



This document was prepared for the ETI by third parties under contract to the ETI. The ETI is making these documents and data available to the public to inform the debate on low carbon energy innovation and deployment.

Programme Area: Marine

Project: PerAWAT

Title: Methodology Report

Abstract:

This report outlines the methodologies and approach adopted in the development of the core modules of the wave farm model software package. It covers the software's architecture; the wave inputs to the simulation; the core hydrodynamic modelling algorithms behind the simulation; the core algorithms behind the farm optimisation module; a set of representative scenarios to assess the applicability of the models; and the key steps for the development and implementation of the software.

Context:

The Performance Assessment of Wave and Tidal Array Systems (PerAWaT) project, launched in October 2009 with £8m of ETI investment. The project delivered validated, commercial software tools capable of significantly reducing the levels of uncertainty associated with predicting the energy yield of major wave and tidal stream energy arrays. It also produced information that will help reduce commercial risk of future large scale wave and tidal array developments.

Disclaimer:

The Energy Technologies Institute is making this document available to use under the Energy Technologies Institute Open Licence for Materials. Please refer to the Energy Technologies Institute website for the terms and conditions of this licence. The Information is licensed 'as is' and the Energy Technologies Institute excludes all representations, warranties, obligations and liabilities in relation to the Information to the maximum extent permitted by law. The Energy Technologies Institute is not liable for any errors or omissions in the Information and shall not be liable for any loss, injury or damage of any kind caused by its use. This exclusion of liability includes, but is not limited to, any direct, indirect, special, incidental, consequential, punitive, or exemplary damages in each case such as loss of revenue, data, anticipated profits, and lost business. The Energy Technologies Institute does not guarantee the continued supply of the Information. Notwithstanding any statement to the contrary contained on the face of this document, the Energy Technologies Institute confirms that the authors of the document have consented to its publication by the Energy Technologies Institute.



**ETI MARINE PROGRAMME PROJECT
PerAWaT MA1003
WG1 WP1 D1B METHODOLOGY REPORT**

Client	Energy Technologies Institute
Contact	Geraldine Newton-Cross
Document No	104327/BR/02
Issue	2.0
Classification	Not to be disclosed other than in line with the terms of the Technology Contract
Date	29 June 2010

Author: J Cruz, E Mackay, M Livingstone,
D McCowen

Checked by:

R I Rawlinson-Smith

Approved by:

R I Rawlinson-Smith

Garrad Hassan and Partners Limited

IMPORTANT NOTICE AND DISCLAIMER

1. This report is intended for the use of the Client on whose instructions it has been prepared, and who has entered into a written agreement directly with Garrad Hassan and Partners Limited (“GH”). GH’s liability to the Client is set out in that agreement. GH shall have no liability to third parties for any use whatsoever without the express written authority of GH. The report may only be reproduced and circulated in accordance with the Document Classification and associated conditions stipulated in this report, and may not be disclosed in any public offering memorandum without the express written consent of GH.
2. This report has been produced from information relating to dates and periods referred to in this report. The report does not imply that any information is not subject to change.

KEY TO DOCUMENT CLASSIFICATION

Strictly Confidential	:	Recipients only
Private and Confidential	:	For disclosure to individuals directly concerned within the recipient’s organisation
Commercial in Confidence	:	Not to be disclosed outside the recipient’s organisation
GH only	:	Not to be disclosed to non GH staff
Client’s Discretion	:	Distribution at the discretion of the client subject to contractual agreement
Published	:	Available to the general public

REVISION HISTORY

Issue	Issue date	Summary
1.0	07.05.2010	D1b Methodology Report - Original issue (electronic version only)
2.0	29.06.2010	Updated version following feedback from the ETI

CONTENTS

COVER PAGE**DISCLAIMER****REVISION HISTORY****LIST OF TABLES****LIST OF FIGURES****EXECUTIVE SUMMARY VI****INTRODUCTION IX**

1	OVERVIEW OF THE DEVELOPMENT STRATEGY FOR GH WAVEFARMER	1
	1.1 GH Software Architecture	1
	1.2 Synergies with Specific GH Software	2
	1.3 Current GH WaveFarmer Architecture	2
	1.4 Overview of the Envisaged GH WaveFarmer Architecture	6
2	WAVE INPUT TO THE GH WAVEFARMER BASE MODULE	8
	2.1 Wave Data Requirements	8
	2.2 Review of the Current Wave Input Capabilities	10
	2.3 Definition of Target Capabilities	10
3	CORE ALGORITHMS: INDIVIDUAL WEC HYDRODYNAMICS AND INTERNAL SYSTEMS MODELLING	12
	3.1 Modelling Wave-Structure Interactions	12
	3.2 Frequency-Domain WEC Hydrodynamics	13
	3.2.1 Introduction to BEM	15
	3.2.2 Applications of BEM to WEC Modelling	18
	3.2.3 A Linear Hydrodynamic Model	23
	3.3 Time-Domain WEC Hydrodynamics	25
	3.3.1 The Time-Domain Equation of Motion	26
	3.3.2 System Causality and Calculation of the Impulse Response Function	29
	3.3.3 Numerical Solution form of the Time-Domain Equation of Motion	31
	3.3.4 State-Space Representation of the Radiation Forces Convolution Integral	32
	3.4 Selection of a Supporting Hydrodynamic Solver	38
	3.5 Current GH WaveFarmer Capabilities – GH FD and GH TD	43
	3.6 Modelling External Forces	44
	3.6.1 Modelling the PTO	46
	3.6.2 Control Actions	50
	3.6.3 Mean Drift Force	55

3.6.4	Moorings	56
3.6.5	Structural Restraint Forces	60
3.7	Equation of Motion Solvers for a Modular Simulation Tool	60
4	CORE ALGORITHMS: LAYOUT OPTIMISER	64
4.1	Review of Previous Optimisation Work – Arrays of WECs	64
4.2	Review of Optimisation Techniques	69
4.2.1	Genetic Algorithms	70
4.2.2	Tabu Search	70
4.2.3	Simulated Annealing	70
4.2.4	Artificial Neural Networks	70
4.2.5	Particle Swarm Optimisation	71
4.2.6	Commercial Codes	71
5	IMPLEMENTATION STRATEGY	72
5.1	Key Design Variables	72
5.2	Outline of the Representative Scenarios	74
5.3	Definitions for Maximising the Energy Yield	80
5.4	Performance vs. Survivability Conditions	81
5.5	Detailed Numerical Model Implementation Plan	83
5.5.1	Wave Data Input	83
5.5.2	Equation of Motion Solver – GH Multibody	84
5.5.3	The Hydrodynamic Model	84
5.5.4	Power Take-Off (PTO) Module	85
5.5.5	Control System	94
5.5.6	Moorings Implementation	95
5.5.7	Optimiser Implementation	95
5.5.8	A Summary of the Key Implementation Steps – FD and TD Core Algorithms	104
	REFERENCES	105
	NOMENCLATURE	117
	KEY TO ACRONYMS	122
	APPENDIX A – DESCRIPTION OF OCEAN WAVES (LINEAR THEORY)	124
	APPENDIX B – ESTIMATION OF THE WAVE SPECTRA FROM MEASUREMENTS	133

LIST OF TABLES

Table 3.1: Commerical BEM Hydrodynamics Codes..... 40

Table 3.2: Selection Matrix detailing the relative capabilities of commercially available BEM solver codes..... 42

Table 3.3: Potential Moorings Configurations for WEC devices..... 58

Table 5.1: List of Representative Scenarios..... 77

Table 5.2: Governing calculations for the initial PTO template. The template is designed to describe a hydraulic or electrical rectification and smoothing type arrangement. 88

Tabel B.1. Linear transfer functions for various wave signals. d is the water depth and z is the height of the measurement from the still water level (positive upwards)..... 134

LIST OF FIGURES

Figure 1.1: Current frequency-domain (MATLAB) code	4
Figure 1.2: Current time-domain (MATLAB) code	5
Figure 1.3: Summary of GH WaveFarmer's envisaged structure under the PerAWaT programme	7
Figure 3.1: ε_{opt} non-dimensional frequency for different configurations (Mynett et al., 1979)	19
Figure 3.2: ε_{opt} non-dimensional frequency for different non-rigid supports (Mynett et al., 1979)	20
Figure 3.3: Initial OWC configuration studied (Brito Melo et al., 1998);	21
Figure 3.4: Left - One degree-of-freedom experimental model of the sloped IPS buoy (Lin, 1999); ...	22
Figure 3.5: AQUADYN's discretisation of the AWS geometry (Alves, 2002)	23
Figure 3.3: The role of system identification techniques in approximating a convolution integral	34
Figure 3.4: Time-domain data exchange between the external force definition modules and the equation of motion solver	45
Figure 3.5: 'Template' Type PTO Model. This template could approximate systems with a simple rectification and smoothing function. Alternative templates could be produced if necessary. Input from the user sets the template to approximate the PTO being modelled	49
Figure 5.1 Overview of the numerical approach – WG1	81
Figure 5.2: Flowchart – Optimiser I/O structure (Scenario 1A)	101
Figure 5.3: Flowchart – Optimiser I/O structure (Scenario 1B)	102
Figure 5.4: Flowchart – Optimiser I/O structure (Scenarios 2A and 2B)	103
Figure A1. The ratios of H_s and period parameters for various values of peak enhancement factor γ . Circles are values obtained by integrating the spectrum, solid lines are the approximations given in Eq. A30-A33	129

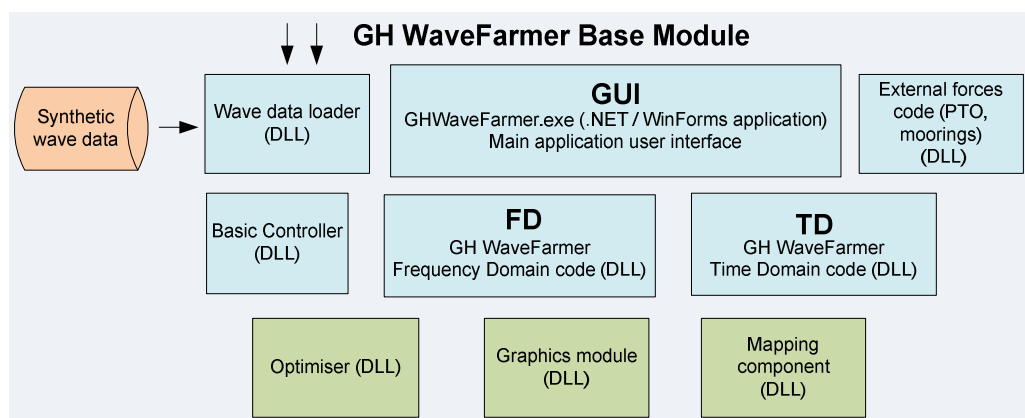
EXECUTIVE SUMMARY

The present report (WG1 WP1 D1B) outlines the methodologies and approach to be adopted in the development of the core modules of the wave farm model software package. The report is an extension of an interim deliverable (WG1 WP1 D1A) and should be considered its final version.

The report is organised in five sections which give a detailed overview of:

- The software's architecture (Section 1);
- The wave inputs to the simulation (Section 2);
- The core hydrodynamic modelling algorithms behind the simulation (Section 3);
- The core algorithms behind the farm optimisation module (Section 4);
- A set of representative scenarios to assess the applicability of the models and the key steps for the development and implementation of the software (Section 5).

The basic structure of the software's base module, which corresponds to the Beta2 release, is detailed in the figure below. There is a direct link between the sections of this report and the modules described in the figure: Section 1 introduces the structure; Section 2 covers the 'wave data loader'; Section 3 cover the 'basic controller', 'FD', 'TD' and 'external forces' modules; finally, Section 4 covers the 'optimiser' module. The 'graphics' and 'mapping' modules will be partly based on existing GH software (given their post-processing nature). The 'optimiser' module will also benefit from existing tools at GH such as the equivalent modules of GH WindFarmer.



LEGEND

	GH WaveFarmer modules
	Shared modules /applications
	Non-GH components
	Input data

Summary of GH WaveFarmer's envisaged structure under the PerAWaT programme

After introducing the planned structure for the software and the synergies with existing software at GH (Section 1), the following sections of this report describe the baseline theory and methodology behind the key components of the Base module. Section 2 overviews the theoretical principles and the base functionalities necessary to load wave data into the simulation. Section 3 addresses the hydrodynamic modelling component (including a bibliographic review) in the frequency and time-domain, along with the principles behind the modelling of the external forces (namely the moorings, structural restraint and power take-off forces). Control aspects are also covered in Section 3, while Section 4 describes previous work in the field of arrays of WECs, the optimisation methods under consideration and the baselines methodologies to be developed for the Beta1 and Beta2 deliverables (GH WaveFarmer Base Module). The core modules will allow comparisons with the nonlinear approach conducted by the University of Oxford via the results presented in deliverables WG1 WP1 D8 to D12. Equally, WG1 WP2 D4 from Queens University Belfast will also allow comparisons between the several numerical approaches (namely the integration of the WG1 WP1 results in the calibration of the sub-grid elements that describe the WECs). To ensure cross-cutting comparisons a table that summarises the validation exercises (which will be replicated numerically, thus resulting also in verification exercises) has been discussed in the technical meetings and will be presented in WG2 WP1 D1.

The final section of the report (Section 5) builds on the previous sections and presents in detail the:

- Key designs variables (Section 5.1);
- Representative scenarios (Section 5.2);
- Definitions for maximising the energy yield (Section 5.3);
- Definitions for survivability conditions (when compared to the performance conditions) (Section 5.4);
- Key steps for the implementation of the core solvers (frequency and time-domain) (Section 5.5).

The latter topic can be considered the key output of this report, as it outlines the strategy for the subsequent deliverables of WG1 WP1. The implementation process aims to develop the frequency and time-domain core algorithms code for the beta releases by systematically completing a series of implementation steps. Note that GH has an existing numerical modelling code (Cruz et al., 2009) which will act as the basis for the software development. The key steps can be summarised as follows:

1. Definition of the wave climate inputs and associated sensitivity studies (use of different spectral parameter vectors as inputs);
2. An upgrade of the equation of motion solver to incorporate the GH Multibody modelling engine.
3. Development of a stand-alone WAMIT results postprocessor designed to save WAMIT output data in a documented format. The user will have the option of running the processor from within the software. The hydrodynamics module will read in the processed WAMIT data so that it can be used for formulation of each of the hydrodynamic force terms.

4. Creation of a radiation impulse response function system identification algorithm based on the frequency-domain fitting technique. The performance (and accuracy) of the resulting state-space simulation will be compared with the existing time-domain numerical convolution method using an irregular wave input and a simple viscous damper PTO model. Favourable results will lead to a system identification option being incorporated as a pre-processing stage.
5. Creation of a user interface capable of receiving constrained mathematical expressions. The interface will be able to limit the user to entering a linear expression if necessary. The mathematical expression interface will allow frequency and time-domain simulations to be defined using the simple mathematical expression PTO model, with its associated control representation, and will act as the basis for the input of user-defined functions in the PTO templates.
6. Construction of a linearised dynamics moorings model. This initial moorings model will ask the user to enter inertial, damping and stiffness coefficients representing the complete moorings system.
7. Construction of the first PTO Template, which will be capable of representing some hydraulic and electrical PTO designs with a single internal state. The state derivative equation will be solved by the equation of motion solver and the template will be designed to operate under specific control logic called at every time-step.
8. Construction of the structural restraint forces and quasi-static moorings models, including a user interface designed to obtain data on the geometrical configuration and force properties of the system.
9. Construction of the optimiser module is a staged approach (1A to 2B) alongside all of the above.
10. Construction of a final post-processing module, allowing the specification of batch runs leading to the creation of site specific power matrices.

INTRODUCTION

The present report (WG1 WP1 D1B) outlines the methodologies and approach to be adopted in the development of the core modules of the wave farm model software package. The report is an extension of an interim deliverable (WG1 WP1 D1A) and should be considered its final version. The main addition to the sections presented in Issue A is in the definition of the key implementations steps to create both the frequency and the time-domain simulations based on linear and quasi-nonlinear hydrodynamics. The core modules will allow comparisons with the nonlinear approach conducted by the University of Oxford via the results presented in deliverables WG1 WP1 D8 to D12. Equally, WG1 WP2 D4 from Queens University Belfast will also allow comparisons between the several numerical approaches (namely the integration of the WG1 WP1 results in the calibration of the sub-grid elements that describe the WECs). To ensure cross-cutting comparisons a table that summarises the validation exercises (which will be replicated numerically, thus resulting also in verification exercises) has been discussed in the technical meetings and will be presented in WG2 WP1 D1.

The report is organised in five different sections; a brief introduction to each is given below:

- In Section 1 the potential synergies that can be achieved by developing the core modules in a fashion consistent with standard Garrad Hassan (GH) software architectures are briefly explored. The current architecture of the existing wave energy converter (WEC) hydrodynamic modelling tools developed by GH is also described and an overview of the envisaged structure for the tools developed under PerAWaT presented;
- In Section 2 an overview of the wave input to the core modules is presented. Quantities such as the wave spectrum and the key spectral parameters are introduced and defined. Estimation techniques to derive the wave spectrum from real data are also considered
- The basis of both the frequency and the time-domain models is presented in Section 3, using linear (Airy) wave theory. An introduction to the principles of fluid-structure interaction modelling, with emphasis to the Boundary-Element Method, is given and applications to WEC modelling described in detail. Particular emphasis is given to the practical aspects of solving the time-domain equation of motion, the selection of a supporting hydrodynamic solver and the modelling of the external forces (namely the power take-off force, the mooring force and the impact of the control methodology).;
- In Section 4 the optimisation methodology is overviewed and examples of WEC array optimisation exercises conducted to date are reviewed. Different optimisation techniques are presented in preparation of the implementation stage;
- The final Section of this report (Section 5) describes the implementation strategy for the methodology introduced in the previous sections of the report. The key findings of this report are compiled, namely:
 - Key design variables (when optimising an array of WECs) – Section 5.1;
 - Description of representative scenarios to assess the functionality of the developed software – Section 5.2;
 - Definitions for maximising the energy yield – Section 5.3;

- Overview of performance vs. survivability conditions – Section 5.4;
- Detailed numerical model implementation plan – Section 5.5.

1 OVERVIEW OF THE DEVELOPMENT STRATEGY FOR GH WAVEFARMER

Garrad Hassan and Partners Ltd (GH) has been developing software products for the renewable-energy industry for more than 20 years and now offers a range of powerful tools for various purposes. Historically the focus has been solely on wind energy, but as the company diversifies into other areas of renewable energy, the software products it offers are also broadening in scope. **GH Bladed**¹ is the industry-standard software for modelling wind turbines, while the tidal version (GH Tidal Bladed) is already being used commercially as a design tool in the emerging field of tidal-stream turbine development. **GH WindFarmer** is a well-established wind-farm design tool which allows designers to optimise the layout of a wind-farm within specified constraints. It also allows realistic visualisation of the proposed farm, among many other features. **GH SCADA** allows real-time remote monitoring and control of an operating wind-farm, while **GH Forecaster**² provides accurate forecasts of wind-farm energy production from between a few hours up to as much as a week in advance.

In the future, the GH portfolio will grow to include **GH WaveFarmer** (the main focus of this report), and **GH TidalFarmer**. These new tools will be designed to model wave and tidal energy farms (respectively). The use of software models to reduce the uncertainty in farm energy yield is commercially attractive to end-users such as project developers and utilities, whilst individual device performance modelling is important to device manufacturers and their investors. The fundamental objective of the PerAWaT project is the development, implementation and validation of the core (or base) code that will, outside of the project, be developed into a commercial software product. The core tools will be capable of modelling the most critical design variables for determining the energy yield of an array of wave or tidal energy devices.

1.1 GH Software Architecture

Currently the GH software portfolio consists of several independently-designed, stand-alone software products with little integration or sharing of functionality. The development of GH WaveFarmer will take place in the context of a broader evolution of GH software products towards a more modular, component-based, and integrated architecture. Some components will be shared at many different levels, from the “skin” of the user interface, through shared core components like optimisers and file management, to outputs (report-generation and graphics). Sharing code is beneficial for the PerAWaT project for several reasons, including:

- It reduces the amount of code which needs to be tested, debugged, and maintained (all expensive tasks).
- It allows the software developer to focus on the innovative tasks (there is less “reinventing the wheel”).

¹ Wherever the term GH Bladed is used in this report, it refers to both the wind-turbine modelling product and to GH Tidal Bladed.

² GH Forecaster is currently not available for purchase, but is used by GH to provide an energy forecasting service.

- When a shared module gets an upgrade, all the products which use that module will benefit with little or no extra development effort.

Therefore, as and when it is deemed appropriate software developed under PerAWaT will make full use of the developing ‘standard’ GH Architecture so as to capture as many of these benefits as possible whilst not distracting from the overall objective of the development of stand alone ‘Beta’ tools.

1.2 Synergies with Specific GH Software

Possible code sharing opportunities that may be pursued under PerAWaT are described below.

The first is a new **multibody dynamics** code recently released in GH Bladed. This is a sophisticated piece of functionality which has been designed to be very generally applicable: the code is not specific for wind turbine components and it deals in a general sense with interactions between rigid or flexible bodies subjected to gravitational, hydro/aerodynamic and other externally-applied loads. It also provides a platform for structural calculations based on a modal approach – a functionality not envisaged for the base version of GH WaveFarmer, but that in the future could be worth pursuing. The code can output time-series of loads and motion at any point of interest in the system. GH WaveFarmer has a similar, though not identical, requirement for multibody analysis, so there is potential to explore shared functionalities between the two.

GH Bladed also offers the user an option to add an **external controller DLL** which can be interfaced to the wind turbine simulation. This allows the user to experiment with different control algorithms/strategies more easily. On a related subject, GH Bladed has a linearisation module which is useful for controller design. GH WaveFarmer might be able to share the functionality of both these, in particular to allow technology developers to use custom-made control strategies without sharing the intrinsic details of each algorithm. If such functionality can not be shared, it is envisaged that a similar module will be built in the GH WaveFarmer base module.

GH Bladed also has an optional “**Real-time Hardware-in-loop testing**” module. This allows a computer running Bladed to operate as a “virtual turbine”, interfacing electronically with actual controller hardware. Such an arrangement has obvious benefits for controller testing. There might be a requirement for a similar product for WEC controllers.

GH Forecaster would provide an excellent basis for a **wave-power prediction module** which could be interfaced with GH WaveFarmer, should there be a demand for this. Equally, the adaptation of the MCP (Measure, Correlate, Predict) methodology for wave energy is a potential extension to PerAWaT, as the use of short-term measurements campaigns together with long-term numerical predictions would allow the estimation of the (bankable) long-term site specific resource in a much faster way. Preliminary work on both these topics has been carried out by GH as part of an nPower Juice funded project (preliminary results were presented at the 2008 Offshore Mechanics and Arctic Engineering Conference).

1.3 Current GH WaveFarmer Architecture

The GH WaveFarmer code in its present form can be configured to model single WECs on a device specific basis. The aim in the future is to adopt a more general-purpose approach, which will read in a user supplied device description and model arrays of multiple interacting devices. An initial, geometry specific array modelling extension to the code has already been completed as part of an internal R&D

project; this culminated in a joint publication with the University of Oxford presented at the 2009 European Wave and Tidal Energy Conference.

GH WaveFarmer is currently implemented as a set of MATLAB .M files. The two “master” .M files which drive the rest of the functionality are GH_WF_TD.m (for time-domain analysis) and GH_WF_FD.m (for frequency-domain). When these are run from MATLAB they call functions in subsidiary .M files, as shown in Figures 1.1 and 1.2, respectively.

The basic functionalities of each of the subsidiary .M files are also described in Figures 1.1 and 1.2. For the frequency-domain code this includes specific routines to import WAMIT data, calculate the absorbed energy for a variety of PTO settings (limited to linear dampers) under two control strategies (passive – same PTO setting applied to all incident wave frequencies; active – PTO setting chosen as that that maximises the absorbed energy for each individual frequency), a post-processing unit (Freq_plotting.m) and an initial calculation of the energy absorbed for a incident wave spectrum (using the superposition principle).

The time-domain code allows the definition of nonlinear external constraints (e.g. PTO, moorings) via a specific .M file (time_pto_v#_#.m) and uses further hydrodynamic data (radiation force memory function – see Section 3.3.1) obtained from the F2T add-on to WAMIT and loaded into the simulation using f2tdataimportk.m. The additional input are introduced via GHTD3v#_#.m while the time-domain equation of motion is solved using the Adams-Bashforth algorithm in Timedomainsolver5_v#.m (see also Section 3.7).

In both cases the existing basic functionalities are the starting point for the envisaged structure (Section 1.4). The methodology for this expansion to the array tool being developed under the PerAWaT project is described in Section 5.

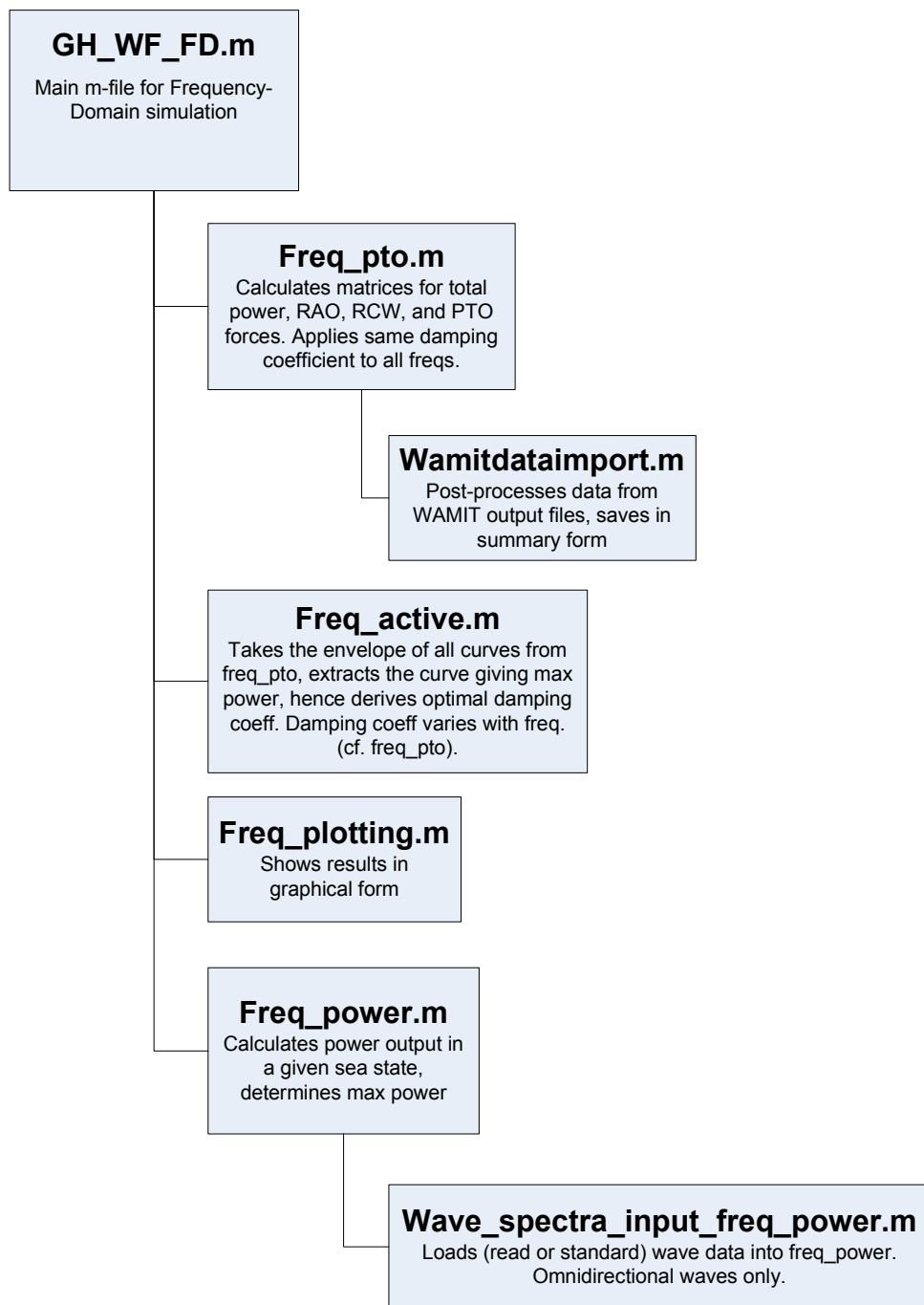


Figure 1.1: Current frequency-domain (MATLAB) code

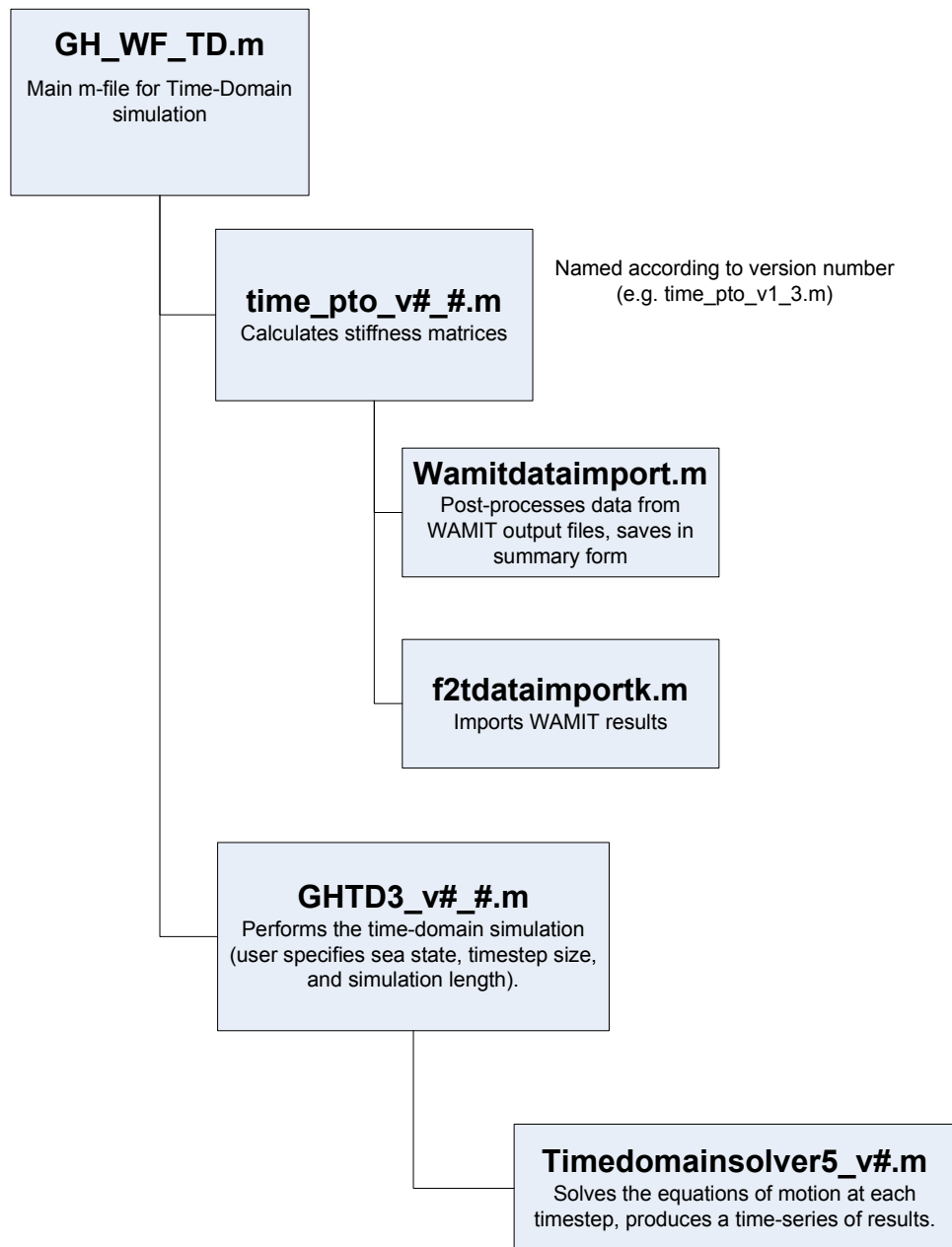


Figure 1.2: Current time-domain (MATLAB) code

1.4 Overview of the Envisaged GH WaveFarmer Architecture

The GH WaveFarmer Base Module shown in Figure 1.3 represents the code which will be developed under the PerAWAT project, i.e. the “Beta 1” and “Beta 2” deliverables. Note that it is likely that some of the Base Module code will share components with other existing GH software products (thus this distinction between the base module components in blue – PerAWaT specific – and the base module components in green – existing GH code). Any code that falls into the latter category will be delivered as executable code only, as it will have been developed independently of PerAWAT. The rest of the Base Module functionality will be delivered as both source code and executables. The base module will be a fully functional version of GH WaveFarmer, but will exclude certain more advanced pieces of functionality which are not being developed under PerAWaT.

The next Sections of this report describe the baseline theory and methodology behind the key components of the Base module. Section 2 overviews the theoretical principles and the base functionalities necessary to load wave data into the simulation. Section 3 addresses the hydrodynamic modelling component (including a bibliographic review) in the frequency and time-domain, along with the principles behind the modelling of the external forces (namely the moorings, structural restraint and power take-off forces). Control aspects are also covered in Section 3, while Section 4 describes previous work in the field of arrays of WECs, the optimisation methods under consideration and the baselines methodologies to be developed for the Beta1 and Beta2 deliverables (GH WaveFarmer Base Module).

Finally, Section 5 presents the implementation strategy to develop the methodology, establishing the starting point for the implementation reports. The key design variables and representative scenarios are also outlined.

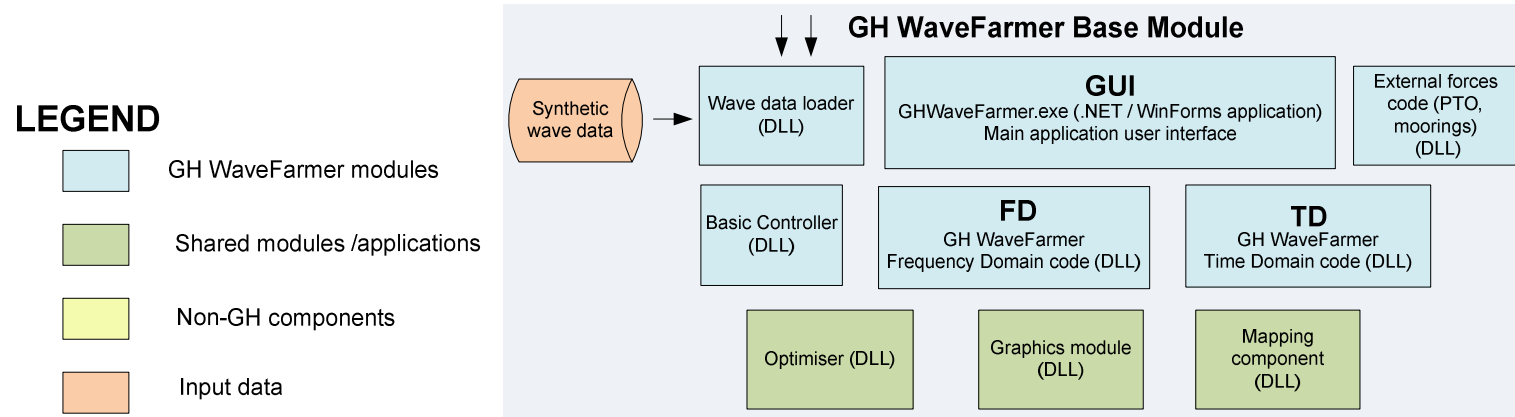


Figure 1.3: Summary of GH WaveFarmer’s envisaged structure under the PerAWaT programme

2 WAVE INPUT TO THE GH WAVEFARMER BASE MODULE

Both the frequency-domain (FD) and time-domain (TD) simulations in the GH WaveFarmer code are based on linear (Airy) wave theory. Before discussing the wave input, it is important to distinguish nonlinear waves from nonlinear forces. Nonlinear waves refer to waves which do not obey the assumptions of linear theory (wave height small compared to wavelength) whereas nonlinear forces can either refer to nonlinear wave-induced forces or nonlinear external forces (such as the PTO and the mooring force). The FD and TD models developed by GH under PerAWaT will both use linear wave inputs. The FD simulations are, by definition, limited to linear forces, but the TD simulations will use linear wave-induced forces and nonlinear external forces from the PTO and moorings. As part of the verification and validation exercises, the necessity to use nonlinear wave-induced forces will also be assessed, and the software will be developed in a way that allows the integration of such load profiles. The applicability of linear and nonlinear wave inputs and hydrodynamics will be determined primarily by comparing the results from the GH models with the nonlinear hydrodynamic models developed by UoOx. If proved necessary, a quasi-nonlinear approach will be developed by GH to address the key aspects of wave-induced nonlinearities.

This Section describes the target capabilities of the wave data loader module (see Figure 1.3) to the FD and TD simulations. The standard concepts, definitions and terminology used to describe ocean waves in the context of linear theory are presented in Appendix A, and methods for estimating the spectrum from measurements are described in Appendix B. The section begins with a discussion of the requirements for wave data in the simulations. This is followed by a review of the present capabilities in Section 2.2. The target capabilities are defined in Section 2.3. Note that the key steps for implementation are outlined in Section 5.5.1.

2.1 Wave Data Requirements

The overall requirement for the wave module is to provide sufficient information about the wave climate to enable the calculation of the average annual energy yield of an array of WECs. The main problem associated with this is that currently it is not known how much information is required in order to obtain an accurate estimate of the energy yield. In general, the energy produced by an array in a given sea state is dependent on the full directional spectrum. However, there is a significant amount of information contained within the directional spectrum and for the purpose of estimating energy yield statistics it is useful to describe the sea state using a limited number of parameters (e.g. significant wave height - H_s , wave energy period - T_e , bandwidth, mean direction, directional spread). The joint distribution of these parameters can then be estimated and the simulation can be run using standard shaped spectra for a representative range of sea states.

Using a limited number of parameters to describe the wave spectrum decreases the required number of simulations. However, for sea states with a given parameter vector, the measured spectra may display a range of different shapes. This will result in a range of different power outputs for a given sea state parameter vector. Increasing the number of parameters used to describe the spectra will decrease the range of spectral shapes for a given parameter vector, but increases the number of simulations which need to be conducted. Therefore, there is an inherent compromise between the number of simulations which need to be run and the accuracy of the estimated energy yield. In the limit case, where the spectra are not parameterised at all, the full history of measured spectra must be used in the simulation. This becomes

problematic when examining the long-term variability in energy-yield, since many computations will be required.

An advantage of parameterising the response of an array or WEC is that in many situations a long record of measured directional spectra will not be available for the site of interest. A requirement for the tools developed under PerAWaT is that they produce an estimate of the energy yield using information that will be available during the initial stages of a project. Typically, only a limited period of in-situ measurements will be available at the initial stages. It is therefore necessary to use long-term reference data from other sources in order to calculate long-term statistics. Usually, the long-term reference data will come from a numerical wave model. Data from numerical wave models are estimates rather than measurements. They require careful calibration to remove as much of the bias as possible and to quantify the remaining uncertainty (see e.g. Mackay et al., 2010). Modules for the analysis and calibration of model data will be developed as add-ons to the base module. For the models developed in WG1 WP1 it will be assumed that the input wave data has been calibrated and the errors are known. The base module will therefore have a ‘wave data loader’ (compatible with the outputs of the add-ons) and also a ‘synthetic wave data’ creator (able to generate the parameterised inputs described above).

The approach taken by most WEC developers at present is to describe the response of the WEC or wave farm in terms of a small number of spectral parameters in a power matrix, usually in terms of H_s and T_e . Various approaches have been proposed to address the limited descriptive ability of the power matrix. The DTI preliminary wave energy device performance protocol (DTI, 2007) suggests that several tables could be used to describe the response of the machine, specifying the mean, standard deviation, minimum and maximum power for each cell of the power matrix. This approach has the advantage that it is relatively simple. However, the distribution of spectral shapes for a given H_s and T_e is likely to vary with location and water depth, so a set of tables will have to be generated for each site of interest.

The alternative to this approach is to include further parameters to describe the power response. Saulnier et al. (2007) examined the sensitivity of the power produced by an axisymmetric point absorber to various spectral bandwidth parameters (measures of the spread of the energy about the mean frequency of the spectrum). The authors suggest that 3-dimensional power matrices could be used to describe the device’s power response, binned by H_s , T_e and spectral bandwidth. Kerbiriou et al. (2007) proposed a slightly different approach, where the power response is calculated as the sum of the contributions from each wave system making up an individual sea state. Each measured directional spectrum is partitioned into separate wave systems and each system is represented by a set of five parameters: the total energy, peak frequency, spectral bandwidth, mean direction and directional spread.

There is, as yet, no consensus on a standard method for parameterising the power response of a WEC or an array of WECs. A heuristic approach will be taken in the PerAWaT project. To start, the response of an array will be calculated using full directional spectra covering a period of one year. The effect of various levels of parameterisation will then be examined. From this, conclusions will be drawn about the trade-off between the accuracy of the estimate of annual energy yield and the number of parameters used to describe the response. A detailed description of the approach is given in Section 5.5.1.

2.2 Review of the Current Wave Input Capabilities

The current GH WaveFarmer FD and TD code, described in Section 1.3, can run simulations for both regular (monochromatic) waves and unidirectional irregular (polychromatic) waves. The basic concepts and definitions used to describe regular linear waves are described in Appendix A1 and irregular waves are described in Appendix A2. At present there is no capability to run simulations for directionally spread seas, but this capability will be developed during PerAWaT.

For regular waves the specified inputs are the wave period and direction (note that results are nondimensionalised by the wave amplitude; for absolute motion in the TD a wave height must be specified, while the RAO is the standard motion output in the FD). These parameters are entered directly into the FD and TD simulations and no input is required from the wave module.

For the irregular wave simulations the only input required by the simulations is a spectrum. In the case of the TD simulations a random sea surface elevation is generated by the TD solver from the input wave spectrum. The simulation of sea surface elevation from spectra is described in Appendix A7. The spectrum used in the simulation can either be specified as a standard form or loaded from a file, containing a measured frequency spectrum. The standard shapes used for the frequency spectrum are described in Appendix A5. These spectra are specified by a number of sea state parameters defined in Appendix A3.

To summarise, the present wave inputs to the FD and TD simulations are:

- Regular waves specified by wave height, period and direction
- Unidirectional irregular waves:
 - Measured spectrum loaded from a file
 - Standard shape spectrum (Pierson-Moskowitz, Bretschneider or JONSWAP) specified in terms of H_s , T (either T_p , T_e , T_m or T_z), JONSWAP peak enhancement factor and direction

2.3 Definition of Target Capabilities

The target capabilities for the wave module are split into two categories: the base module and add-on modules. The base module will have the capability to create standard shape spectra and load wave spectra and parameters from the add-on modules, but these add-on modules will be developed outside of PerAWaT.

The wave base module developed in PerAWaT will have the following capabilities:

- Generate standard shape frequency spectra and directional spreading functions for a given sea state parameter vector
- Load directional spectra from measured data
- Create a probabilistic parametric description of a site-specific wave climate from measured spectra.
- Output unidirectional and directional spectra to FD and TD simulations

The use of directional spectra, both from standard shapes and measured data, is a simple extension to the present capabilities of the wave module (although the implementation of the directionally spread waves in the TD simulations is less straightforward). Directional wave parameters are defined in Appendix A4 and standard shapes for the directional distribution are discussed in Appendix A6.

The most significant extension of the wave module from the current capabilities is the probabilistic, parametric description of a site-specific wave climate. As discussed in Section 2.1, there is currently no consensus on which sea state parameters should be used to describe WEC or array response. The approach taken in PerAWaT will be to develop a flexible parameterisation of the sea state and then estimate the joint distribution of these parameters from measured data. The joint distribution of these parameters can then be used to specify the range of sea states for which the response of the WEC or array should be calculated in order to estimate the average annual energy yield. The main advantage of this approach is that it will allow the optimiser to iterate using a small number of parameters rather than using the full range of measured sea states to describe the long-term, site specific wave climate. More detail on the proposed procedure is given in Section 5.5.1.

The add-on modules developed outside of PerAWaT will have the following capabilities:

- Analysis of unprocessed wave data
- Shallow water spectral wave model
- Calibration of model data and estimation of uncertainty

The module for analysis of unprocessed data will take raw measurements from standard wave measuring devices (buoys, ADCP, wave gauge arrays, etc.) as input. Quality controls will be applied to the raw data and the frequency and directional spectra will be estimated using the methods described in Appendix B.

The main purpose of using a shallow water spectral wave model in this context is to estimate wave conditions at a wave farm site using boundary conditions from a nearby data source (either a large-scale spectral wave model such as WAM or WW3 or another measurement location). This approach is usually necessary to estimate the long-term distribution of sea-states at the site of a potential wave farm. The representation of arrays of WECs in spectral wave models is being investigated by QUB in WG1 WP2. The models developed by GH are for small array sizes in relatively deep water, where it can be assumed that bathymetric effects within the array can be neglected. For larger arrays this assumption may be less valid, and the QUB approach will allow bathymetric effects to be calculated explicitly. The integration of QUB's software in the Beta2 version will be the immediate use of this functionality.

If model data is used to estimate the long-term distribution of sea states at a site, then it will require careful calibration as well as quantifying the uncertainty. Methods for calibrating model data for use in wave energy studies are discussed in Mackay et al. (2010). For the simulations conducted in PerAWaT only measured data will be used.

3 CORE ALGORITHMS: INDIVIDUAL WEC HYDRODYNAMICS AND INTERNAL SYSTEMS MODELLING

3.1 Modelling Wave-Structure Interactions

Two different numerical approaches are commonly employed to determine the nature of wave interaction with fully or semi-immersed bodies of unknown shape. The first is to solve for the complete set of fluid properties at all locations in a mesh covering the control volume containing the body of interest. The solution process is based on treatment of discretised Navier-Stokes equations (although Potential or Euler flow assumptions are sometimes made) and is known as Computational Fluid Dynamics (CFD), a reference to the need for a numerical solution to the numerous equations describing the complete spatial variation and time variation (under non-steady flow) in the fluid. Generation of a suitable mesh for the discretisation, and the selection of an appropriate turbulence model (for viscous flow), including boundary layer treatment, are important factors in ensuring that an accurate solution is obtained in a practical amount of computation time.

CFD solutions have the advantage of producing a thorough and flexible solution to the problem, however the need to solve for the entire control volume means that computational effort for all but the simplest models can become prohibitively high if an accurate, time dependant solution is desired. This is particularly the case for the modelling of WECs, which much be subjected to irregular wave inputs over a long period of time and actively respond to the fluid forces, operating with a continuously varying wetted surface area and overall position in the control volume. In addition, the generality of CFD codes (which frequently cover a wide scope of applications through the inclusion of numerous mathematical models and calculation options) means that the end result can vary significantly due to decisions made by those responsible for defining the calculation specification. Finally, creation of a suitable simulation model in the unconstrained CFD environment can in itself be time consuming and the diversity of WEC designs is such that convergence on a common simulation configuration is not guaranteed. The recent merger between Germanischer Lloyd (GL) and GH brings new opportunities in the field of CFD modelling given GL's expertise in the field and this is currently being explored as a means of an additional verification data set.

An alternative approach avoids the need to calculate an overall solution for all points in the flow. The technique, typically referred to as a 'Boundary Element Method' (BEM), or panel method, focuses on determining the velocity potential solely on the body surface, which is divided into panels (see Section 3.2.1). This approach is the industry standard when assessing offshore engineering problems such as the motion of a floating body in response to an incident wave climate. The solution is generally restricted to potential flow, with each panel being modelled as a fluid source contributing to the net flow over the surface. The excitation and radiation velocity potentials are then solved for using Green's Theorem, with the free-surface source potential as the Green function. In a 'low-order' solution method, the panels are flat and are assumed to have constant properties over their area. More recent 'higher-order' options, which use linear, quadratic or B-spline approximations to the body geometry and velocity potential distribution have been developed (Newman and Lee, 2002). In these, the panels used to describe the geometry and / or the velocity potential are curved. A BEM solution (either low or high-order) quantifies a set of frequency dependant hydrodynamic coefficients for the body geometry (the solution of the radiation problem, i.e. a forced motion in an otherwise undisturbed fluid) and the wave exciting force (the solution of the diffraction problem, i.e. the force due to the incident wave field when the body is fixed). These can then be used in

conjunction with the higher-level hydrodynamic analysis presented in Sections 3.2 and 3.3 to evaluate the response of a body as a function of the incident waves in either the frequency or time-domain.

BEM based hydrodynamic modelling is now well established in the context of theoretical WEC modelling and will be adopted for the initial GH WaveFarmer releases, the subject of the methodology presented here. Comparison with both empirical results and those from more computationally intensive numerical modelling in the PerAWaT project will provide a basis for the review of the GH WaveFarmer hydrodynamic modelling approach. These comparisons have been formalised in WG0 D1 (see Section 2, Figure 2.2).

3.2 Frequency-Domain WEC Hydrodynamics

Numerical modelling of WECs is typically initiated in the frequency-domain, relying on the principles of linear wave theory. Such models, although limited by the simplifying assumptions of the theory, provide a suitable platform for overall concept design and configuration assessment. Linear wave theory itself is well documented in many references: selected examples are Lé Méhauté (1976), Newman (1977), Mei (1989; revised and extended edition in 2005), and Falnes (2002), among many others. In the majority of these examples wave energy conversion is explicitly mentioned and studied. A short description of some of these titles is presented below. Note that throughout Section 3 Falnes (2002) is used as the key reference.

The underlying principles of linear wave theory condition the approach. In particular:

1. The free-surface and the body boundary conditions are linearised;
2. The fluid is incompressible and the flow is irrotational (potential flow);
3. Viscous effects like shear stresses and flow separation are not considered;
4. The seabed is assumed to be flat (and uniform);
5. Under these above mentioned assumptions all variables can be expressed as a complex amplitude times $e^{i\omega t}$, where ω is angular wave frequency (regular waves, sinusoidal motions).

In the first two references mentioned above, the underlying theoretical principles are thoroughly reviewed. Le Méhauté (1976) presented a complete survey of wave theories and general hydrodynamic aspects. Waves and wave effects were also discussed in Newman (1977), with particular emphasis to the definitions of damping and added mass, exciting force and moment, and also the response (or motion) of floating bodies.

Mei (1989) dedicated a sub-chapter (7.9 in the 1989 edition; 8.9 in the 2005 edition) to the absorption of wave energy by floating bodies. The basic principles of the energy conversion chain are described, and examples of concepts that can be classified as terminators (beam-sea absorbers), attenuators (head-sea absorbers) and omnidirectional absorbers are given. When the characteristic dimension of the wave energy converter is much smaller than the wavelength λ the latter are often called point absorbers. An interesting effect is associated with this type of concept. The so-called point absorber effect was first reported by Budal and Falnes (1975) which implies that in a one degree-of-freedom approach (e.g.: heave) a body

radiating axisymmetric waves can absorb all the available power in a wave front with width equal to $\lambda / 2\pi$. Note that terminators and attenuators can also absorb more power than the one contained in a wave front with their own width (particularly clear for solo devices), so this effect is not exclusive to omnidirectional absorbers. The point absorber effect was also pointed out by Evans (1976) and Newman (1976), who emphasised the paradox that linear wave theory carries in this particular case: an infinitely small body would require infinitely large amplitudes of motion to capture all the energy, but linear wave theory is limited to small amplitudes ($A / \lambda \ll 1$, where A is the incident wave amplitude). The author also derived two key findings: the symmetrical nature of the radiation force, meaning that the added mass and damping matrices are also symmetrical, and the relation between the radiation and the diffraction problems (as pointed out earlier by Haskind, 1957). All these authors recognised a limitation that two dimensional symmetric bodies have when absorbing waves: with one degree-of-freedom, only 50% of the incident wave power can be absorbed. This limitation can be overcome by adding linearly independent degrees-of-freedom (e.g.: two uncoupled modes lead to an upper limit of 100%).

The performance of a wave energy converter is usually measured by the capture width, the length of wave crest that contains the absorbed power. In other terms, the capture width can be defined as the ratio between the mean absorbed power and mean wave power per unit crest width. This parameter has the dimension of length, but it is sometimes useful to present it in the non-dimensional form as the ratio between the capture width and the width of the device; this ratio is often called relative capture width. The two-dimensional equivalent of the relative capture width is the hydrodynamic efficiency. Given that it is limited to a unit width device and to a unit width wavefront it has a maximum value of 100%, whereas in a three-dimensional layout a device can absorb more power than the one contained in a wave front with its own width, as three-dimensional effects allow it to absorb energy from the total wavefront incident upon it.

In Mei (1989) the case of a special two-dimensional terminator, the Edinburgh Duck, was presented in detail, particularly with regard to the equations of motion and to the hydrodynamic efficiency. This contribution follows directly from Mynett et al. (1979). Finally, a review of the theoretical principles of wave energy conversion was given in Evans (1976, 1981a). But the most complete compilation of mathematical work related to the absorption of waves by oscillating bodies can be found in Falnes (2002), where the basics of wave-body interactions are presented alongside the principles of optimum control for maximisation of converted energy. A special chapter is dedicated to oscillating water columns, emphasising the amount of work carried out for this specific technology at an early stage.

It is relevant to recognise the dedicated conferences and meetings have been organised over the past few decades. The biennial European Wave and Tidal Energy Conference (EWTEC), which dates back to an early symposium held in Gothenburg in 1979, is one of the most relevant and its proceedings are a proof of the continuous interest that wave energy has engaged in both the scientific and the industrial communities over the years, a legacy for future generations and a starting point for those who are willing to develop new concepts. Other relevant compilations of publications include the proceedings of the 1985 IUTAM Symposium in Lisbon edited by DV Evans and AF Falcão, which focus many different subjects of the hydrodynamics of wave energy converters (from survivability to optimisation) that are remarkably up-to-date. One final reference to one of the annex reports of the 1993 Generic Technical Evaluation Study of Wave Energy Converters, sponsored by the European Union (at the time Commission of the European Communities), entitled 'Device Fundamentals Hydrodynamics' (coordinated by University College Cork). The contributions relative to basic hydrodynamic aspects, optimum control and laboratory testing are particularly relevant to those who are beginners in the field.

It is beyond the scope of this report to present a thorough review of linear wave theory. Such an exercise can be found in one of the available references mentioned earlier. However it is relevant to briefly summarise the equations that define the physical problem (see example in Section 3.2.3) and the main simplifying assumptions that are implemented in a frequency-domain model, when solving the wave-body interaction problem. Firstly, a revision on the numerical methods typically implemented when conducting frequency-domain modelling of WECs are presented (Section 3.2.1), along with some specific examples (Section 3.2.2). These first two Sections are extracted from the contribution of one of the authors of this report to Cruz (2008).

3.2.1 Introduction to BEM

Panel methods, also referred to as Boundary Element Methods (BEM) in a wider engineering perspective, are computational methods used to solve partial differential equations which can be expressed as integral equations. Typically, BEM are applicable to problems where the Green function can be calculated. A thorough review on panel methods in computational fluid dynamics is presented in Hess (1990). Relevance is given to aerodynamics, but the main assumptions (e.g.: potential flow) and principles are applicable to generic fluid mechanics problems. A sub-chapter focusing exclusively in free surface applications is also presented. The two common problems given as examples are:

1. a ship at constant forward speed in an undisturbed wave field;
2. a fixed structure facing incoming regular waves.

Note that an extension of the second case also includes the problem of an oscillating body in an undisturbed media, which is particularly relevant in wave energy conversion.

In the first case, Rankine type sources were originally used and both the submerged portion of the hull and the surrounding free surface were panelised. In the second case the singularities are more complex and only the body is discretised. Newman (1985) developed a practical technique to address such issues and later applied it to a variety of case studies. Many references can be found in the literature, but given the introductory nature of this section Newman's key communications are followed.

A review on the basic principles that rule the application of panel methods in marine hydrodynamics is given in Newman (1992). It is emphasised that many of the common problems in this subject, like wave resistance, motions of ships and offshore platforms, and wave structure / interaction can be addressed following potential flow theory, where viscous effects are not taken into account. The objective is therefore to solve the Laplace equation with restrictions imposed by boundary conditions. The domain is unbounded (with the solution being specified at infinity), so a numerical approach that arranges sources and (optionally) normal dipoles along the body surface can be considered to solve the hydrodynamic problem. Two different representations can be considered, following Lamb (1932): the potential or the source formulation. In the first one, Green's theorem is used, and the source strength is set equal to normal velocity, leaving the dipole moment, which is equal to the potential, unknown. On the other hand, the source formulation relies solely on source terms with unknown strength to describe the potential. In both cases, similar Fredholm integral equations can be solved.

The pioneer work of Hess and Smith (1964) is mentioned by Newman, in which the source formulation was used for three-dimensional bodies of arbitrary shape. For the first time, a linear system of n algebraic equations was derived by establishing boundary conditions at a collocation point on each of the n panels that were used to describe the fluid domain.

Hess and Smith (1964) also derived the analytical expressions for the potential and velocity induced by a unit density source distribution on a flat quadrilateral panel, avoiding numerical integration that could lead to erroneous results when the calculation point is in the vicinity (or on) the panel.

To conclude his keynote paper, Newman (1992) also points out the basic differences between the source and the potential formulation. It is mentioned that the computational effort required for both approaches is roughly equivalent. The differences mainly involve:

1. issues linked with thin bodies, where normal dipoles prove to be more stable than sources;
2. the fluid velocity, that in the source formulation can be evaluated from the first derivatives of the Green function, whereas in the potential formulation the second derivatives are necessary. Nevertheless the latter is not robust when using flat panels to discretise a curved surface, given that the velocity field induced by the dipoles changes quickly over distances similar to the panel dimensions;
3. ‘irregular frequencies’, which are related to flawed solutions in problems involving bodies that pierce the free surface. It is a common problem of both approaches but more likely to appear in the source formulation (Yeung, 1982).

When choosing a method to solve a specific problem there are two main versions that can be followed: a low-order method, where flat panels are used to discretise the geometry and the velocity potential, and a high-order method, which uses curved panels, allowing (in theory) a more accurate description of the problem. The high-order method has inherent advantages and disadvantages when compared with the low-order equivalent. Lee et al. (1996a) and Maniar (1995) showed the increase in computational efficiency, i.e., the method converges faster to the same solution when the number of panels is increased in both. The possibility of using different inputs for the geometry, like an explicit representation, also contributes to an increase in accuracy. Another significant advantage relies on the continuity of the pressure and velocity on the body surface, which is relevant for structural design. The main disadvantage is linked with the lack of robustness that the method yields, failing to converge in some cases. Such issues can be particularly severe when a field point is in the vicinity of a panel or near sharp corners.

The concerns associated with the computational burden have been progressively losing their initial importance as computers evolved. However such issues remain clear when developing a new code, particularly when studying complex problems. It is also clear that the pre-processing, linked with the calculation of the panel representation and relevant parameters, like areas and moments, and the solution of the linear system itself, are the steps which require the majority of the effort.

Newman and Lee (1992) performed a numerical sensitivity study on the influence that the discretisation has on the calculation of wave loads. The effects of the number of panels and their layout were investigated. Convergence tests were also performed. A classic case is the one described in Eatock Taylor and Jeffreys

(1985), where the hydrodynamic loads calculated are of ‘uncertain accuracy’. Recent hardware developments allow much more detailed studies.

Typically, increasing the number of panels used in the geometric and hydrodynamic representations will lead to an increase in accuracy. One important exercise that should never be neglected when developing a code is the numerical verification of the results, ensuring that the solution is not divergent or convergent to the wrong solution. Naturally validation, i.e., the comparison with physically derived results, is also a key factor. The computational time required to solve the problem also increases with the number of panels, so an optimal ratio between accuracy and the number of panels can be derived. Equally relevant is the panel layout, which can be solely responsible for invalid solutions.

A few basic qualitative guidelines are pointed out by Newman and Lee (1992). These can be summarised in the following way:

- i. near the free surface, short wavelengths demand a proportionately fine discretisation;
- ii. local singularities, induced by (e.g.) sharp corners, tend to require fine local discretisation;
- iii. discontinuities on the characteristic dimension of the panels should be avoided; ideally a cosine spreading (also referred to as spacing) function should be used for the panel layout (width of the panels is proportional to the cosine of equally-spaced increments along a circular arc);
- iv. problems involving complex geometries can require a high number of panels even for simple calculations (e.g.: volume).

Convergence tests are usually the answer to select the optimal discretisation. For representative wavelengths and for the same mesh layout, the number of panels is increased and the output evaluated. For a high enough value, the increase in the number of panels will not lead to a significant change in the solution. The authors mention the word ‘error’ when comparing different numerical solutions, which according to many references is fundamentally wrong (Roache, 1998; Eça and Hoekstra, 2000). Recently several authors have conducted studies in this area using numerical results from different concepts (e.g.: Cruz and Payne, 2006; Sykes et al., 2007).

Newman and Lee (1992) also mention that when using the low-order method (flat quadrilateral panels), a numerical ‘error’ of 0.1% to 10% can be expected, emphasising the need to validate all the results. The authors are directly associated with the development of a BEM code named WAMIT, at the Department of Ocean Engineering of the Massachusetts Institute of Technology (MIT). This code was initially verified through comparison with analytical solutions. Validation exercises were also conducted using experimental results. Together with these procedures, benchmarking with similar codes also has an important role to ensure that a code does not converge to the wrong answer. Examples of topics studied by this research group include wave loads on offshore platforms, time-domain ship motions, ship interactions in a channel, wave energy conversion and, on a more theoretical level (with implications to all fields), the development of a panel method based on B-splines. This high-order approach is justified by some fundamental differences, namely the possibility of describing more accurately the geometry and the velocity potential. Recent developments are presented in Newman and Lee (2002).

Other research groups have been actively involved in BEM code development. A particular strong one with regard to the study of wave energy conversion can be found at the École Centrale de Nantes (Laboratory of Fluid Mechanics). A complete suite of packages for several seakeeping problems has been under development since 1976 at ECN, resulting in:

1. AQUADYN, for general problems without forward speed;
2. AQUAPLUS, which assumes an encounter frequency for a moving vessel;
3. CUVE, which solves the problem of a vessel with internal tanks.

AQUADYN is a BEM code very similar to WAMIT, in particular to its low-order panel method solver. Several examples of the use of AQUADYN can be found in the literature (e.g.: Brito-Melo et al., 1998). Details about specific studies related to wave energy conversion involving AQUADYN and WAMIT, two of the most prominent BEM codes used in the field, are given in Section 3.2.2.

3.2.2 Applications of BEM to WEC Modelling

It is fair to say that Salter's early work regarding wave energy absorption by different shapes, published in a wide audience journal like Nature (Salter, 1974), led to similar studies in research groups spread worldwide. The first numerical simulations soon followed. A first attempt to numerically reproduce Salter's experiments was made by Katory (1976), in which inconsistent results were obtained (e.g.: the derived added mass matrix was not symmetric). Mynett et al. (1979) presented the first comprehensive numerical study with regard to cam shaped wave energy converters, following the experimental work performed by Salter on such shapes and the theoretical work of Mei (1976) and Evans (1976), where the principles of basic power take-off systems were described and characterised using linear wave theory. A modified hybrid element method, originally derived by Bai and Yeung (1976), was used. The forces, motions and the efficiency of the device were assessed (note that efficiency should be understood as the hydrodynamic efficiency, the 2-D equivalent of relative capture width). The simulations were validated by direct comparison with the available experimental results, allowing the confirmation of the high efficiency of the cam shape in a broad band of wave frequencies. An interesting sensitivity study was also conducted, evaluating the impact of the change of shape, submergence ratio, water depth and the inclusion of a non-rigid support structure.

Some key findings can be identified in Figures 3.1 and 3.2, which illustrate the relative influence of such parameters for constant water depth by plotting the efficiency (ε) as function of the non-dimensional frequency (numerical predictions). Figure 3.1, where the optimal efficiency (ε_{opt}) is compared for selected configurations, shows the predominant influence of the submergence depth (s) with regard to other parameters like the angle θ , which partially defines the shape. Note that when $\theta = \pi/2$ and $s = 0$ the theoretical limit for a semi-circle is reached, so $\varepsilon_{opt} = 0.5$ for all frequencies. It is equally interesting to witness the predominant influence of s when compared to θ . For both $s = a$ and $s = a/2$ there is little difference between the results for $\theta = \pi/2$ and $\theta = \pi/4$. This apparent independence between the

hydrodynamic efficiency and the inclination of the beak in the cam shape motivates the numerical work (investigation of the change of shape of the Duck) conducted recently at the University of Edinburgh (e.g. Cruz, 2009).

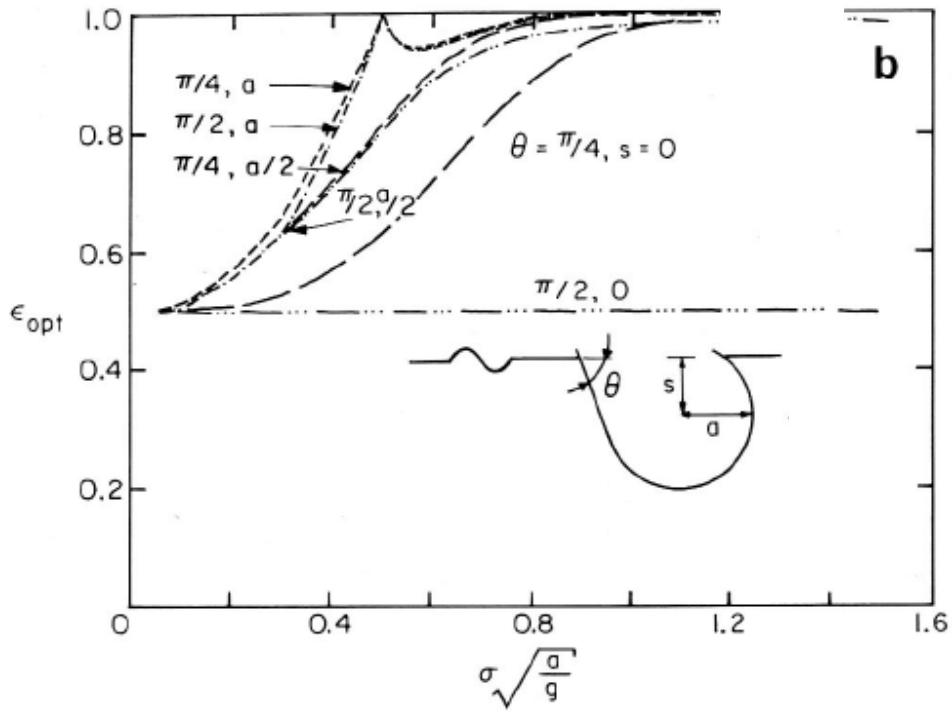


Figure 3.1: ϵ_{opt} non-dimensional frequency for different configurations (Mynett et al., 1979)

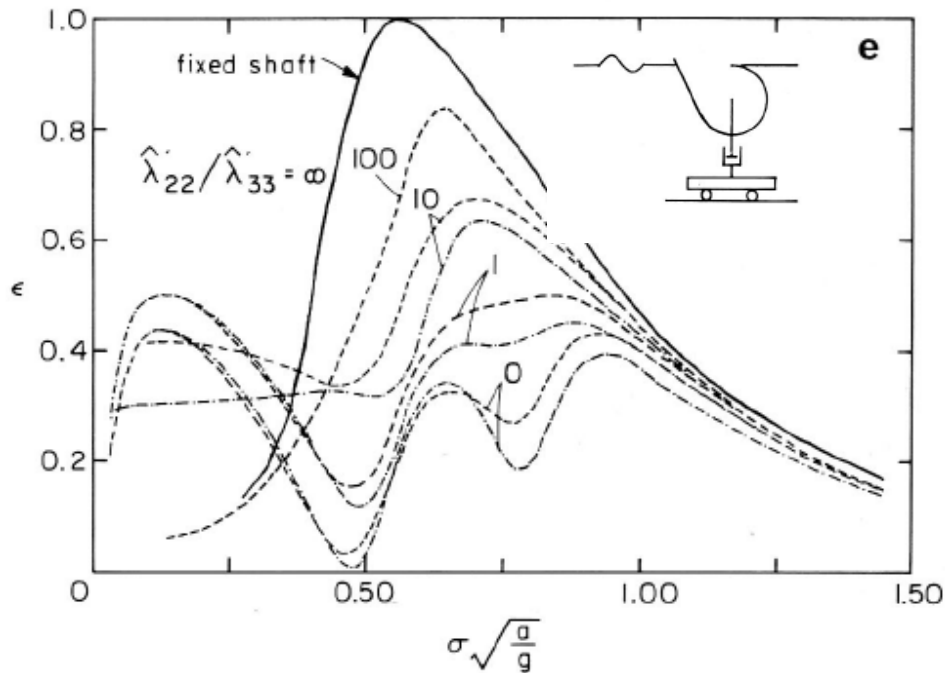


Figure 3.2: ε_{opt} non-dimensional frequency for different non-rigid supports (Mynett et al., 1979)

Figure 3.2 shows a similar plot, now comparing the effect of the external damping ratio $(\hat{\lambda}_{22}' / \hat{\lambda}_{33}')$, where the index '2' denotes heave and '3' pitch. The two curves per damping ratio correspond to two different values of the external carriage mass (which holds the support system). It is clear that as the ratio decreases so does the efficiency.

Mynett et al. (1979) therefore corresponds to the first numerical study concerning cam (or Duck) shapes. In Standing (1980) numerical comparisons regarding the response amplitude operator in pitch and the capture width for a Duck string were evaluated by means of a BEM code named NMIWAVE, from the National Maritime Institute, in a direct follow up of Mynett et al. (1979). Most of the subsequent work at the University of Edinburgh was experimental, with different models at different scales being tested in narrow and wide wave tanks. Pizer (1992, 1993, 1994) applied a pure BEM approach to the duck geometry as did Cruz (2009) using WAMIT.

The use of pure BEM codes to study wave energy converters (WECs) was at first also linked with the study of Oscillating Water Column (OWC) plants. Brito-Melo et al. (1998, 2000a) modified the AQUADYN code originally developed at ECN (Nantes), producing a specific version dedicated to OWCs (AQUADYN-OWC). The major modification was associated with the supplementary radiation problem imposed by the oscillatory movement of the water in the inner chamber, which was solved by modifying the boundary condition through the pressure distribution. The study, conducted in the scope of the development of the Pico plant, showed an increasing level of depth: the initial configuration assumed an isolated structure

surrounded by an infinite fluid domain (Figure 3.3, left), whilst the final geometry included the neighbouring coastline and bathymetry (Figure 3.3, right). Comparisons were made with a 1:35 scale model, validating the numerical results.

WAMIT has also been used, in its low-order option, to model OWCs. Lee et al. (1996b) studied three different configurations: a moon pool in infinite water depth, a bottom-mounted OWC and an OWC with extended walls (in the direction of wave propagation). Two approaches were conducted to incorporate the inner free-surface effects. Firstly, the source code was modified to take into account a new dynamic boundary condition. Secondly, a virtual surface was fitted to the inner free-surface, with predetermined velocity distributions ruling the movement. The study lacks experimental validation but a partial verification exercise was performed, comparing the outputs of both approaches, which were found to be closely correlated. Several numerical problems were identified, like the difficulty in implementing the principles associated with resonance in a linear code, and the influence of thin walls, which can lead to inaccuracies when representing the linear system of equations. Numerical sensitivity exercises were also conducted by evaluating different discretisations of the geometry and by comparing the derived values for the exciting force from direct pressure integration and from the Haskind relation.

Delauré and Lewis (2003) applied WAMIT in the modelling of an OWC, following a similar approach to the second one employed by Lee et al. (1996b), where generalised modes of motion were used to model the inner free-surface. The article follows up on a series of contributions from the same authors, where a review of similar applications, parametric studies and benchmarking with experimental results were presented (Delauré and Lewis, 2000a; 2000b; 2001). The agreement between numerical and experimental results was shown to be particularly good for small amplitude waves and for an ‘open chamber’ configuration (no external damping). One of the results confirms Newman’s earlier work (Newman, 1992), by pointing out the differences between the results from the potential and the source formulation, with the latter being judged less suitable for problems involving thin wall structures such as OWC plants.

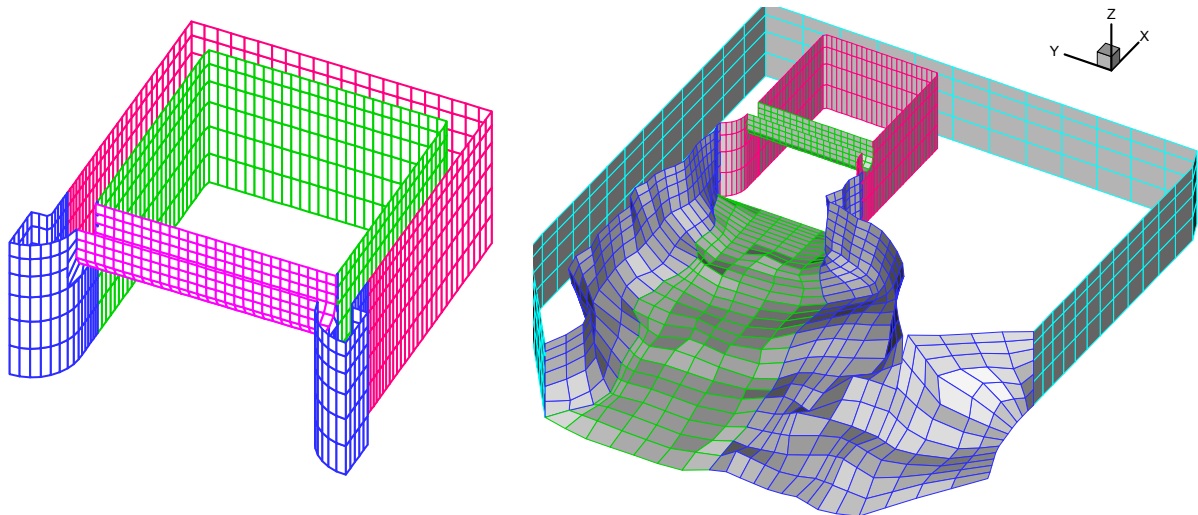


Figure 3.3: Left- Initial OWC configuration studied (Brito Melo et al., 1998);

Right - final OWC configuration studied (Brito Melo et al., 2000a)

At the Wave Power Group of the University of Edinburgh, Pizer (1994) used a custom made BEM code, previously developed at the University of Strathclyde during the author's PhD studies, to compare numerical with experimental results from a solo duck. In the process of verifying the code, selected analytical results, such as a floating hemisphere, were also used. More recently within the same research group, Payne (2006) used WAMIT to perform the hydrodynamic modelling of a sloped IPS buoy, comparing the results with those from two experimental models: a one degree-of-freedom model (Figure 3.4, left) and a freely floating model (Figure 3.4, right). The one degree-of-freedom version was developed by Lin (1999). WAMIT results, particularly in terms of the body motions, showed a shift in the frequency with regard to the experimental equivalents, a tendency that was linked with the influence of the discretisation of the inertia matrix. A numerical sensitivity study to quantify the influence of the radii of gyration was conducted to confirm that effect. The complexity of the model, namely the dynamometer that acts as the power take-off system can also be indicated as partially responsible for such discrepancies. Such a tendency was also clear in Pizer (1994). An initial review of the application of BEM codes to wave energy research, both in theoretical studies and when comparing numerical and experimental results, is also available in Payne (2006).

To conclude, and to emphasise the importance of BEM modelling in the staged development of a WEC, two examples which have reached the full-scale concept stage are given. Firstly, the Archimedes Wave Swing (AWS), for which the first numerical calculations were performed by Pinkster (1997), who derived the hydrodynamic coefficients for selected geometries. The AQUADYN code was also extensively applied to the AWS, allowing the recalculation of the hydrodynamic coefficients and also the exciting force for a wide range of configurations (e.g. Prado et al., 2005). Modifications to the AQUADYN code to estimate the wave profile directly above the full-scale pilot plant, which was installed in late 2004 offshore Póvoa de Varzim in Northern Portugal, were also made (Cruz and Sarmiento, 2007). Figure 3.5 shows one of the early numerical discretisations of the AWS pilot plant.

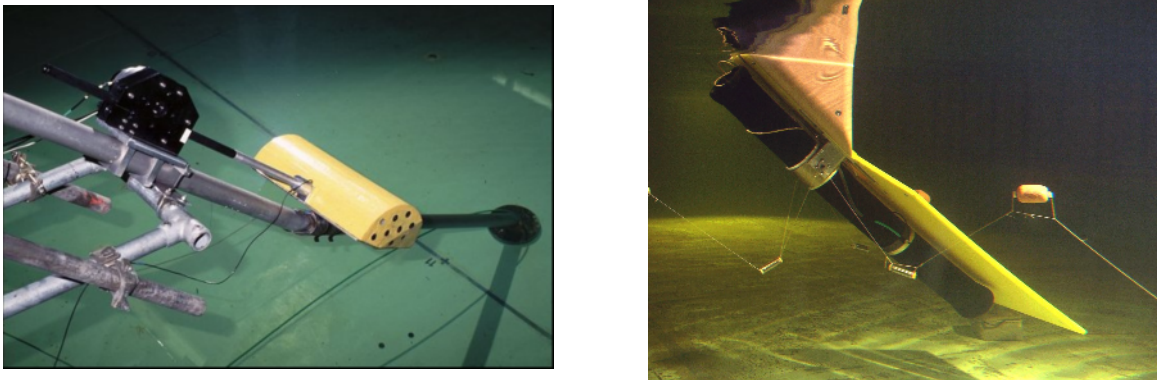


Figure 3.4: Left - One degree-of-freedom experimental model of the sloped IPS buoy (Lin, 1999);

Right - Freely-floating model of the sloped IPS buoy (Payne, 2006)

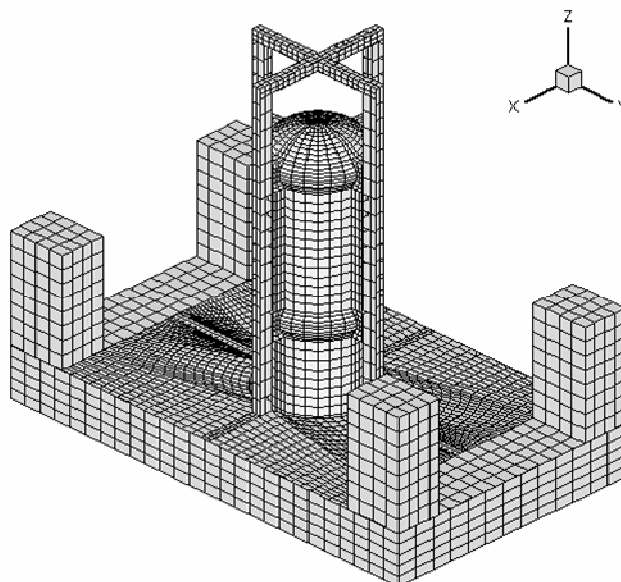


Figure 3.5: AQUADYN's discretisation of the AWS geometry (Alves, 2002)

In a similar way, and also from an early stage, the Pelamis wave energy converter (WEC) has been developed using a variety of computer codes of different scope and complexity. In the basis of all the developed tools is the computation of the hydrodynamic coefficients, exciting force and motions in several degrees-of-freedom using a linear BEM code named 'Pel_freq'. A detailed description of the complete software suite can be found in Retzler et al. (2003), where validation exercises are described at several scales, though initial comparison with results from a 1:35 scale model were presented in Yemm et al. (1998). An updated version of the 2003 article was given in Pizer et al. (2005). It is emphasised that the outputs of the frequency-domain code are extensively used as inputs in the time-domain simulation also developed by Ocean Power Delivery (linear and nonlinear), and in interfaces with other numerical tools for selected problems (e.g.: mooring load analysis).

3.2.3 A Linear Hydrodynamic Model

The theoretical basis for the frequency-domain GH WaveFarmer hydrodynamic modelling is described below. The intention is to describe the manner in which the hydrodynamic forces experienced by the WEC, which is essentially modelled as a number of connected bodies responding to incident wave action, are compiled to form the core software simulation tasks of evaluating the frequency response and solving the complete time-domain equation of motion.

The analysis is completed initially for the case of a single body design oscillating in one degree of freedom, but the approach may be subsequently expanded to produce a matrix formulation describing a much more complex system.

Neglecting losses, the equation of motion of the body of mass m_m , oscillating in the degree of freedom, x under wave action is given by:

$$m_m \ddot{x} = f_f + f_{ext} \quad [3.1]$$

where f_f represents the total wave and fluid force and f_{ext} the total external force created by the moorings and power take-off (including controller action) .

If the amplitude of the wave and body motions is sufficiently small for linear wave theory to be assumed then the fluid force term, f_f may be decomposed as follows (e.g. Thomas in Cruz, 2008; Falcão, 2007):

$$f_f = f_{hs} + f_e + f_r \quad [3.2]$$

where f_{hs} is the hydrostatic spring force on the buoy, f_e is the wave exciting force that would be experienced by the body if it were to be held in a fixed position, and f_r is the radiation force applied to generate unit amplitude waves in an otherwise undisturbed environment.

A single frequency, sinusoidal wave input creates a time-domain variation in excitation force that can be expressed as:

$$f_e = \Re(F_e e^{j\omega t}) \quad [3.3]$$

where F_e is a complex force composed of incident and diffracted wave components, F_{inc} and F_{diff} respectively:

$$F_e = F_{inc} + F_{diff} \quad [3.4]$$

F_{inc} can be calculated directly from the pressure distribution due to the incident waves over the body surface area, however it is much more difficult to determine F_{diff} directly, for an arbitrary geometry, without the use of specialist hydrodynamics codes, the subject of the review in Section 3.4. The incident wave component alone is typically much larger than the diffracted wave component for slender bodies, and in such cases it is often referred to as the ‘Froude-Krylov’ force (Falnes, 2002).

Continuing with the linear wave model, the radiation force complex amplitude at frequency ω , $F_r(\omega)$ is a function of the body motion x which, assuming an oscillatory response, can take the form: $x = \Re(X(\omega)e^{j\omega t})$ so that:

$$F_r(\omega) = -G(\omega)X(\omega) = -(-\omega^2 m_r(\omega) + j\omega B_r(\omega))X(\omega) \quad [3.5]$$

where the transfer function $G(\omega)$ incorporates components in phase with the body's acceleration and velocity. In the time-domain this becomes:

$$f_r = \Re(F_r e^{j\omega t}) = -m_r(\omega)\ddot{x} - B_r(\omega)\dot{x} \quad [3.6]$$

The coefficients $m_r(\omega)$ and $B_r(\omega)$ are referred to as the 'added mass' and 'added damping' respectively and are frequency dependant parameters that are most conveniently determined either experimentally, or using a specialist hydrodynamics code, for all but the simplest body geometries.

Combining Equations (3.1), (3.2), (3.3) and (3.6) with an appropriate linear hydrostatic force term, $f_{hs} = -K_{hs}x$ produces the following equation of motion:

$$(m_m + m_r)\ddot{x} + B_r(\dot{x}) + K_{hs}x = \Re(F_e e^{j\omega t}) + f_{ext} \quad [3.7]$$

If the external force is modelled simply as a linear system, providing a reaction force with complex amplitude $F_{ext}(\omega)$, then assuming the system has an oscillatory response, $x = \Re(Xe^{j\omega t})$, a frequency dependant expression for the body displacement can be derived from Equation (3.7) as:

$$X = \frac{F_e + F_{ext}}{-\omega^2(m_m + m_r) + j\omega B_r + K_{hs}} \quad [3.8]$$

Equation (3.8) applies strictly to linear, monochromatic waves of frequency ω , however extension to approximate the body motion in irregular waves is possible through superposition of results for a range of frequencies and phases.

The direct way in which the device response can be calculated makes the linear, frequency domain modelling outlined above well suited to rapid design iteration at the concept stage. A formulation of this nature is the basis of the Frequency Domain Core simulation code.

3.3 Time-Domain WEC Hydrodynamics

In reality a WEC design is unlikely to be completely linear in nature. A typical PTO arrangement is often comprised of both rectification and smoothing elements designed to operate in conjunction with the control system to supply the generator with a reliable, steady energy input, whilst also influencing the device hydrodynamic response in such a way as to maximise the absorption of energy from the waves themselves. The nonlinear effects of PTO components such as accumulators or nonlinear damping elements are felt by the bodies interacting with the waves. The mooring forces acting on the WEC may also be discontinuous or nonlinear, either as a direct result of their mechanical properties, or indirectly due to their physical configuration. If the aim is to accurately review the performance of a detailed WEC model incorporating a realistic PTO, control system and moorings design then at least partially nonlinear modelling in the time-domain becomes a requirement. What follows is a brief introduction to the time-domain simulation task, the aim being to provide a review of the relevant theory, particularly from a hydrodynamics perspective, and also to illustrate the interacting technical requirements for effective numerical implementation. The

approach taken is similar to that described by previous time-domain modelling studies, including initial work by Count and Jefferys (1980) and more recently Duclos et. al (2001), Falnes (2002), Kristiansen and Egeland (2003), McCabe (2005), Thomas (1981, 2008) and Falcão (2007, 2008) amongst many others. The time-domain hydrodynamics approach is closely linked to the frequency domain formulation described above and care has been taken to outline the most critical implementation steps in the formation of time-domain force expressions from the BEM solver outputs.

The assumption remains that for device performance orientated calculations, the fluid force can be linearly decomposed as described by Equation (3.2). In reality, the most vigorous sea states may produce additional nonlinear wave effects that are likely to be more relevant from a survivability perspective. The point at which a fully nonlinear wave model becomes necessary should be better quantified by a comparison between linear wave models and the fully nonlinear wave hydrodynamics simulations to be undertaken by the UoOx as part of the PerAWaT programme.

3.3.1 The Time-Domain Equation of Motion

By adopting the wave force decomposition described by Equation (3.2), it is possible to evaluate the time-domain wave hydrostatic, excitation and radiation forces individually. The simplest of these to determine is the hydrostatic component, which remains as a linear spring term if a constant water plane cross-sectional area is assumed for the floating body, but may alternatively take a nonlinear form corresponding to the geometry variations experienced at greater displacements.

The excitation force component can adopt the linear form described by Equation (3.4), with the variation in complex force amplitude with wave frequency, $F_e(\omega)$ being an output of most standard hydrodynamics packages (see section 3.4). The time-domain force expression can then be obtained from Equation (3.3), written as the superposition of the force contributions from each of the wave frequencies in the incident wave train (which is compiled as the linear superposition of n sinusoidal, regular wave components, each assigned with a random phase shift, ϕ):

$$f_e = \sum_n f_{e,n} = \sum_n \Re \left(F_{e,n} e^{j(\omega t + \phi_n)} \right) \quad [3.9]$$

Some of the more advanced packages also calculate a nonlinear Froude-Krylov force term; the inclusion of such a component in the time-domain equation of motion may form the subject of a further study later in the PerAWAT project. This would constitute a quasi-linear approach, the output of which would also be compared with the UoOx results.

The radiation force component is directly dependant on the system response, making the task of developing a suitable time-domain expression much more complex.

Consider again the frequency variation for the radiation force amplitude given by Equation (3.5):

$$F_r(\omega) = -G(\omega)X(\omega)$$

The transfer function $G(\omega)$ may be easily replaced with a form that allows the force amplitude to be expressed in terms of the body's velocity rather than displacement (a conversion that is useful later in the analysis to allow a mechanical impedance-based analogy to be drawn):

$$F_r(\omega) = -H(\omega)U(\omega) \quad [3.10]$$

Following the approach of Falnes (2002), if the system is causal (no radiation force acts on the body until the body itself is in motion), then $H(\omega)$ is the Fourier transform of the system response function, $h(t)$:

$$H(\omega) = \int_0^{\infty} h(t) e^{-j\omega t} dt \quad [3.11]$$

which can be expanded to the mechanical impedance form:

$$\begin{aligned} H(\omega) &= \int_0^{\infty} h(t) (\cos(\omega t) - j \sin(\omega t)) dt \\ &= B_r(\omega) + jE_r(\omega) \end{aligned} \quad [3.12]$$

where $B_r(\omega)$ is the radiation 'resistance' or damping and $E_r(\omega)$ is the 'radiation reactance'. The reactance term is more commonly written in terms of the 'added mass', $m_r(\omega)$ where:

$$\omega m_r(\omega) = E_r(\omega) \quad [3.13]$$

So that:

$$H(\omega) = B_r(\omega) + j\omega m_r(\omega) \quad [3.14]$$

For most bodies, the radiation damping, $B_r(\omega)$ tends to 0 as ω tends to ∞ (Kristiansen and Egeland, 2003). This is not the case for the added mass term, which tends to a finite value, $m_r(\infty)$. Falnes (2002) notes that it is useful to isolate this behaviour through consideration of an alternative, related transfer function, $D(\omega)$, which takes a similar form to $H(\omega)$:

$$D(\omega) = \frac{B_r(\omega)}{j\omega} + m_r(\omega) - m_r(\infty) \quad [3.15]$$

It is assumed that $B_r(\omega)$ decays sufficiently fast as $\omega \rightarrow 0$ to make $D(\omega)$ non-singular at $\omega = 0$.

Equivalent forms of Equation (3.10) can now be written as:

$$\begin{aligned}
F_r(\omega) &= -H(\omega)U(\omega) \\
&= -j\omega D(\omega)U(\omega) - j\omega m_r(\infty) \\
&= F_r'(\omega) - j\omega m_r(\infty)
\end{aligned} \tag{3.16}$$

$$\text{where: } F_r'(\omega) = -j\omega D(\omega)U(\omega) = -K(\omega)U(\omega) \tag{3.17}$$

$K(\omega)$ is another new transfer function, which can be expanded using Equations (3.14), (3.15) and (3.17):

$$\begin{aligned}
K(\omega) &= j\omega D(\omega) = H(\omega) - j\omega m_r(\infty) \\
&= B_r(\omega) + j\omega(m_r(\omega) - m_r(\infty))
\end{aligned} \tag{3.18}$$

The time-domain variation in the radiation force can now be found from the inverse Fourier transforms of Equations (3.16) and (3.17) :

$$f_r(t) = f_r'(t) - m_r(\infty)\dot{u}(t) = f_r'(t) - m_r(\infty)\ddot{x}(t) \tag{3.19}$$

$$f_r'(t) = -d(t) * \dot{u}(t) = -k(t) * u(t) \tag{3.20}$$

where $k(t)$ is defined by the inverse transform: $k(t) = \frac{1}{2\pi} \int_{-\infty}^{\infty} K(\omega) e^{j\omega t} d\omega$

Finally, substituting Equations (3.19) and (3.20) into the Equations (3.2) and (3.1) yields the, Cummins, (1962) form of the complete time-domain equation of motion:

$$(m_m + m_r(\infty))\ddot{x} + f_{hs}(x) + \int_{-\infty}^t k(t-\tau) \dot{x}(\tau) d\tau = f_e(t) + f_{ext}(x, \dot{x}, \dots, t) \tag{3.21}$$

It is also common for the above expression to take the alternative form developed by (Wehausen, 1971):

$$(m_m + m_r(\infty))\ddot{x} + f_{hs}(x) + \int_{-\infty}^t l(t-\tau) \dot{x}(\tau) d\tau = f_e(t) + f_{ext}(x, \dot{x}, \dots, t) \tag{3.22}$$

Where the two convolution transfer functions are related by: $k(t) = \frac{d}{dt}l(t)$. Both $k(t)$ and $l(t)$ are ‘impulse response functions’ and are also referred to as ‘*memory functions*’ due to their significance in representing the state of the fluid as a result of recent buoy motion when incorporated into the convolution. Jefferys (in Count, 1980) notes that the velocity formulation of Equation (3.21) is the more convenient

because the body velocity is stored as one of the system states during computation, whereas additional calculation is required to obtain an acceleration value.

For stationary structures (zero forward speed) radiation impulse response functions depends exclusively on the geometry of the body. Similar relationships can be derived for the exciting force and the response amplitude operators ('RAO's – which map the incident wave amplitude directly to the body motion). The former will be strongly conditioned by the wave input (see below), while the latter, although relevant for some examples in the offshore industry (e.g. Floating Production Storage and Offloading vessels - FPSOs), does not apply when $f_{ext} \neq 0$, which is always the case if either power is being extracted from the fluid or if the device is not freely floating

3.3.2 System Causality and Calculation of the Impulse Response Function

Values of $m_r(\omega)$, $m_r(\infty)$, $B(\omega)$ and the diffraction force are functions of the body geometry and can be calculated by one of the commercial hydrodynamics packages reviewed in section 3.4. Some packages also calculate the form of the response functions, $k(t)$, however it is worth noting that the information stored in $m_r(\omega)$ and $B(\omega)$ is in fact also stored in $m_r(\infty)$ and $k(t)$ as a result of the causality of the system. Moreover, it is possible to convert between the two, so that either or both forms may be obtained from the BEM solver. Once again, the following is compiled from (Falnes 2002).

Consider an arbitrary, causal impulse response function, $c(t)$ that is similar to $k(t)$. The causality of $c(t)$ dictates that $c(t) = 0$ for all negative t but has a finite value for all positive t . As such, $c(t)$ is neither an even nor an odd function, but can nevertheless be decomposed into appropriately constrained even and odd components, $c_e(t)$ and $c_o(t)$ respectively:

$$c(t) = c_e(t) + c_o(t) \quad [3.23]$$

It is necessary that $|c_e(t)| = |c_o(t)|$ for all t (for $c(t)$ to be 0 for $t < 0$), so:

$$c(t) = 2c_e(t) = 2c_o(t) \text{ for } t > 0 \quad [3.24]$$

The inverse Fourier transform that relates $c(t)$ to its frequency-domain counterpart is:

$$c(t) = \frac{1}{2\pi} \int_{-\infty}^{\infty} C(\omega) e^{j\omega t} d\omega \quad [3.25]$$

If $C(\omega)$ is expanded to the complex form: $C(\omega) = B(\omega) + jE(\omega)$, where the real and imaginary terms could be a resistance and reactance respectively, then Equation (3.25) becomes:

$$\begin{aligned}
c(t) &= \frac{1}{2\pi} \int_{-\infty}^{\infty} [B(\omega) + jE(\omega)] [\cos(\omega t) + j \sin(\omega t)] d\omega \\
&= \frac{1}{2\pi} \int_{-\infty}^{\infty} [B(\omega)\cos(\omega t) - E(\omega)\sin(\omega t)] d\omega \\
&\quad + \frac{j}{2\pi} \int_{-\infty}^{\infty} [B(\omega)\sin(\omega t) + E(\omega)\cos(\omega t)] d\omega
\end{aligned} \tag{3.26}$$

If an impulse response function is real as a function of time, then its Fourier transform obeys: $C(\omega) = C^*(-\omega)$, which in turn leads to $B(\omega) = B(-\omega)$ (even function of ω) and $E(\omega) = -E(-\omega)$ (odd function of ω). This allows the products $B(\omega)\cos(\omega t)$ and $E(\omega)\sin(\omega t)$ to be identified as even, yielding a finite value once the integration in Equation (3.26) is completed. In contrast, the odd products, $B(\omega)\sin(\omega t)$ and $E(\omega)\cos(\omega t)$, cause the imaginary term to vanish. Equation (3.26) can now be written in a form that is comparable to Equation (3.23):

$$c(t) = \frac{1}{\pi} \int_0^{\infty} B(\omega)\cos(\omega t) d\omega - \frac{1}{\pi} \int_0^{\infty} E(\omega)\sin(\omega t) d\omega \tag{3.27}$$

or $c(t) = c_e(t) + c_o(t)$, where:

$$c_e(t) = \frac{1}{\pi} \int_0^{\infty} B(\omega)\cos(\omega t) d\omega \quad \text{and} \quad c_o(t) = -\frac{1}{\pi} \int_0^{\infty} E(\omega)\sin(\omega t) d\omega \tag{3.28}$$

Note that $E(\omega)\sin(\omega t)$ is an even function of ω but an odd function of t . Substituting Equations (3.18) into (3.24) yields the result:

$$c(t) = \frac{2}{\pi} \int_0^{\infty} B(\omega)\cos(\omega t) d\omega = \frac{2}{\pi} \int_0^{\infty} X(\omega)\sin(\omega t) d\omega \tag{3.29}$$

Applying Equation (3.29) to the case of the impulse response function $k(t)$ in Section 3.3.1, which has a resistance $B(\omega) = B_r(\omega)$ and a reactance $X(\omega) = \omega(m_r(\omega) - m_r(\infty))$ (see Equation 3.18), produces the useful expression:

$$\begin{aligned}
k(t) &= \frac{2}{\pi} \int_0^{\infty} B_r(\omega) \cos(\omega t) d\omega \\
&= -\frac{2}{\pi} \int_0^{\infty} (\omega(m_r(\omega) - m_r(\infty))) \sin(\omega t) d\omega
\end{aligned} \tag{3.30}$$

which allows $k(t)$ to be explicitly calculated from just one of a body's hydrodynamic coefficients, $B_r(\omega)$ or $m_r(\omega)$.

The role of $B_r(\omega)$ and $m_r(\omega) - m_r(\infty)$ as the resistive and reactive components of a causal impulse response function has the additional advantage that one hydrodynamic coefficient can be calculated from the other using the Kramers-Kronig relations, further limiting the required BEM solver output:

$$\begin{aligned}
m_r(\omega) - m_r(\infty) &= \frac{2}{\pi} \int_0^{\infty} \frac{-B_r(y)}{\omega^2 - y^2} dy \\
B_r(\infty) &= \frac{2\omega^2}{\pi} \int_0^{\infty} \frac{m_r(\omega) - m_r(\infty)}{\omega^2 - y^2} dy
\end{aligned} \tag{3.31}$$

3.3.3 Numerical Solution form of the Time-Domain Equation of Motion

Equation (3.21) can be solved directly, with the convolution term being re-evaluated at each time-step. Values of k and \dot{x} must be stored as a discrete time series, but the fact that $k(0) = 0$ is useful in reducing the integro-differential form to a second order ordinary differential equation, which can be solved as an 'initial value problem'.

Defining the state vector:

$$\underline{z} = \begin{bmatrix} z_1 \\ z_2 \end{bmatrix} = \begin{bmatrix} x \\ \dot{x} \end{bmatrix} \tag{3.32}$$

produces the formulation:

$$(m_m + m_r(\infty))\ddot{z}_2 + K_{hs} z_1 + \int_{-\infty}^t k(t - \tau) \dot{z}_2(\tau) d\tau = f_e(t) + f_{ext}(z_1, z_2, \dots, t) \tag{3.33}$$

which can be rearranged to give:

$$\dot{\underline{z}} = \begin{bmatrix} \dot{z}_1 \\ \dot{z}_2 \end{bmatrix} = \begin{bmatrix} z_2 \\ \frac{f_e(t) + f_{ext}(z_1, z_2, \dots, t) - K_{hs} z_1 - \int_{-\infty}^t k(-\tau) \dot{z}_2(\tau) d\tau}{(m_m + m_r(\infty))} \end{bmatrix} \quad [3.34]$$

Although the analysis here is restricted to a single degree of freedom only, Equation (3.33) can be expanded in vector form to incorporate multiple degrees of freedom for multiple bodies. Further details on the numerical formulation to account for the modular external force contributions can be found in Section 3.7.

In reality, it is frequently the case that k decays rapidly with time and only the most recent time history of velocity (or acceleration) terms needs to be stored to obtain an accurate numerical approximation to the convolution integral. Nevertheless, the evaluation of the convolution term has some additional complications:

- Numerical evaluation of the convolution is most easily completed if the equation of motion is solved with a fixed time-step solver. For a variable time-step solver to be used, the time-step sizes corresponding to the velocity time history must also be stored. Each time-step size will then have to be accounted for individually in the numerical evaluation process, a potentially complex operation. The type of solver selected is dependant on a number of factors however, such as the supply of external force information (see section 3.7) and the numerical ‘stiffness’ of the WEC model being solved.
- Storage of even a limited history of velocity (or acceleration) values and evaluation of the convolution integral can be computationally expensive for a system of multiple bodies moving in multiple degrees of freedom. This is particularly the case if the solution is obtained using small time-steps.
- The presence of the convolution term in Equation (3.33) can be prohibitive in the application of standard state-space control theory techniques, which may be of use in a WEC’s control system design.

For these reasons, a number of attempts have been made to replace the convolution with a more directly computable, state-space alternative. A review of these alternative approaches is critical in determining the most effective solution method for the GH WaveFarmer simulation tool.

3.3.4 State-Space Representation of the Radiation Forces Convolution Integral

The radiation convolution in the time-domain equation of motion is effective as a method of representing the complete state of the system as a result of previous events. A close approximation to this effect can be achieved by replacing the convolution with a high order ordinary differential equation, or a state-space system in which many states are recorded; forms that explicitly describe the dynamics of the system and can much more readily be evaluated numerically. It is interesting to note however that the free vertical motion of an immersed floating body decays to zero with t^n rather than exponentially (Ursell, 1964) and so in this case it is only possible to approximate the real system using a finite order differential or state-space

form. Nevertheless, as Taghipour et al. (2008) note, the difference in most cases is of academic interest only and, once found, a high order ordinary differential or state-space form could be used to accurately represent the convolution component of the radiation force.

The process of determining an approximate state-space representation is referred to ‘system identification’ and is illustrated graphically in Figure 3.3. System identification studies with regard to WEC modelling have been completed by a number of authors; all have the common aim of optimising a vector of parameters that can be used to compile the state-space matrices, A' , B' , C' and D' , through some form of comparison with the exact system impulse response, k .

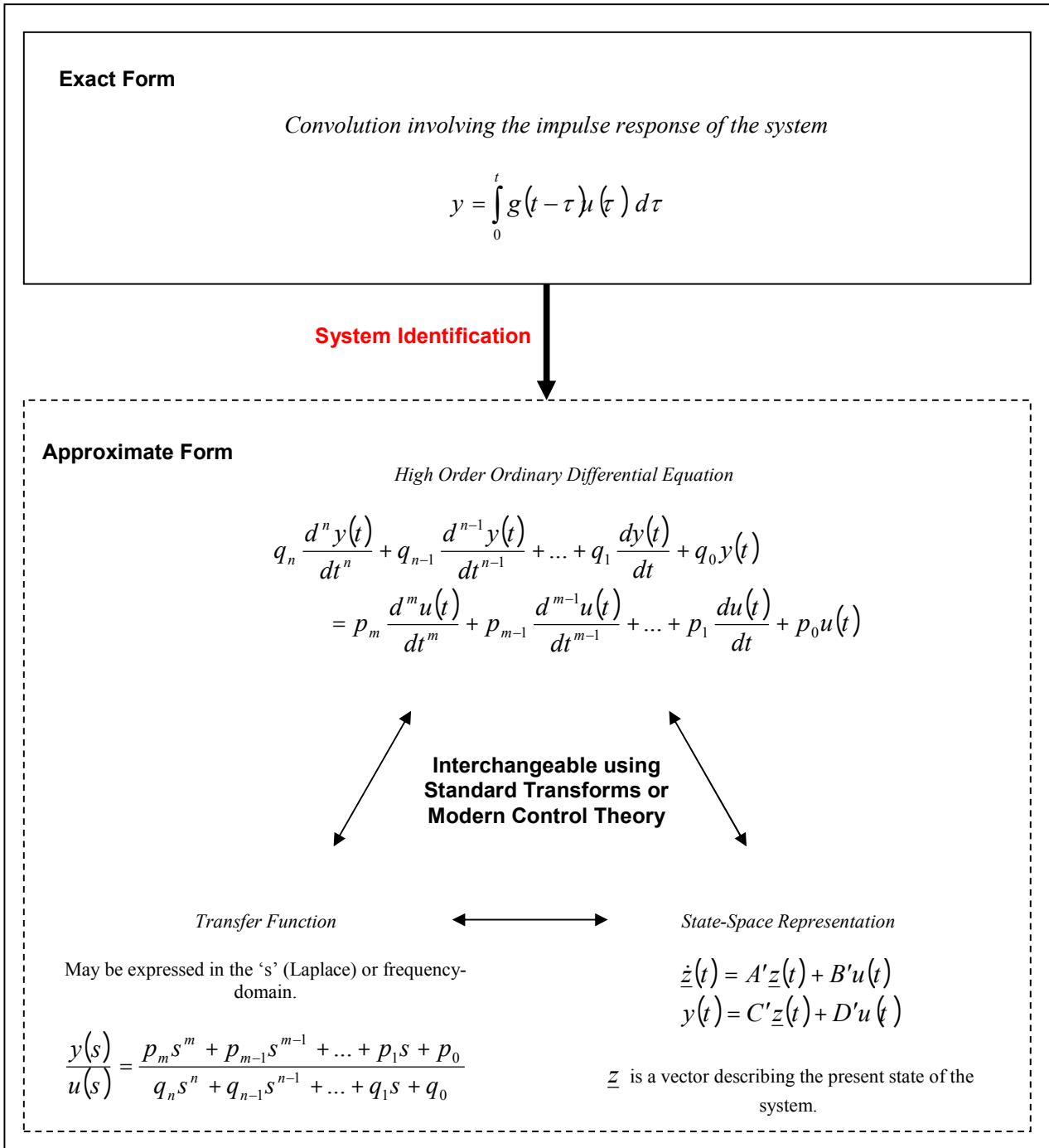


Figure 3.3: The role of system identification techniques in approximating a convolution integral

The system identification process generally follows one of the following four approaches; however there is significant variation in precisely which algorithms and fitting techniques are used for parameter optimisation.

1. Transfer function estimation in the frequency-domain. The impulse response function $K(j\omega)$ is expressed, typically in a complex form, as a combination of the hydrodynamic coefficients, B_r and m_r . A typical expression is Equation (3.18):

$$K(\omega) = B_r(\omega) + j\omega(m_r(\omega) - m_r(\infty))$$

If $K(\omega)$ maps the velocity to the convolution component of the radiation force, $F_r'(\omega)$, as described by Equation (3.17), then it is possible to write:

$$\frac{-F_r'(\omega)}{U(\omega)} = K(\omega) = B_r(\omega) + j\omega(m_r(\omega) - m_r(\infty)),$$

a form that suggests that $K(\omega)$ can be matched to a parameterised transfer function:

$$K(\omega) \approx \frac{N(\omega)}{D(\omega)} = \frac{p_m s^m + p_{m-1} s^{m-1} + \dots + p_1 s + p_0}{q_n s^n + q_{n-1} s^{n-1} + \dots + q_1 s + q_0} \quad [3.35]$$

The vector of unknown parameters, $\theta = [p_m, p_{m-1}, \dots, p_0, q_n, q_{n-1}, \dots, q_0]$ satisfy the expressions:

$$\begin{aligned} \Re\left(\frac{N(\omega)}{D(\omega)}\right) &= B_r(\omega) \\ I\left(\frac{N(\omega)}{D(\omega)}\right) &= \omega(m_r(\omega) - m_r(\infty)) \end{aligned} \quad [3.36]$$

which must be solved using a mathematical algorithm, such as a Gauss-Newton method, or an equivalent, potentially requiring some prior linearization, or the specification of weighting factors. Mathworks' MATLAB incorporates functions such as 'invfreqs.m' specifically designed to assist in the solution process. It should be noted that for impulse response functions, the transfer function $\frac{N(\omega)}{D(\omega)}$ can be specified as having a relative degree of 1.

The final stage of the process is to convert the transfer function to a time-domain state-space form using a technique such as 'direct', 'parallel' or 'series programming', all of which are a well-documented part of modern control theory.

A frequency-domain fitting approach has been adopted successfully in the past by McCabe et. al (2006) and Taghipour et al. (2008).

2. Time-domain fitting of the impulse response function, $k(t)$ to that of the proposed state-space form. The technique is based on the fact that a state-space system:

$$\begin{aligned}\dot{z}(t) &= A'z(t) + B'u(t) \\ y(t) &= C'z(t) + D'u(t)\end{aligned}\quad [3.37]$$

has a general response to an impulse, $u(t) = \delta(t)$:

$$h(t) = y(t) = C'(\theta)\exp(A'(\theta)t)B'(\theta) + D'(\theta)\delta(t)\quad [3.38]$$

The response, $h(t)$ produced by Equation (3.38) can be compared with $k(t)$, in order to determine the vector of parameters, θ ; which in this case are the elements of the state-space matrices, A' , B' , C' and D' . The optimum fitting task is nonlinear in the parameters θ and again requires a Gauss-Newton type algorithm (Taghipour et al. 2008). Alternatively, Kristiansen and Egeland (2003) note that the MATLAB function 'imp2ss.m' in the Robust Control Toolbox, which uses the Henkel Singular Value Decomposition method (Kung, 1978), is available to complete this task. It is worth noting that this function employs the inverse Tustin method to generate the final continuous time-domain state-space model from a discrete form, which generally ensures a stable result, but introduces an additional approximation to the process. Yu and Falnes (1995) provide a detailed description of the time-domain identification procedure, applying the technique to the analysis of a heaving point absorber.

3. A direct realisation technique; one option being based on the use of the Markov parameters of the resulting state-space system in discrete time (Ho and Kalman, 1966; Taghipour et al., 2008). This method tends to be complex to implement and upon completion requires a conversion from discrete back to continuous time using an algorithm that produces a stable continuous time result. The discrete to continuous time conversion again introduces an additional approximation to the result.
4. Mathematical approximation to the convolution process itself. The most widely known example of this involves the use of Prony's Approximation in an approach adopted by the SEAREV team at the École Centrale de Nantes (Duclos et al. 2001). The radiation convolution of the form:

$$-f' = \int_0^t k(t-\tau)\dot{x}(\tau) d\tau\quad [3.39]$$

can be solved by approximating the function by a series of exponentials:

$$k(t) \approx \sum_{i=1}^N \alpha_i e^{\beta_i t}\quad [3.40]$$

The parameters to be determined, θ are the values of α_i , β_i , which are found using Prony's method, a discrete time algorithm used to obtain values that fit a sampled impulse response. A

Prony approximation function is available in MATLAB's Signal Processing Toolbox. Once again, the resulting discrete (z domain) transfer function result must be converted back to the s or time-domains to allow the continuous time parameters to be obtained.

Substituting Equation (3.40) into Equation (3.39) allows the convolution to be written:

$$-f'(t) \approx \sum_{i=1}^N \int_0^t \alpha_i e^{\beta_i(t-\tau)} \dot{x}(\tau) d\tau = \sum_{i=1}^N S_i(t) \quad [3.41]$$

$$\text{with} \quad S_i(t) = \int_0^t \alpha_i e^{\beta_i(t-\tau)} \dot{x}(\tau) d\tau \quad [3.42]$$

which can be differentiated to give:

$$\dot{S}_i(t) = \beta_i S_i(t) + \alpha_i \dot{x}(t) \quad [3.43]$$

It is now possible to evaluate $-f'(t)$ through integration of the set of equations described by Equations (3.41), (3.42) and (3.43), rather than completing the numerical convolution. The S_i can each be thought of as additional system states and the final state-space form encompasses the complete system, mapping the wave excitation force and external force inputs to the body's motion response.

A fully developed GH WaveFarmer code could potentially incorporate multiple system identification algorithms; however as an initial stage, it will be prudent simply to implement one of the above techniques, in parallel with the exact numerical convolution, so that the potential benefits of state-space representation can be fully assessed.

3.4 Selection of a Supporting Hydrodynamic Solver

BEM solvers are widely specified for the determination of the added mass and radiation damping coefficients required to complete the hydrodynamic calculations outlined in Sections 3.2 and 3.3. A code selected to support the GH WaveFarmer hydrodynamics must:

- Be able to complete frequency-domain calculation of the radiation damping (B_r) and added mass (m_r) hydrodynamic coefficients for any body geometry, in multiple degrees of freedom.
- Compute the hydrostatic spring for a mean water-plane area.
- Calculate, at least in a frequency dependant, linear form, the amplitude of the wave exciting force, $F_e(\omega)$.
- Be able to complete calculations at both finite and infinite water depths.
- Perform calculations for multiple bodies in close proximity.
- Operate on a standard laptop computer with a hardware specification that delivers only moderate performance by present standards.
- Explicitly output all data.

In addition, it is desirable for the code to:

- Calculate the impulse response function $k(t)$ for each degree of freedom (although it should be noted that this could alternatively be completed in GH WaveFarmer through the numerical implementation of Equation (3.30).
- Be able to evaluate a nonlinear Froude-Krylov component to the incident wave excitation force, for an instantaneous water-plane area (which could potentially be useful to GH WaveFarmer for more accurate calculation at a later stage).
- Incorporate a user friendly interface and employ convenient data output formats.

The commercial codes listed in Table 3.1 have been identified for comparison. All meet the minimum criteria listed above, operate as stand-alone applications on a windows-based platform and are designed for use on typical personal computer systems. The developers tend to offer a number of alternative perpetual or temporary licensing options, which may also be expandable to include related packages.

The modelling capabilities of each of the options have been compared in Table 3.2. One of the principal differences is in the user environment and data input and output formats. The majority of codes operate through a graphical user interface, which allows the user to control the calculation process and view data

output, however WAMIT operates entirely through a command line and MOSES has the option to do so. Input formats for body definition vary widely, with no common format.

The added mass and radiation damping coefficients are calculated by all codes; however it is not clear whether any other than WAMIT calculate the radiation impulse response functions. Only WaveLoad and AQWA calculate nonlinear Froude-Krylov excitation forces, with the other codes simply generating a linear, frequency dependant, complex force amplitude. It is not clear however whether the nonlinear data is produced by WaveLoad and AQWA in an accessible format. WaveLoad, AQWA and TiMIT, the time-domain code produced by MIT, can calculate nonlinear hydrostatic forces as a function of actual, rather than mean body geometry.

Product Name	Developer
AQWA	ANSYS Inc. (Pennsylvania, USA, Worldwide) Engineering software developer with range of widely used commercial FEA and CFD codes. Produce AQWA as 'AQWA Diffraction' (Basic Model Generation, Hydrostatics, Radiation, Diffraction Analysis), 'AQWA Suite' (Simple Moorings model and Motion Simulation), or Suite 'with Cable Dynamics' (Dynamic Mooring Model)
WAMIT	WAMIT Inc. 'Spin-off' from Massachusetts Institute of Technology (MIT).
HydroStar	Bureau Veritas (Worldwide) Part of Veritas Marine's 'VeriSTAR Offshore' software solutions stream, which also includes moorings (Ariane 7) and structural analysis tools.
Moses	Ultramarine Inc. (Texas,USA) Specialize in Engineering design and analysis with corresponding software development.
Neptune	Zentech Inc. (Texas,USA) An engineering consultancy and software development company. Specializes in providing services to marine, petroleum, and construction industries. Also develop 'ZenMoor' mooring analysis tool as well as specialist software for the oil industry.
WADAM (SESAM)	Det Norske Veritas (DNV) (Norway, Worldwide). Established risk management services provider. Developed as part of the 'SESAM' modular suite, which incorporates pre and post-processing and structural analysis tools. Typically run from within 'HydroD' loads and motion response software.
WaveLoad	Martec Ltd. (Nova Scotia, Canada) (Member of the Lloyd's Register Group). Specialises in engineering analysis services and creation of simulation software. Part of the 'Trident' software suite.

Table 3.1: Commerical BEM Hydrodynamics Codes

Product Name	Capabilities									Additional Notes
	Multiple Bodies	Input/Output Format	User Interface	Frequency Domain Calculation of Added Mass and Damping Coefficients	Calculation of Radiation Force Impulse Response Functions	Calculation of Incident Wave Excitation Forces	Calculation of Hydrostatic Forces	Calculation of Mean Drift Forces	Specification of water depth. (Ability to cope with shallow water)	
AQWA	Yes	Graphical body modeling with built-in mesh generation and modification capabilities. Geometry checking	Graphical User Interface (GUI) for definition of model and environment parameters. Output data viewed through GUI.	Yes	Output is unclear, but likely to be calculated internally for use in the time-domain calculations	Yes. Linear and also time domain non-linear Froude-Krylov force component based on instantaneous wetted surface area.	Yes. Linear and non-linear. Non-linear restoring forces computation in the time domain based on instantaneous wetted surface area.	Yes	Yes	Now maintained as part of the extremely popular ANSYS Solver Products range. AQWA itself was first developed in 1985 and is widely used in the marine industry
WAMIT	Yes	Body geometry specified by a user-supplied text file. Additionally, if the high order solution method is selected, which uses B-splines to describe the body geometry and pressure on the body surface, then the user can supply a list of rectangular panels or direct B-spline information. Exact geometry definition is possible if user has access to a FORTRAN compiler. Library of .dll files available for a range of commonly used geometries. Geometric models can also be imported from the CAD program 'MultiSurf' (AeroHydro Inc.); however this requires an additional license for interface modules RG2WAMIT and RGKernel.	Command Prompt in Windows to initiate calculations. Output data stored in specially formatted text files.	Yes	Yes, using the 'F2T' utility specifically designed for this purpose.	Yes Linear Either from direct integration of the body surface pressure or from Haskind relationships.	Yes. Linear restoring forces. Non-linear restoring forces computed in the time domain by the TIMIT, MIT's time domain code.	Yes	Yes	Calculation processes and output data can be readily controlled by external software due to the lack of GUI. Well-documented output text-file format useful during software development. Supplied in FORTRAN 90/95 Source Code.
HydroStar	Yes	Body geometry input is through line or 'frame' designs. Automated mesh generation and geometry checking. Data output can be read by the VeriSTAR NSO ('New Strudl Offshore') structural analysis software.	Graphical User Interface Module.	Yes	Unknown	Yes Linear	Yes Linear restoring forces.	Yes	Yes	Used extensively in the Oil and Gas industries. In development for over 20 years.

Moses	Yes	Body geometry defined through the amalgamation of ‘hulls’, other larger bodies, tubes and/or plate elements. Interactive graphics allow the generation of unusual shapes. User can select from and modify a library of shapes. Option to create macros that rapidly generate bodies and complete post-processing tasks. Automatic mesh generation. Mesh refinement options.	User interface in the form of a specifically designed window with a command line, toolbar and display area. Option to use a simple terminal window instead, which can operate in ‘silent’ mode, only producing output when requested.	Yes	Unknown	Yes Linear	Yes Linear restoring forces.	Yes	Yes	MOSES is a computer language rather than a ready-made program. Incorporates a complex, non-linear moorings model.
Neptune	Unknown	Integral drawing facility for body definition. Automatic mesh generation with editing facilities and geometry checking. Graphical post-processing of results.	Graphical User Interface	Yes	Unknown	Yes Linear	Yes Linear restoring forces.	Yes	Unknown	Available documentation is sparse.
WADAM (SESAM)	Optional Module	Panel data can be imported from WAMIT, ‘Prefem’ (a DNV product) or Patran-Pre (an MSC Software Product). Mesh generation and refinement. Output is in the form of a hydrodynamic results interface file for use in ‘Postrep’ (DNV post-processing and statistics software). The WADAM print file is directly accessible from HydroD and can be exported to allow hydrostatic data to be viewed in Microsoft Excel.	Graphical User Interface	Yes	Unknown	Yes Linear	Yes Linear restoring forces.	Yes	Unknown	The 3D Radiation-Diffraction theory used by WADAM is based on software developed by MIT. WADAM is often run from ‘HydroD’ (also developed by DNV and part of SESAM).
WaveLoad	Yes	Graphical body geometry definition and mesh generation. Models can be imported from the Trident FEA software, which in turn can import geometries in a neutral computer aided design (CAD) file format. Specification of mooring lines and other constraints. Graphical post-processing and option to return results to Trident FEA.	Graphical User Interface	Yes	Output is unclear, but likely to be calculated internally for use in the time-domain calculations	Yes. Linear and also time domain non-linear Froude-Krylov force component based on instantaneous wetted surface area in ‘Wave Load-TD’ (time domain code).	Yes. Linear and non-linear. Non-linear restoring forces computation in the time domain based on instantaneous wetted surface area.	Yes	Yes	

Table 3.2: Selection Matrix detailing the relative capabilities of commercially available BEM solver codes

3.5 Current GH WaveFarmer Capabilities – GH FD and GH TD

In its current format GH WaveFarmer is capable of solving the frequency and the time-domain equations of motion in matrix form for a single WEC device described by multiple bodies moving in multiple degrees of freedom (as outlined in Section 1). Figures 1.1 and 1.2 illustrate the links between main routines that have been developed with this objective. A first exercise that expands the single WEC tool to array calculations in the frequency-domain has been presented by GH at the 2009 European Wave and Tidal Energy Conference.

With regard to the time-domain solution, the radiation convolution integral is discretised and evaluated numerically using stored velocity values from previous time-steps. A fixed time-step 2nd order Adams-Bashforth integrator is used to provide relatively high orders of accuracy based on past time-step results. The code could be expanded to incorporate additional, fixed or variable time-step equation of motion solvers however it should be noted that solver selection can be restricted by external force calculation practicalities, in addition to the common stability and numerical performance considerations; see Section 3.7.

Each body is initially represented by a full six degrees of freedom in the system matrices, however motion in certain directions can be physically ‘locked’, in which case corresponding components are removed and the matrix dimensions are reduced accordingly. The user can specify particular modes using an indexing system to identify the degrees of freedom responsible for the relative motion driving the PTO system.

At present WAMIT (see Section 3.4) is used to compute the radiation damping and added mass hydrodynamic coefficients, $B_r(\omega)$ and $m_r(\omega)$ (including $m_r(\infty)$), as well the impulse response function, $k(t)$ (using the ‘F2T’ utility) for each body geometry and each degree of freedom. A potential extension to the code is the capability of loading hydrodynamic parameters that have been calculated by other hydrodynamic solvers listed in Section 3.3. The wave exciting force is also calculated by WAMIT so that, in combination with the incident wave-train generated by GH WaveFarmer, the total wave excitation force component can be calculated at each time-step.

The PTO force calculation is at present limited to a linear damping, although this can be replaced in the time-domain solver by a nonlinear mathematical expression based on the instantaneous motion of the bodies. Simple controller effects are modelled in a ‘passive’ or ‘active’ sense in the form of an additional damping specified as either a constant coefficient, the ‘passive’ case, or a frequency dependent damping coefficient, the ‘active’ case. Mooring forces are specified by a (at maximum) cubic function of displacement.

The description of the external forces and the array optimisation strategies represent the greatest scope for development. Potential PTO, moorings and control system options are discussed in more detail in Section 3.6. It may also be desirable to incorporate a nonlinear wave excitation force component, however, as stated in Section 3.3, the point at which this becomes necessary will be quantified to some extent by the comparisons with the nonlinear simulations being carried out by the UoOx.

3.6 Modelling External Forces

The ‘external forces’ term in the WEC equations of motion described in Sections 3.2 and 3.3 refers to the force contributions to the system other than those resulting from the dynamic wave action. This includes the PTO reaction force, which is dependant on both the PTO hardware configuration and the control system actions, the mooring forces, the structural restraint forces, due to components of the physical device design but not part of the PTO, and the drift forces, as the baseline loading for the moorings system. The nature of each of these forces is device specific and so it is crucial that GH WaveFarmer is flexible in offering a range of external force modelling components.

In a frequency-domain analysis, control system, PTO and mooring effects are restricted to linear mathematical expressions that approximate the WEC design and can be incorporated directly into the frequency-domain system transfer function. Detailed nonlinear external force models can operate in the time-domain only, but provide a more realistic representation, calculating instantaneous force contributions on a time-step-by-time-step basis. In this Section, and unless otherwise stated, the discussion is focused on the time-domain description of the external forces; note that frequency-domain representation will be based on a linearisation of the time-domain equivalent.

The relative advantages and potential limitations of alternative approaches to external force modelling will be discussed below. Initially, however, it is useful to specify the way in which the external force definition modules must interact, both with each other and with the equation of motion solver.

The data transfers required at each time-step in a time-domain simulation are outlined in Figure 3.4.

Note that, in contrast to the frequency-domain, the time-domain PTO and control system modules may incorporate their own internal states, resulting from the dynamic equations describing the system components. For instance, the reaction force provided by a hydraulic PTO at any given time might depend on the current pressure in a number of accumulator components, or the settings in control circuitry, factors that are influenced by the previous simulation history and so must be stored as states describing the present condition of the PTO.

The control system has no direct output to the equation of motion because control actions are implemented by the PTO hardware. Indeed, for cases where the PTO definition is a simple mathematical expression only, the controller may take a form that is sufficiently simple for the two modules to be combined, the control action manifested as a modification to the PTO characteristics. It is likely that distinct PTO and control definition modules will be required only when GH WaveFarmer reaches a comparatively developed stage; nevertheless the complete range of current options with regard to each is discussed below.

A proposed path forward for the GH WaveFarmer Base Module modelling of the external forces is given in Section 5.4

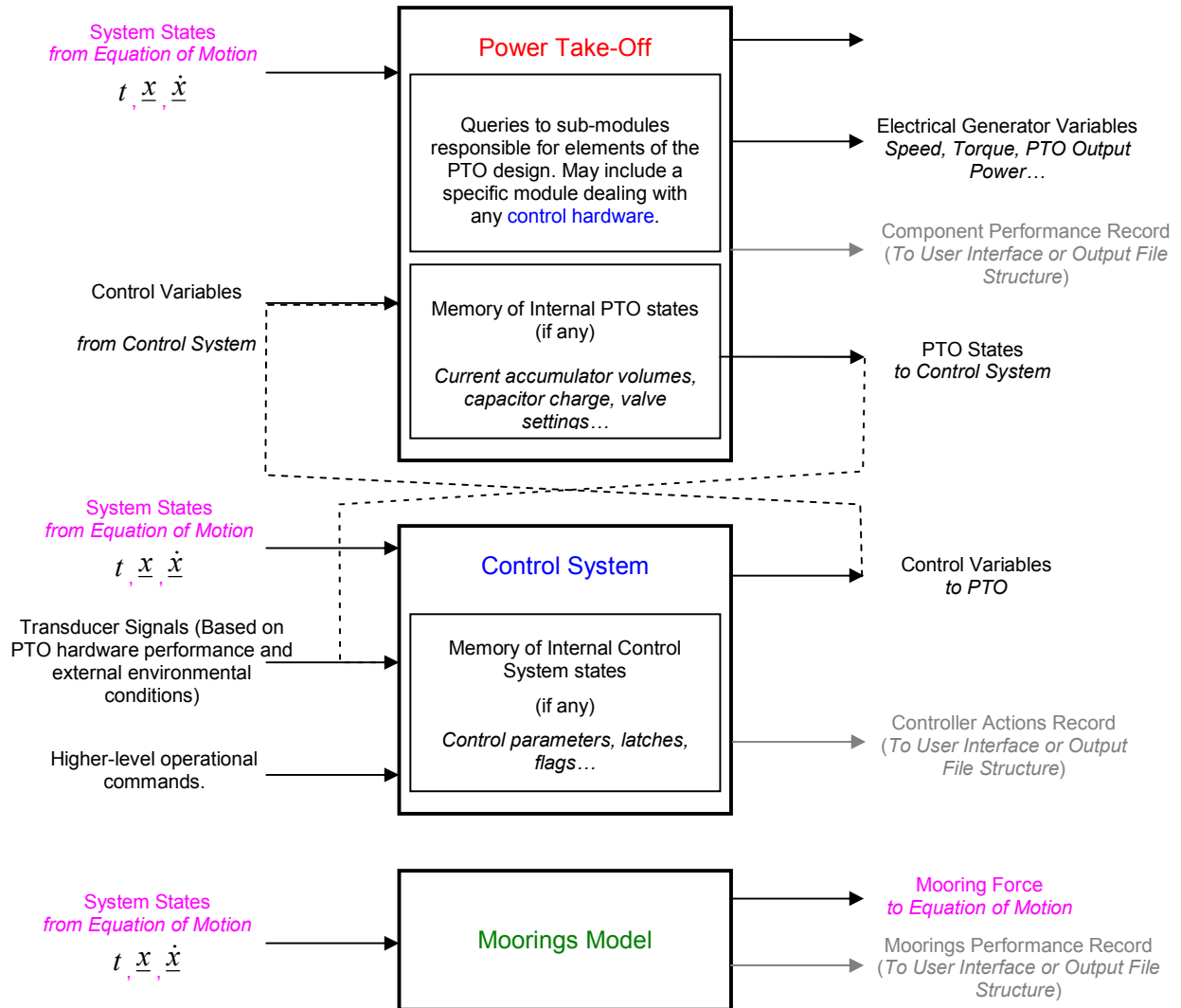


Figure 3.4: Time-domain data exchange between the external force definition modules and the equation of motion solver.

3.6.1 Modelling the PTO

There is significant diversity amongst the PTO designs currently being developed for use in WECs. The variation in the operational principle of each design means that even if devices employ the same medium through which to achieve the PTO energy conversion task, such as the hydraulic approach adopted by Ocean Power Technologies' *PowerBuoy*, Pelamis Wave Power's *Pelamis* device (Henderson, 2006) and the École Centrale de Nante's *SEAREV* (Josset, 2007), then schematic design, component selection, and control hardware configurations have not fully converged on a single, standard form. The result is that GH WaveFarmer must incorporate a correspondingly flexible PTO definition module, potentially providing the user with multiple routes by which to model a manufacturer's design. Such an approach has the added advantage that PTO definitions provided by manufacturers in a variety of forms can be accommodated, from a detailed technical diagram, to a software model (which may include visible code or may operate as a 'black-box') or a simplified spring-damper approximation. Alternative modelling options are discussed individually below.

Simple Mathematical Expression, No Internal States

A basic PTO definition module could simply provide a facility for a user to specify a mathematical expression that calculates the instantaneous PTO force from the body motion. The expression could take a number of standard forms (controlled by the user interface): a polynomial with user specified order and coefficients; a coulomb type force with user specified amplitude; or a combination of exponential or logarithmic terms. The option to sum the effects of more than one expression could also exist and controller influence would be imposed directly on the calculation before the result is returned to the equation of motion. This option, with the additional constraint of linear expressions only, would be the only PTO definition type available to the frequency-domain calculations. The power absorbed by the PTO model could be calculated during simulation, but the power output to the generator would be dependant on a simple 'PTO efficiency' value. The user would not be able to draw conclusions about the performance of individual components in the PTO design.

This approach would allow an approximate PTO model to be built if the performance characteristics are well known

A Simplified PTO 'Template' with Pre-Defined Mathematical Models and States

For a more realistic representation of the PTO forces on the equation of motion, and a better estimation of the energy capture of the device, the PTO could be modelled in terms of its primary constituent roles of rectifying and smoothing the energy input, under control, in conjunction with some form of energy 'consumption' as PTO energy is converted to an electrical output. The user could specify a loss associated with a generalised 'rectification process', which in reality may be an arrangement of control valves, electrical diodes, or similar. In series with this, a 'smoothing process', incorporating an internal state representing the 'charge' in a smoothing system could also be included. The charge may be the equivalent to the stored fluid volume in accumulators positioned either side of a hydraulic motor (which would in turn drive the electrical generator), the electrical charge in a capacitor, or the speed of a flywheel. The charging and discharging characteristics would need to be defined through selection of a fixed format mathematical model. Finally, the energy 'consuming' load model (in reality a conversion to the final electrical energy output), would extract energy from the system with a specified efficiency. Controller influences would be incorporated throughout the system, providing scope for the specification of simple control algorithms.

An initial PTO ‘template’ is shown graphically in [Figure 3.5](#). Alternative templates, supporting a different range of mathematical models, could be added at a later date if required to accommodate additional groups of PTO design.

Although the template based PTO system potentially produces a more accurate estimation of electrical power output and PTO force influence on the equation of motion, the definition remains relatively rigid and provides only a limited amount of information to the PTO designer, who may be interested in the performance of specific physical components.

Basic GH WaveFarmer Component Library

A more flexible approach to PTO modelling would be to construct a library of basic PTO components that can be connected and configured by the user. Each component would incorporate its own mathematical model, which would need to be solved in conjunction with the time-domain equation of motion. Components would initially need to be kept simple to limit the computational burden of such a system. Even so, the flexibility of this modelling approach would require the creation of a suitable graphical user interface, as well as the inclusion of an error checking code to verify the user’s design. Furthermore, a pre-processor would be needed to compile the PTO design into a form suitable for numerical evaluation. More detailed and realistic components could be gradually added to the library as GH WaveFarmer develops.

An internal GH WaveFarmer component library represents the most challenging implementation option and could be expected to require quite significant development time. It is unclear whether this level of detailed modelling is both necessary, from a numerical accuracy perspective, and capable of servicing the wave energy industry in the short-term, given the need to build up a minimum number of components before commercial PTO design modelling can begin.

Link with other Commercial Software Modelling Tools

Some users, particularly device manufacturers, may use a commercial mechanical, hydraulic or electrical systems simulation package as part of their PTO design process. If this is the case, then it would be useful to create a simulation interface that allows users to examine the performance of their existing models in conjunction with the GH WaveFarmer hydrodynamics. Previous work at GH has shown that creation of such a time-domain simulation interface is possible, the principal challenge being to guarantee sufficiently good data exchange performance to maintain practical simulation times (Livingstone, 2009).

An interfaced commercial simulation package would additionally present the user with an alternative environment in which to model a WEC’s control system.

Dynamic Link Library (.DLL) Communication

GH WaveFarmer is designed for use by a range of organisations, each of which will have different relationships with WEC manufacturers. As a result, it may at times be important to ensure that internal details of the PTO design can be specified for the GH WaveFarmer simulation but hidden from view. A manufacturer supplied PTO model in the form of a dynamic link library (.DLL) would meet this requirement. At each time-step, GH WaveFarmer’s equation of motion solver would send equation of motion (e.g. displacement and velocity) information through a .DLL interface and receive a PTO force in return. In the case of more complex designs, PTO state derivatives would also need to be supplied for use by the GH WaveFarmer integrator. The success of such an arrangement would be dependant on the precise specification of the required .DLL input/output (I/O) format, but the creation of a .DLL link would

additionally facilitate rapid switching of PTO definitions, a useful feature even if the PTO design does not need to be protected. Despite the hidden nature of the PTO design, a user would be able to verify performance claims by comparing the output of specified regular or irregular wave simulations with published or experimental data.

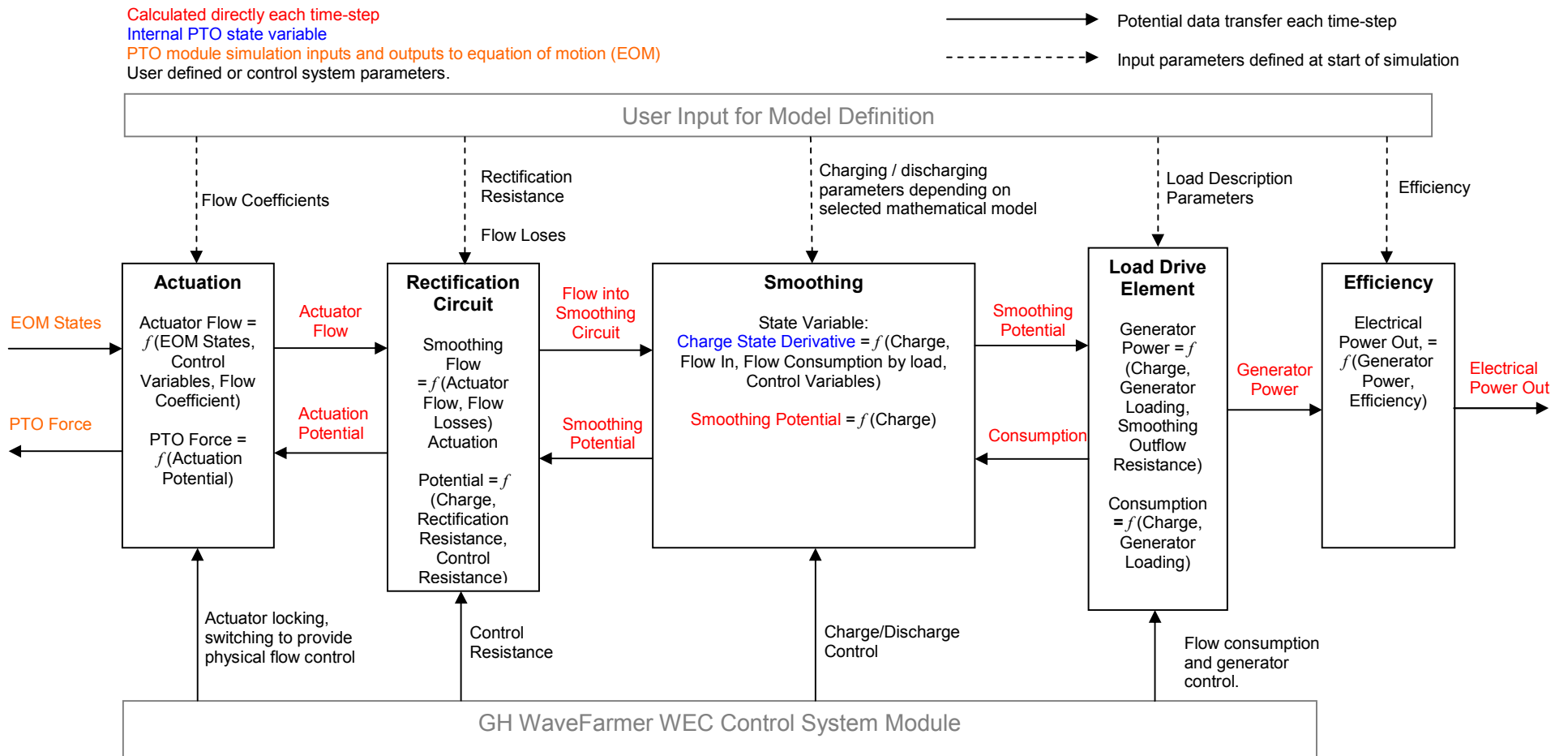


Figure 3.5: 'Template' Type PTO Model. This template could approximate systems with a simple rectification and smoothing function. Alternative templates could be produced if necessary. Input from the user sets the template to approximate the PTO being modelled.

3.6.2 Control Actions

The design of WEC control strategies to maximise the energy capture of a device have been the subject of research since the early days of the wave energy industry. A brief overview of established control techniques is necessary to provide a context for the proceeding discussion on control implementation in the GH WaveFarmer software.

Basic WEC Control Theory

Before attempting to describe the complex control task associated with a real WEC device, potentially incorporating nonlinear PTO and hydrodynamic forces, it is useful to return momentarily to a linear, heaving point absorber model. The device is a buoy of mass m_m connected to the sea bed by a PTO comprised of a parallel spring and viscous damper. The PTO spring stiffness is represented by K_m and the PTO damping coefficient is B_m . The hydrostatic force operates as a spring with stiffness K_{hs} . Adopting the linear hydrodynamics model described by Equation (3.2), the equation of motion for such a device can be written as:

$$m_m \ddot{x} + B_m \dot{x} + (K_{hs} + K_m)x = f_e + f_r \quad [3.44]$$

where, as before, f_e represents the wave exciting force and f_r the wave radiation force. Adopting complex notation, whereby an arbitrary quantity, x harmonically oscillating with amplitude x_0 at frequency ω with phase ϕ is expressed as:

$$x = x_0 \cos(\omega t + \phi) = x_0 \frac{e^{j(\omega t + \phi)} + e^{-j(\omega t + \phi)}}{2} = \frac{x_0}{2} e^{j\phi} e^{j\omega t} + \frac{x_0}{2} e^{-j\phi} e^{-j\omega t}$$

and the complex amplitude, X is defined: $X = x_0 e^{j\phi}$ so that:

$$x = \frac{1}{2} X e^{j\omega t} + \frac{1}{2} X^* e^{-j\omega t} = \Re(X e^{j\omega t}) \quad [3.45]$$

Equation (3.44) can be written assuming a oscillatory buoy response, $x = \Re(X e^{j\omega t})$ (Falnes, 2002):

$$\begin{aligned} & \left((j\omega)^2 m_m + j\omega B_m + (K_{hs} + K_m) \right) X e^{j\omega t} + \left((-j\omega)^2 m_m - j\omega B_m + (K_{hs} + K_m) \right) X^* e^{-j\omega t} \\ & = F_e e^{j\omega t} + F_e^* e^{-j\omega t} + F_r e^{j\omega t} + F_r^* e^{-j\omega t} \end{aligned} \quad [3.46]$$

Or in terms of the buoy velocity, $u = \Re(U e^{j\omega t})$; $U = j\omega X$:

$$\begin{aligned} & \left(j\omega m_m + B_m + \frac{(K_{hs} + K_m)}{j\omega} \right) U e^{j\omega t} + \left(-j\omega m_m + B_m - \frac{(K_{hs} + K_m)}{j\omega} \right) U^* e^{-j\omega t} \\ & = F_e e^{j\omega t} + F_e^* e^{-j\omega t} + F_r e^{j\omega t} + F_r^* e^{-j\omega t} \end{aligned} \quad [3.47]$$

Defining a ‘mechanical impedance’:

$$Z_m = j\omega m_m + B_m + \frac{K_{hs} + K_m}{j\omega} = B_m + j \left(\omega m_m - \frac{K_{hs} + K_m}{\omega} \right) = B_m + jE_m \quad [3.48]$$

Equation (3.47) can be re-written as:

$$\left(Z_m U - (F_e + F_r) \right) e^{j\omega t} + \left(Z_m^* U^* - (F_e^* + F_r^*) \right) e^{-j\omega t} = 0 \quad [3.49]$$

which is satisfied for all t if $ZU - (F_e + F_r) = 0$ or:

$$F_e + F_r = Z_m U \quad [3.50]$$

So the mechanical impedance is the relationship between the forcing term amplitudes and the buoy velocity amplitude. Now an expression for the complex radiation force amplitude is given by Equation (3.5):

$$F_r(\omega) = -G(\omega)X(\omega) = -\left(-\omega^2 m_r(\omega) + j\omega B_r(\omega) \right) X(\omega)$$

Defining a ‘radiation impedance’, Z_r (Falnes 2002), (Thomas in Cruz 2008), we can write this as:

$$F_r(\omega) = -\left(j\omega m_r(\omega) + B_r(\omega) \right) U(\omega) = -Z_r U \quad [3.51]$$

$$Z_r = B_r + j\omega m_r = B_r + j\omega m_r \quad [3.52]$$

Combining Equations (3.51) and (3.50) yields:

$$F_e = (Z_m + Z_r) U \quad [3.53]$$

which can be rearranged to give the velocity response to wave excitation:

$$U = \frac{F_e}{(Z_m + Z_r)} = \frac{F_e}{\left(B_m + B_r + j \left(\omega(m_m + m_r) - \frac{K_{hs} + K_m}{\omega} \right) \right)} \quad [3.54]$$

The instantaneous power absorbed by the PTO damper is given by:

$$P_m = F_m u = B_m u^2 = B_m \left(\frac{1}{2} U e^{j\omega t} + \frac{1}{2} U^* e^{-j\omega t} \right)^2 = \frac{B_m}{4} \left(U^2 e^{2j\omega t} + U^{*2} e^{-2j\omega t} + 2UU^* \right) \quad [3.55]$$

Taking the time average eliminates the purely oscillatory terms in time and the expression simplifies to:

$$\bar{P}_m = \frac{B_m}{2} (UU^*) = \frac{1}{2} B_m |U|^2$$

Substituting for U using Equation (3.54):

$$\bar{P}_m = \frac{1}{2} B_m |U|^2 = \frac{\frac{1}{2} B_m |F_e|^2}{\left(B_m + B_r \right)^2 + \left(\omega(m_m + m_r) - \frac{K_{hs} + K_m}{\omega} \right)^2} \quad [3.56]$$

Falnes (2002) notes that if the mass and stiffness properties of the system are fixed, then maximum power absorption is achieved for the wave frequency ω with a PTO damping B_m corresponding to the case when $\frac{\partial \bar{P}_m}{\partial B_m} = 0$:

$$B_{m \text{ opt}} = \left(B_r^2 + \left(\omega(m_m + m_r) - \frac{(K_{hs} + K_m)}{\omega} \right)^2 \right)^{\frac{1}{2}} \quad [3.57]$$

which can be substituted back into Equation (3.56) to give the corresponding optimum power absorption:

$$\bar{P}_{m \text{ opt}} = \frac{\frac{1}{4} |F_e|^2}{B_r + \left(B_r^2 + \left(\omega(m_m + m_r) - \frac{(K_{hs} + K_m)}{\omega} \right)^2 \right)^{\frac{1}{2}}} = \frac{\frac{1}{4} |F_e|^2}{B_r + B_{m \text{ opt}}} \quad [3.58]$$

For any PTO damping, B_m and a fixed wave frequency ω , power absorption is maximised further if the PTO mass and stiffness are such that the reactance term in Equation (3.56) evaluates to zero:

$$\begin{aligned} \omega(m_m + m_r) - \frac{(K_{hs} + K_m)}{\omega} &= 0 \\ \Rightarrow \omega &= \omega_n = \sqrt{\frac{K_{hs} + K_m}{(m_m + m_r)}} \end{aligned} \quad [3.59]$$

Substituting Equation (3.59) into Equation (3.54) shows that if this resonance condition is satisfied, then the buoy's velocity is in phase with the excitation force:

$$U = \frac{F_e}{(Z_m + Z_r)} = \frac{F_e}{(B_m + B_r)} = \frac{f_{e0}}{(B_m + B_r)} e^{i\phi_{fe}} \quad [3.60]$$

where f_{e0} is the absolute excitation force amplitude.

Maximum power is produced for this frequency with a PTO damping given by substituting Equation (3.59) into Equation (3.57), which then reduces to:

$$B_{m \text{ opt}}(\omega_n) = B_r(\omega_n) \quad [3.61]$$

It follows from Equation (3.58) that the maximum possible power absorption by the system is:

$$\bar{P}_{m \text{ max}} = \frac{|F_e|^2}{8B_{m \text{ opt}}(\omega_n)} \quad [3.62]$$

If the mechanical and radiation impedances defined above are written generally in terms of their resistive and reactive components (Equation 3.48 and 3.52), then Equation (3.59) may alternatively be written:

$$E_m + E_r = 0 \Rightarrow E_m = -E_r \quad [3.63]$$

For optimal damping in this condition, Equation (3.61) states that $B_m = B_r$, so the mechanical impedance or ('PTO Matrix') that produces greatest possible energy absorption at the wave frequency is simply the complex conjugate of the radiation impedance at that frequency (Edinburgh University Wave Power Project, 1987):

$$Z_{m \text{ max}} = Z_r^* \quad [3.64]$$

The above analysis suggests two potential control approaches. Selection of either depends on the controller's ability to influence the PTO properties.

1. Constant reactance tuning of the PTO damping (real control).

The PTO damping is set to achieve a sub-optimum power absorption level without adjustment of the system's spring and inertial (reactance) terms (Equation 3.57). For a device operating in irregular waves, the damping can be continuously adjusted to match the incident wave frequency content: an 'active' control implementation (which requires prediction of future wave frequencies); or can be set in a 'passive' strategy to a constant value chosen as the value that will yield the highest average absorbed power given the long term wave climate at a site.

2. Phase control to achieve or approximate resonance in the system.

For full ‘reactive’ phase control (also known as ‘complex conjugate’ control in reference to the optimum control condition, Equation 3.59), the control system must be capable of adjusting the effective system reactance. This can be done in a theoretical sense through the specification of an appropriate PTO stiffness, K_m , or the design of a method to alter the effective system mass (e.g. using ballast tanks). The hydrostatic stiffness acting on the system is typically sufficiently large to dictate the addition of an artificial negative stiffness effect or positive mass contribution in order to lower the natural frequency to a level comparable with the incident waves. Such effects are difficult to implement physically, but in principle even an adaptation of the technique to the constraints of a real PTO system would yield greater power outputs than the simpler technique described above. A phase control approach can once again take either an active or passive form.

A time-domain approximation to full phase control, known as ‘latching’, was proposed by Budal and Falnes (Count, 1980) and has been widely investigated since. A latching control strategy is designed to mimic the resonance condition achieved with full reactive phase control, without adjustment of the system reactance. Instead, the relative motion in the PTO mode is physically constrained to a discontinuous form approximating the ‘in-phase’ velocity and excitation force resonance condition described by Equation (3.60). This is done through the specification of a brake or holding force that acts to catch the buoy (or the bodies responsible for the relative motion driving the PTO) at its end points, when its velocity approaches zero; the buoy is then released again at a time calibrated to ensure that the buoy reaches its maximum velocity at a time that corresponds to the peak excitation force of the proceeding wave. The precise release time acts as the control variable and a number of alternative release strategies have been proposed, some relying on knowledge or prediction of future wave frequencies and others based on instantaneous force measurement (Falcão 2008; Barbarit et al. 2004, 2006).

In reality, the control task is further complicated by the true nature of the PTO force contribution to the equation of motion. The result is a trend towards unique, device specific control system designs, however these typically aim to operate the PTO in a way that approximates one of the above strategies as closely as possible with the hardware available.

Controller Implementation Options

The close interaction between the control system and PTO means that the control strategy implementation options are dependent on the detail with which the PTO has been defined. The idealised theoretical control strategies outlined above can be directly combined with the most basic PTO definition option of a simple mathematical expression, in the early GH WaveFarmer beta releases. A user would be able to select from a ‘drop-down’ list containing passive and active constant reactance tuning options, passive and active reactive control and, in the time-domain, an optimal latching strategy based on knowledge of future waves. These effects would then be imposed directly on the calculation of the PTO force.

The PTO ‘template’ definition option would require an associated control system template providing the user with the option to implement a control algorithm based working variables in the template. The nature of the control algorithm would be dependent on the template being used. The typical rectification-smoothing arrangement in the Figure 3.5 template results in a variable magnitude ‘coulomb’ type PTO force contribution to the equation of motion, as the actuator pumps against the charge in the smoothing elements. In this case, a user could implement an approximation to constant reactance tuning through adjustment of the actuator force-flow rate relationship. Similarly, a latching phase control could be implemented through actuator motion locking, with unlatching logic being

based on the internal state of the smoothing charge or hydrodynamic force transducer signals (Livingstone and Plummer, 2010).

The template dependant control input from the user could be obtained through a comparatively unrestrained graphical user interface incorporating an environment in which the user can specify control actions based on the available data signals. Alternatively, a fixed format .DLL or MATLAB script designed specifically to deal with the PTO template could be selected.

The less constrained PTO implementation options require a much more open control implementation, designed on a machine specific basis. The control logic may be an unrestrained .DLL or MATLAB script operating with control variables selected by the user during PTO design, or, in the case of the PTO commercial code interface and .DLL and options, may be incorporated as part of the PTO definition, with no distinct control system-PTO divide being obvious from within GH WaveFarmer.

3.6.3 Mean Drift Force

The excitation force described in sections 3.2 and 3.3 represents the wave frequency loading induced by the incident waves and has a nominal zero mean force exertion over time. However, if a floating device absorbs and reflects a proportion of the wave energy, then the repeated wave impact can be described as having an additional time-averaged baseline loading (typically with much smaller in amplitude) known as the ‘mean drift force’.

The mean drift force is generally calculated for a given wave frequency independently from the excitation force and can be evaluated either through a time averaged momentum flux analysis on a control volume surrounding the body or by directly time-averaging the integrated pressure distribution over the body surface. Hydrodynamics codes such as WAMIT may be used to complete the drift force calculation, but require external force information to describe the energy absorption properties of the device in a power production simulation. A full description of a complex WEC PTO and control system would not be possible in a simple hydrodynamics code external force definition; however the role of mean drift forces as the baseline load for moorings design means that force calculation is likely to be of greatest interest in a survivability environment, when the WEC is not absorbing power.

Retzler (2006) found that during power production, the drift forces measured on a scaled Pelamis WEC were due almost entirely due to energy absorption for all but the highest wave frequencies. In such cases, a mean drift force calculation could be completed based on the expression (Falnes 2002, Retzler, 2006):

$$f_{drift} = \frac{\rho g}{4} \left(|A_i|^2 + |A_r|^2 - |A_t|^2 \right) \quad [3.65]$$

Which is derived from the conservation of the transported wave power and be manipulated to give the more useful form:

$$f_{drift} = \frac{\omega}{g} (J_i + J_r - J_t) = \frac{\omega}{g} (\overline{P_m} + 2J_r) \quad [3.66]$$

where A_i , A_r and A_t are the incident, reflected and transmitted wave complex amplitudes and J_i, J_r, J_t and $\overline{P_m}$ are the incident, reflected and transmitted wave powers and the time averaged WEC absorbed power per unit width of wave front respectively.

If the reflected wave power is small, then

$$f_{drift} \approx \frac{\omega}{g} \left(\overline{P_m} \right) \quad [3.67]$$

Equations (3.65), (3.66) and (3.67) apply to deep water only, but can be modified for the finite depth case (Longuet-Higgins, 1977).

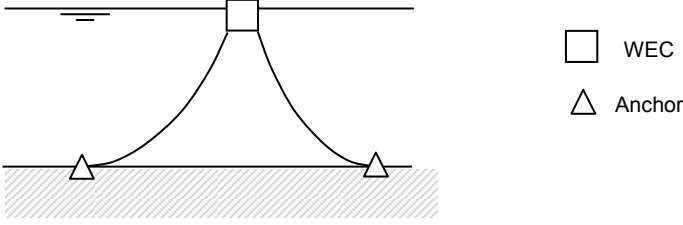
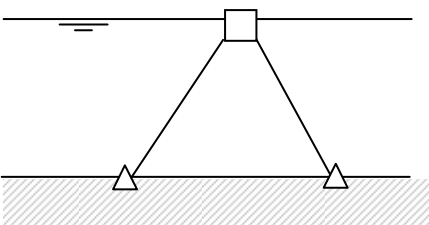
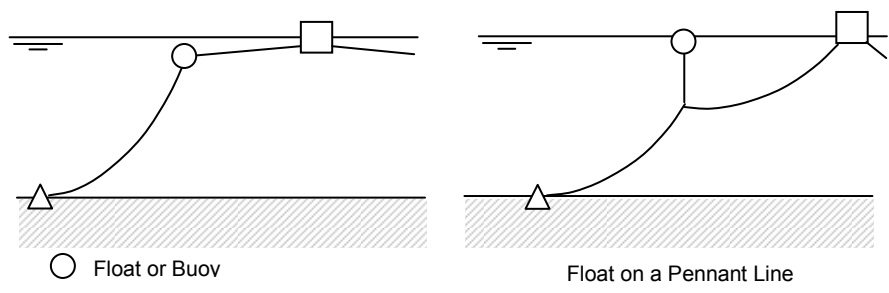
It could be expected that a hydrodynamics code (such as WAMIT) would produce comparable mean drift force to the above approximation if the WEC model were based on a simple viscous damper external force component sized to absorb an equal time-averaged power to the complete, more complex design. The specification of this as an equivalent PTO in WAMIT would not affect the calculation of the hydrodynamic coefficients and excitation force amplitudes, as these are functions of the body geometry only.

3.6.4 Moorings

Moorings for Floating Wave Energy Converters

The design of an appropriate moorings system is important in the development of floating, ocean deployed WECs. Devices are likely to be operating in energetic seas and potentially in arrays designed to efficiently exploit the wave climate over a restricted area of sea bed. The expense of moorings cables, anchor deployment and the potential for significant lengths of expensive offshore electrical cable to be taken up tracking device movement (Fitzgerald and Bergdahl, 2007), as well as long term reliability considerations add further commercial pressure to moorings system designs. From a performance perspective, WECs are designed to actively respond to, rather than passively survive wave loading: it is important that moorings fulfil their station-keeping role without significant impact on the energy absorbed by the device.

All of these factors have led researchers and device manufacturers to consider a range of different mooring strategies. Often these make use of mooring line configurations built up from a number of basic components. Some typical line configurations are shown in Table 3.3 below (Fitzgerald and Bergdahl 2007, Durand et. al 2007, CMPT 1998), however it should be noted that there is potential for use of complex mooring ‘nets’ or ‘webs’ for arrays of devices, which may contain additional line components, but are yet to be the subject of intensive research. Each line may be constructed from a range of different materials (typically chain, wire rope or fibre rope), with transition between materials occurring at any point. Float or clumped mass components facilitate the design of systems with specific loading properties and dynamic responses. Finally, line installation is dependent on an appropriate anchor, able to support the direction and magnitude of the resultant sea-bed load.

Description	Configuration
<p>Catenary Line</p>	 <p>Most basic mooring configuration, not well suited to shallow water. Anchor need only support horizontal loading. Restoring forces provided by the catenary shape created by the line weight.</p>
<p>Tension tether (Taut Line)</p>	 <p>Compliance is based on cable elasticity. Potentially a very simple, efficient approach. Requires an anchor that supports vertical as well as horizontal loading.</p>
<p>Line System with added Float(s).</p>	 <p>Floats support the mass of the mooring line and alter the angle at which it attaches to the WEC. The floats may be submerged, surface floating, or may operate both on and below the surface (creating a nonlinear characteristic as the float is dragged below the surface). The use of a pennant line to specify the float location vertically (and hence control surfacing characteristics) is likely.</p>

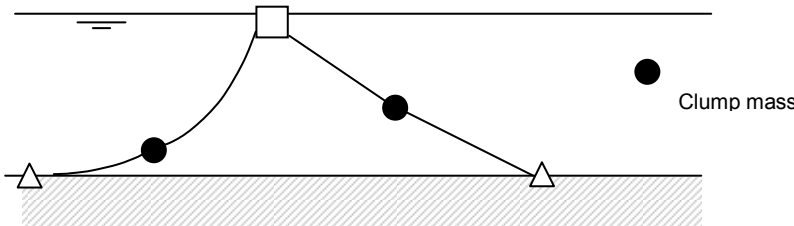
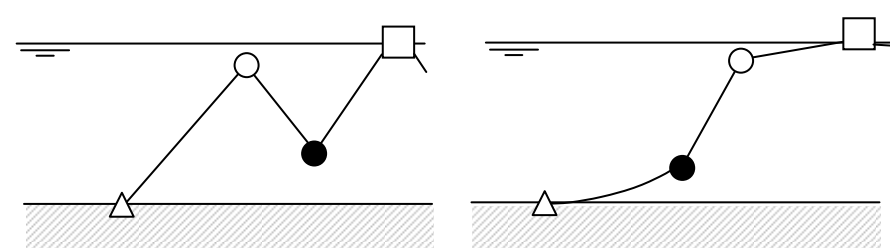
<p>Line System with added clump mass(es).</p>	 <p>Submerged clump masses to provide additional inertia and increase the vertical force component on specific sections of the line.</p>
<p>Combination of floats and clump masses</p>	 <p>A combination of floats and masses for more complete control over line static and dynamic properties.</p>

Table 3.3: Potential Moorings Configurations for WEC devices

Moorings Analysis and Modelling Techniques

Moorings systems analysis can be undertaken with both static and dynamic approaches. The separate roles of each are described below:

A **static analysis** focuses on determining the equilibrium position of the mooring line under alternative mean environmental or device loadings. The analysis is useful in providing a starting point for the specification of line lengths and materials, float and mass properties and any line pre-tensions. Design parameters should be set so that the mooring system can cope statically with extreme wave-induced off-sets. Static load-extension curves can be compiled from the analysis, which is typically based on the solution of the classic catenary equation (CMPT 1998), incorporating the static effects of line mass and hydrostatic force distributions as well as weight and buoyancy loading from clumped masses and floats.

Once a static assessment of the system is completed, it is possible to use the results as part of an otherwise dynamic system simulation by adopting a ‘quasi-static’ approach. The assumption is made that the moorings pass through a series of static equilibriums in response to motion of the WEC, so that the instantaneous moorings force can be calculated directly from the load-extension curves, which may have been implemented computationally as ‘nonlinear spring’ elements. This technique neglects

all of the dynamic forces acting in the mooring system (most notably hydrodynamic damping and inertial components) and so in the past (in the oil and gas industry) has only been applied with significantly increased safety factors (Johanning et al. 2005, DNV-OSE301 and API RP 2SK standards).

The more advanced alternative to quasi-static simulation is to adopt a *dynamic* approach once the initial statics based system design has been completed. This is now the norm in offshore structure design and is particularly important when moorings incorporate large drag elements, or water depths are great. The complete dynamic moorings partial differential equations have no analytical solution and must be solved numerically, through complex solver implementations based on finite-difference ('lumped mass') or finite element models (CMPT, 1998).

As a more immediately accessible alternative, a number of approximate formulations have been developed to account for the most dominant dynamic effects whilst providing a more readily solvable mathematical representation. Application of these is dependant on the mooring system in question: an approximate solution developed by (Polderdijk, 1985) uses a series of tests to assess whether line inertia or, more unlikely, hydrodynamic damping effects can be reasonably neglected. Similarly, a frequency-domain approach, developed by (Goodman and Breslin, 1976) and (Triantafyllou et al., 1986), involving transformation of the partial differential equations to an ordinary differential form, with linearised dynamics, is appropriate for systems where responses either side of a static equilibrium position tend to be small. Modal techniques have also been suggested; however fluid damping forces are often so large that the dynamic response to motion at the top of the line is governed by more localised axial stretching (Koterayama 1978, CMTP 1998).

The Moorings Modelling Options for the GH WaveFarmer Code

A variety of options exist for moorings modelling in the GH WaveFarmer code. The initial focus is on the impact of moorings on the performance of the WEC in power production (the GH WaveFarmer modelling tool is not at present being developed from a survivability perspective).

In the frequency-domain, moorings effects can be expressed in terms of simple damping and spring terms, obtained by linearising the moorings characteristic for wave-frequency loading at small horizontal device displacements from a nominal moored position. Calculation of the appropriate spring, damping and inertial coefficients could be performed either externally by the user, in the most basic implementation, or as a more complex pre-processing task within GH WaveFarmer. Fitzgerald and Bergdahl (2008) describe one method of distilling such characteristics from a moorings design. If more information about the state of the moorings system is required, then the frequency-domain, linearised moorings dynamic equations derived by Triantafyllou et al. (1986) could be solved numerically within GH WaveFarmer, albeit with greater computational effort. Alternatively, an interface could be created with external moorings analysis codes which use frequency-domain techniques to predict moorings dynamic effects.

An initial time-domain implementation option would be a quasi-static approach based on a force lookup on displacement using the load-extension curves produced by an initial static analysis. This initial static analysis process could be completed externally by the user, or be incorporated as a pre-processing task within GH WaveFarmer.

As the GH WaveFarmer modelling tool is developed, there would be a case for incorporating a more accurate, dynamic moorings time-domain modelling option. This would be most readily achieved through a software interface with an existing moorings evaluation code, or a more general finite element analysis tool with moorings modelling capabilities. Potential options include Orcina's

Orcaflex (Orcina Ltd.), Zentech's Zenmoor (Zentech Inc.), Marintek's 'Riflex' (DNV Software) (which is sold with Mimosa and other components as part of DNV's 'DeepC' package) or the 'MODEX' finite element tool (Fitzgerald and Bergdahl, 2007). Creation of a suitable dynamic simulation software interface would be a challenge; however Orcaflex already incorporates an option to operate as a Windows .DLL for static calculations. As a most advanced stage, GH WaveFarmer could include its own time-domain dynamic moorings model; development of an accurate, validated code would be an involved process but there is potential for collaboration with those responsible for existing modelling tools at GL Noble Denton.

In all complete time-domain dynamic simulation options, computation time is likely to be high. It may be that sufficient accuracy can be achieved through a time-domain model based on the linearised expressions developed for the frequency-domain.

In addition to the mooring line systems considered above, it is possible that arrays of WEC devices would be moored in net type arrangements, with just a few appropriately placed anchors for the complete site. Solving for moorings systems with net or web structures is beyond the foreseeable capabilities of the GH WaveFarmer tool and in these cases, the responsibility of creating a representative model for the GH WaveFarmer simulations would fall upon the user.

3.6.5 Structural Restraint Forces

The final contribution to the 'external force' term in the equations of motion is that applied due to physical, structural restraints: the forces present due to the structural connections between wave-loaded bodies, or adjacent parts of the support structure, for which the wave-induced response may not be calculated. The structural forces in their simplest form may fit a linear spring or damping characteristic and could be specified as such in the creation of the WEC model. The appropriate mathematical representations would then be solved as part of the equations of motion. At a later stage of the code development, it may also be desirable to incorporate the facility to model nonlinear restraint forces to represent more realistic connections.

Restraint force specifications will need to be provided by the user as part of the WEC design definition and the flexibility of the user interface, which must limit inputs to linear expressions only (or complete a linearisation process) for the frequency-domain, will be critical in determining the complexity of the forces modelled. Initially it is assumed that forces will be calculated explicitly, without the provision of internal states.

3.7 Equation of Motion Solvers for a Modular Simulation Tool

The modular external forces implementation outlined in Section 3.6 has an impact on the solution methodology for the time-domain simulation. Each of the external force modules may interact with the equation of motion solver in two alternative ways:

1. The full external force model is available to the equation of motion solver in state-space form and returns the external force state derivatives, $\dot{\underline{\zeta}}$ as a function of the external force and equation of motion states:

$$\dot{\underline{\zeta}} = f(t, \underline{z}, \underline{\zeta}) \quad [3.68]$$

In this case, the external force state equation can be solved in conjunction with the equation of motion; the equation of motion solver working with the combined formulation:

$$\begin{bmatrix} \dot{\underline{z}} \\ \dot{\underline{\zeta}} \end{bmatrix} = A' \begin{bmatrix} \underline{z} \\ \underline{\zeta} \end{bmatrix} + B' \underline{u} \quad [3.69]$$

$$\underline{y} = C' \begin{bmatrix} \underline{z} \\ \underline{\zeta} \end{bmatrix} + D' \underline{u}$$

Where \underline{y} is the vector of simulation outputs and \underline{u} is the input vector containing both the hydrodynamic forces, f_f and the instantaneous external forces, f_{ext} as calculated directly from the present values of the equation of motion and external force states.

2. The external force module operates in a closed format, simply returning the instantaneous external force value once supplied with the equation of motion states, \underline{z} :

$$f_{ext} = f(t, \underline{z}) \quad [3.70]$$

Any external force states, $\underline{\zeta}$ and their state derivative functions, $\dot{\underline{\zeta}} = f(t, \underline{z}, \underline{\zeta})$ are not available to the equation of motion solver but are used within the external force module to complete the calculation. In this arrangement, an external force module with internal states must incorporate its own solver to update the external force state values each time-step. The external force module solver must be controlled to exchange data at specified intervals with the equation of motion solver.

The simple mathematical expression, template and internal component library modelling options for the PTO (see section 3.6.1) may be written to fall into the first category, as may all internal WaveFarmer modelling options for the moorings, control system and structural restraint forces. PTO and mooring models built in other commercial software tools, and potentially the .DLL modelling options (depending on the .DLL format), are more may fit into the second category, however this will depend on the precise form of the interface; the distinguishing feature being whether the software returns data in the format of equation 3.68 (state derivatives) or equation 3.70.

If all of the external force modules in the simulation fit category 1, then the equation of motion solver can be readily implemented as one of many standard explicit or implicit algorithms, subject to the usual limits on solution accuracy and stability. As an example, consider the initial value problem:

$$\dot{\underline{q}} = f(t, \underline{q}); \quad \underline{q}(t=0) = \underline{q}_0 \quad [3.71]$$

where the state vector \underline{q} describes the complete system (for example the displacement and velocity of a wave activated body, as well as the external force states) at time t :

$$\underline{q} = \begin{bmatrix} \underline{z} \\ \underline{\zeta} \end{bmatrix} \quad \dot{\underline{q}} = \begin{bmatrix} \dot{\underline{z}} \\ \dot{\underline{\zeta}} \end{bmatrix} = f\left(t, \begin{bmatrix} \underline{z} \\ \underline{\zeta} \end{bmatrix}, \underline{u}\right) = A' \begin{bmatrix} \underline{z} \\ \underline{\zeta} \end{bmatrix} + B' \underline{u} \quad [3.72]$$

The 4th order Runge Kutta solution of such an equation takes the form (Iserles, 1996):

$$\begin{aligned}
 \underline{q}_{n+1} &= \underline{q}_n + \frac{1}{6} \delta (i_1 + 2i_2 + 2i_3 + i_4) \\
 t_{n+1} &= t_n + \delta \\
 i_1 &= f(t_n, \underline{q}_n) \\
 i_2 &= f\left(t_n + \frac{1}{2} \delta, \underline{q}_n + \frac{1}{2} \delta i_1\right) \\
 i_3 &= f\left(t_n + \frac{1}{2} \delta, \underline{q}_n + \frac{1}{2} \delta i_2\right) \\
 i_4 &= f\left(t_n + \delta, \underline{q}_n + \delta i_3\right)
 \end{aligned} \tag{3.73}$$

Each of the intermediate steps, i is evaluated by a call to the function $\underline{\dot{q}} = f\left(t, \begin{bmatrix} \underline{z} \\ \underline{\zeta} \end{bmatrix}, \underline{u}\right)$ defined in Equation 3.72, which is the amalgamation of Equations 3.34 and 3.68.

If some of the external force calculations instead fall into to category 2, so that not all states are visible to the equation of motion solver, then the Runge Kutta equations must solve the initial value problem using the alternative expression for the state derivatives:

$$\underline{\dot{q}} = \begin{bmatrix} \underline{\dot{z}} \\ \underline{\dot{\zeta}}_1 \end{bmatrix} = f\left(t, \begin{bmatrix} \underline{z} \\ \underline{\zeta}_1 \end{bmatrix}, \underline{u}\right) = A' \begin{bmatrix} \underline{z} \\ \underline{\zeta}_1 \end{bmatrix} + B' \underline{u} \tag{3.74}$$

Where the external force category 1 state derivatives, $\underline{\dot{\zeta}}_1$ are solved by the equation of motion solver as before, but the category 2 module states are only supplied implicitly to the state derivative calculation through their use in calculating the instantaneous external forces, f_{ext} imbedded in the input vector \underline{u} . The instantaneous f_{ext} values are now calculated in part directly from the states available to the equation of motion, \underline{q} , but also in part externally by the category 2 external force modules. As stated previously, the category 2 external force modules incorporate their own solvers (not necessarily matching the equation of motion solver) to ‘update’ the external force states $\underline{\zeta}_2$ used in the calculation. Such a formulation is complex to manage using the Runge-Kutta type method, which relies on multiple intermediate calls to the function defining $\underline{\dot{q}}$ (Equation 3.74), because the equation of motion solver must have sufficient control over the category 2 external force module solvers to complete the intermediate steps without prohibiting the external solvers from correctly working through their own solution process.

If category 2 external force modules are involved, it is simpler, and may indeed be necessary, to limit the selection of solvers to others that provide a more direct solution at each time-step. Multi-step type

solvers use previous time-step results, rather than multiple intermediate calculations, to achieve high orders of accuracy. A fourth order implementation of the linear multi-step Adams-Bashforth method (Iserles, 1996) takes the form:

$$\underline{q}_{n+1} = \underline{q}_n + \delta \left(\frac{55}{24} \underline{\dot{q}} - \frac{59}{24} \underline{\dot{q}}_{n-1} + \frac{37}{24} \underline{\dot{q}}_{n-2} - \frac{3}{8} \underline{\dot{q}}_{n-3} \right) \quad [3.75]$$

As before, the external state derivatives from category 1 modules, $\underline{\dot{\zeta}}_1$ are solved in conjunction with the equation of motion states, $\underline{\dot{z}}$ by the equation of motion solver, whilst the category 2 module states are supplied implicitly to the state derivative calculation through their use in calculating the instantaneous external forces, \underline{f}_{ext_2} :

The lack of any intermediate steps simplifies the external force interface and has a further performance related benefit, regardless of the external force module type, derived from the fact that every call to the function $\underline{\dot{q}}$ requires evaluation of all of the external and fluid forces (by whatever means). The computational time required to do this could be relatively large, particularly once delays in external force module interfaces are accounted for and, in the absence of a replacement state-space system, may also involve evaluation of the radiation forces convolution. For this reason, it is desirable to keep the number of calls to $\underline{\dot{q}}$ to a absolute minimum. The intermediate steps in Runge-Kutta type explicit integrators, and the iterative root-finding solution processes required for implicit approaches, are based on multiple $\underline{\dot{q}}$ calls each time-step, whereas a multi-step type solver requires just one, making it an appealing choice assuming stability and accuracy considerations can be met.

4 CORE ALGORITHMS: LAYOUT OPTIMISER

Arrays of wave energy converters (WECs) raise multi-disciplinary issues such as sea space usage, mooring configurations, electrical connections between devices, power transmission to land and hydrodynamic interference between individual WECs. The objective of a software package like GH Wavefarmer is to address the combined effect of all the above with other specific aspects (e.g. type of WEC, site specific issues). Building on from Section 3 of this report a review related to previous work is presented, focusing the hydrodynamic interference of WECs when deployed in arrays. The functionality to estimate the interference and optimise the layout will be implemented in the core algorithms of GH WaveFarmer.

Most studies on array interactions present results for simplified scenarios, assuming regular long-crested sinusoidal waves, linear wave theory and ignoring engineering constraints on the WEC. To extrapolate the methodology for realistic seas with irregular and directional waves and accurately estimate the net effect averaged over a typical year under realistic engineering constraints is one of the core objectives of the wave work groups of PerAWaT.

4.1 Review of Previous Optimisation Work – Arrays of WECs

The initial theoretical work relative to the modelling of arrays of WECs was carried out by Budal, Falnes, Thomas, Evans and McIver (e.g. Falnes, 1980; Thomas and Evans, 1981; McIver, 1984). It was shown that either constructive or destructive interference could occur, thus by arranging the WECs in certain patterns there could potentially be a net gain in the power output compared to N devices operating in isolation (N being the number of WECs in the array). The q -factor was defined as the ratio of the power absorbed by an array relative to the power absorbed by isolated devices:

$$q = \frac{\text{Power absorbed by the array}}{N * \text{Power absorbed by isolated device}}$$

Maximising q therefore implies two objectives:

- Maximising the effects of constructive interference;
- Minimising the effects of destructive interference.

The approaches used in the modelling of arrays of WEC have been varied and include theoretical (analytic), numerical (e.g. using commercial packages such as WAMIT or AQUADYN or adaptation of wave propagation solvers such as SWAN) and experimental methods. Most of these studies have focused on directly modelling the hydrodynamic interactions between the WEC and the wave field and are therefore geometry dependent (typically the ones that are not geometry dependent neglect some of the effects of the presence of the WECs in the wave field). Examples that overview such exercises (including optimisation of arrays of WECs with simple geometries / configurations) are presented in this Section. It should be highlighted from inception that these different key approaches are being extended, developed, implemented and compared in the PerAWaT project, via the work of the different project partners.

The hydrodynamic interactions within an array of floating offshore structures have been extensively investigated within the context of the linear wave theory. Under this theory, two classes of techniques can be broadly classified (Mavrakos and McIver, 1997; Falcao, 2008): the methods that attempt to find a numerical solution without approximations other than those involved in the truncation of a numerical

scheme and the methods that use simplifying approximations, for example based on the dimensions of the array relative to the incident wave length, before a numerical solution is attempted. Two common approximations are the “plane-wave” and the “point-absorber” approximations. The plane wave method is based on a wide spacing approximation which assumes that the device spacing is many wavelengths, whereas the point-absorber method is based on a weak-scattering approximation in which it is assumed that the wavelength is much greater than a typical device dimension. A matrix method using the plane-wave approximation to model the multiple scattering of surface waves in an array of axisymmetric WECs was developed by Simon (1982). A comparison of the calculated hydrodynamic properties of a row of vertical circular cylinders using these two approximate methods with the “multiple-scattering” method (Ohkusu, 1974) led to the conclusion that the plane-wave method does not hold for the long-wave regime while for short waves regime the point-absorber approximation becomes inaccurate (Mavrakos and McIver, 1997). However, and in agreement with previous work, it was found (Mavrakos and McIver, 1997) that in most circumstances of practical interest hydrodynamic forces can be accurately calculated using the plane-wave approximation (although such a conclusion is layout dependent). When the number of bodies is large, asymptotic approximations may be required to mitigate the computational burden associated with explicit methods (Newman, 2001). Thompson et al. (2007) developed a new method which aimed to exploit the simple geometry of a long array of equally spaced circular cylinders, referred to as large array approximation (LAA). Work on the scattering of surface waves by arrays of vertical cylinders was recently performed at MIT (Li and Mei, 2007). This is based on Bragg resonance in the physics of solid state and crystallography. This work could possibly be extended to the hydrodynamics of arrays of wave energy devices, provided that the radiated wave field is accounted for.

Due to the complexity of explicitly modelling the hydrodynamics, an alternative approach has been promoted by other authors: to model a generic WEC extracting energy at various points in the wave field and examine the wake effects. A phase-resolving model which solves the mild-slope equations and examines the effect of placing objects in the wave-field which reflect, absorb and transmit various fractions of the incident energy have been used by Beels et al. (2006). Venugopal and Smith (2007) used the Boussinesq wave model implemented in MIKE21, in order to model WEC's mounted on the sea bed. A similar approach using the spectral wave model SWAN is presented by Millar et al. (2007) and Smith et al. (2007). In all of these approaches the WEC's power absorption and radiation properties are assumed as a simulation input – meaning that in a practical scenario these would need (at best) to be calibrated against other numerical or experimental data.

The modelling of a wave farm in an adapted mild-slope wave propagation model MildWAVE studied by Beels (2006) was developed at the Ghent University and uses the mild-slope equations of Radder and Dingemans in a numerical finite difference scheme. It is applied to estimate wave propagation over uneven bottoms and wave disturbance inside a harbour. This phase-resolving model is able to generate linear water waves over a mildly varying bathymetry and to calculate instantaneous surface elevations (and velocity potential) throughout the domain. The simulation of the energy extraction of a WEC was made through sponge layers which absorb the generated and scattered waves. A sponge layer coefficient ranging from 0 to 1 determines the energy that is reflected, transmitted and absorbed. Head-on irregular long-crested waves were generated but no iteration in the layout or values of absorbed energy were presented. Also, it is unclear how the PTO control strategy on each individual WEC and other external constraints (e.g. moorings) can be implemented with this method.

Venugopal and Smith (2007) carried out a numerical investigation in the change of the wave climate around an array of hypothetical wave devices. These wave devices were modelled as porous structures with different absorption and transmission levels. The MIKE 21 suite wave models, both Spectral and Boussinesq wave models, were used for this purpose. The spectral wave model was used to obtain

phase averaged wave parameters on the area, whereas the nonlinear Boussinesq wave model was used to study the interaction between waves and an array of bottom mounted hypothetical wave energy devices. The Boussinesq model produces phase resolved outputs and is widely used for various studies in ports, harbours and coastal areas. It is noted that this model can only be applied to fixed structures and does not have the capability of handling dynamics of a moving structure. An array of five overtopping devices with dimensions of 10 m width and 160 m length was considered and the results expressed in terms of a *wave disturbance coefficient* defined as the ratio of significant wave height at a certain location in the model domain to a reference significant wave height at the boundary. The results showed a reduction in the wave heights downstream of the devices and an increase due to reflection upstream of the devices. Only one array layout was considered with no iterations on the best position of the devices. No information regarding the power output of the array was made available and only one wave heading was considered.

The approach of phase-averaged models such as SWAN presents some drawbacks as the transmission through obstacles is modelled with a proportional decrease of energy across the whole spectrum. As WECs resonate with certain frequencies in the spectrum, greater reductions in energy at these frequencies are caused and the shape of the spectrum is changed. To address this issue, Alexandre et al. (2009) applied frequency-dependent transmission coefficients in SWAN to investigate how the nearshore conditions were altered by the presence of an array of heaving point absorbers. It was observed that an incident Bretschneider spectrum is modified to a bi-modal spectrum if a wave device is tuned to match peak frequency of the spectrum. Another identified obstacle is that phase-averaged methods only account for wave energy transmission and any radiated waves are neglected. In addition to this, as the separation between WECs in an array is of the order of a few wavelengths, a phase-averaged model such as SWAN may not be applicable for modelling interactions within an array. Assuming such caveats can be surpassed, by adding the frequency dependence this approach has the potential to merge the GH and UoOx approaches with the QUB methodology, if extrapolated to the array interactions rather than investigation of the nearshore effects.

With regard to explicit approaches to estimate the hydrodynamic interactions in arrays of WECs, there have been several studies employing a combination of analytical and numerical approaches. Justino and Clément (2003) studied different array configurations made of five spherical submerged wave energy devices. Optimal and sub-optimal impedance matrices were assessed and results compared with those obtained for a single sphere. AQUADYN was used to compute the hydrodynamic coefficients in the frequency-domain. Cruz et al. (2009) investigated the influence of layout and farm control on the energy absorption characteristics of an array of vertical cylinders in both regular and irregular waves in the frequency-domain. These results were compared with a study previously presented by Siddorn and Taylor (2008) in which a semi-analytical method for an uncontrolled array of truncated cylinders was employed in order to verify the solution of the radiation and diffraction problems. Fitzgerald (2006) and Fitzgerald and Thomas (2007) evaluated the variation of the q -factor for an array of five heaving semi-submerged spheres by iterating on their relative position. The point absorber approximation was employed and exact solutions derived for a single wave frequency and angle of incidence. This work was extended and the variation of the q -factor with frequency and angle of incidence was investigated. The influence of real seas would also require that the frequency variation be assessed in conjunction with the spacing between devices. The formulation of the problem required the solution of a constrained nonlinear optimisation problem and the chosen procedure was implemented in Fortran and employed the NAG routine E04UCF. The NAG routine E04UCF searches for an optimal value of the objective function using a sequential quadratic algorithm.

Sequential quadratic programming (SQP) is one algorithm for nonlinear continuous optimisation problems. The method is based on solving a series of subproblems designed to minimise a quadratic

model of the objective subject to a linearization of the constraints. If the problem is unconstrained, then the method reduces to Newton's method for finding a point where the gradient of the objective vanishes.

An important consistency condition derived from point absorber theory has been highlighted in (Fitzgerald and Thomas, 2007), showing that the mean value of the q -factor (for regular waves) across all angles of incidence is unity for optimal motions:

$$\frac{1}{2\pi} \int_0^{2\pi} q(\beta) d\beta = 1$$

Although not directly applicable to the irregular waves case, this result highlights the importance of adapting the layout to the predominant site conditions (in a real site, dominated by swell conditions, it is unlikely that the directional spectra will show the same energy content for all directions). As a guideline, it is immediately clear that the array optimisation process should attempt to ensure strong constructive interference at a particular angle of incidence (i.e. the dominant wave direction) while minimising the regions of destructive interference at other relevant angles of incidence.

An analytic method to describe the interaction of waves with an array of two WEC devices modelled as floating truncated circular cylinders under the assumptions of linear wave theory is presented in Child and Venugopal (2007). Only regular waves are considered and an exact solution of the problem is derived in order to compute wave and body motion amplitudes. The hydrodynamic heave exciting force, the added mass and damping coefficients, and the power absorbed by each element of the array is calculated.

The work is extended by implementing a genetic algorithm (GA) optimisation and a heuristic method called parabolic intersection (PI) to search for array configurations that maximise the absorbed power for a given regular incident wave (Child and Venugopal, 2009). A GA is a directed random search technique which can find the global optimal solution in complex multi-dimensional search spaces. A GA is modelled on natural evolution in that the operators it employs are inspired by the natural evolution process (Pham and Karaboga, 2000). These operators, known as genetic operators, manipulate individuals in a population over several generations to improve their fitness gradually. The best individuals, as evaluated by the user supplied "fitness function", will either undergo a random alteration to their defining variables (mutation), exchange parameters with other highly rated individuals (crossover) or will pass on to the next generation unaltered (elitism). To solve the problem under study the individuals were taken as array configurations and their fitness assessed using an exact hydrodynamic interaction technique. The parabolic intersection method implemented in Child and Venugopal (2009) involves a combination of logic and conjecture. Some approximations are made such as considering the progressive part of either radiated or scattered waves as the principal cause of interference and neglect the remaining components. The main areas of constructive and destructive interference relative to the body will then be given by the locations where the interacting wave field is in or out of phase with the ambient incident wave field. The curves consisting of points with zero relative phases approximately form a family of parabolas, centred on the device. The procedure then consists of positioning a second device nearby on one of the curves of positive interference. Superimposing a similar set of curves around the second device on to the original pattern highlights the intersections between the families of parabolas as the locations where most positive interference is likely. The procedure is repeated until the array has been constructed.

An explicit hydrodynamic interaction technique was used to assess the performance of the resulting arrays, quantified by the power enhancing effect of the arrangement (q). The q -factor is presented for regular waves for a range of frequencies and directions. In contrast with other similar investigations where the point absorber approximation was employed and therefore the influence of diffracted waves were neglected, the effects of device scattering were included in the computations applying the theory of Garret (1971) and the interaction method of Kagemoto and Yue (1986). The inclusion of scattered waves allowed the analysis of closely spaced arrays and is presently considered one of the best available methods for performing numerical computations of wave interactions with very large arrays of structures. It was also shown that a significant reduction in performance may occur if arrays effects are not taken into account. Arrays of structures containing many thousands of individual elements or infinite arrays have been subject of study by Maniar and Newman (1997) and McIver (2001).

It should be noted that the positive interference parabolic curves are function of both the wave number and the wave heading and thus the q -factor for a specific array is also a function of the same variables. For a specific site, characterised (e.g.) by a specific directional spectrum, the choice of the array layout that provides best performance is therefore not a trivial task.

The genetic algorithm marginally outperformed the parabolic intersection method in Child and Venugopal (2009) in terms of their prescribed objective function for some cases. Nevertheless, the PI method produced some viable competitors with much less computational effort. As many configurations are possible under the PI method, it is reasonable to expect further improvements in the performance.

Closely spaced arrays have also been investigated, both numerically and experimentally. The behaviour of twelve closely spaced point absorbers in unconstrained and conditions has been analysed in irregular waves by Backer et al. (2009). Instead of optimising the device locations, this study focused on large structures containing multiple closely spaced oscillating bodies such as the Wave Star, the Manchester Bobber or the Buldra Platform (Fred Olsen). By fixing the geometry, the study aimed to determine the optimal PTO parameters. It has been shown that applying the optimal control values for one buoy in isolation to multiple closely spaced buoys results in a suboptimal solution for the array. The optimisation of the parameters of the control matrices in this numerical study in the frequency-domain was carried out with a sequential quadratic programming method. Two techniques were tested, the diagonal and individual optimisation respectively and the power absorption of the array compared for the different case studies.

Closely spaced arrays of heaving wave energy devices were also subject of experimental studies by Weller et al. (2009). The power absorption of a two-dimensional array of heaving devices in both regular and irregular waves in a wide flume was investigated showing that the presence of positive interactions is largely dependent on the incident wave period and the performance of adjacent devices. The same authors also carried out a numerical study of five heaving hemispherical bodies (Weller et al., 2009) in which different diagonal mechanical damping matrices were obtained for maximum or constant net power over a range of wave frequencies.

A theoretical analysis of the ocean wave energy absorption by a periodic linear array of oscillating water columns (OWC) has been described by Falcão (2001). A linear power take-off (PTO) mechanism is assumed with a complex characteristic constant allowing for phase control is considered. It showed that the capture width of an individual OWC can be substantially magnified by the array effect, provided that the devices are optimally phase-controlled. However, if the turbine constant is constrained to be real, the energy absorption is, at most, only marginally increased by hydrodynamic interference.

The study of arrays of WECs in the time-domain has fewer examples than the studies in the frequency-domain. Babarit (2009; 2010) studied the influence of the distance between two interacting WECs on the capture width in both regular and irregular waves. A numerical model in the time-domain was derived and the hydrodynamic coefficients calculated using a custom-made code developed by the Ecole Central de Nantes (Achil3D). Also developed by the same institute are the Smooth Particle Hydrodynamics (SPH) method for solving the Euler equations and the Spectral Wave Explicit Navier-Stokes Equations (SWENSE) approach to simulate the wave-structure interactions in viscous flow. Two identical semi-submerged heaving cylinders with hydraulic PTO were considered. It was concluded that the wave interactions were stronger on the front system and that the energy absorbed by the rear system always presented lower values. The Fast Multipole Method (Greengard and Rokhlin, 1987) is suggested as a potential alternative to cope with large arrays, an area which current diffraction potential solvers struggle to solve. It has been also suggested that the alteration of the energy absorption due to wave interaction effects decreases with the square root of the distance for regular waves although it seems to decrease at a faster rate for irregular waves. Folley and Whittaker (2009) assessed the sensitivity of the performance of a WEC array to control parameters concluding that the maximum annual average power capture is significantly reduced for irregular waves when compared to the maximum power capture for regular waves and that the optimum array configuration is also significantly modified. It also suggested that as the difference in performance between an optimal array configuration and a sub-optimal array configuration may be relatively small for irregular waves, other factors such as mooring arrangements, access requirements, smoothness of generated power and site utilisation may have a more dominant effect on the final economically optimum array configuration than the theoretical hydrodynamic optimum array configuration.

To conclude, it should be noted that a even more detailed optimisation exercise could include the optimisation of a device operating in isolation before the optimisation of the array is attempted (WEC design). A tool for the simulation, visualisation, evaluation and optimisation of the performance of a single WEC has been implemented by Weber and Thomas (2005). WAMIT was imbedded in Mathematica as an hydrodynamic solver in which different geometries were simulated with a combination of several functional arguments such as incident wave frequency range, wave direction and water depth and others geometrical, kinematic and dynamic design parameters. This tool enabled the evaluation of a sensitivity analysis about the optimised parameter set.

4.2 Review of Optimisation Techniques

The problem of multiple wave scattering effects by an array of WECs is computationally expensive for a large number of bodies as typically WEC arrays are dependent on multiple variables. These include (among others): the incident wave field (regular or irregular waves), dominant wave direction, directional spread, wave height, the control strategy adopted (PTO damping, active, passive, individual or group strategy), the type of WEC, the array layout, whether motions are constrained or unconstrained, etc.

In general, the effects of WEC on waves may include attenuation of wave height (frequency dependent), reflection of incoming waves, radiation of waves and other interactions (linear and nonlinear). The main mechanisms for recovery in the wake of WECs are the directional spread of the incident wave field, the diffraction of waves around the WEC and regeneration by wind (only significant at larger distances).

The main relevant optimisation techniques applied in the studies mentioned in the previous Section consisted on sequential quadratic programming (SQP), a method entitled Parabolic Intersection (PI) and the Genetic Algorithm (GA) technique, which belongs to the so called ‘intelligent’ optimisation algorithms. Other examples of intelligent algorithms are the Tabu Search (TS), the simulated

annealing (SA) and the artificial neural networks (ANN). In general, the objective function of these optimisation exercises is the maximisation of the q -factor value or the energy yield alone without consideration of other constraints such as distance between WECs, mooring constraints, electrical constraints, loads and individual maximum motions and / or power. In addition to this, most studies are carried out in the frequency-domain which is only able to cope with linear forces. It is known that (at least) some PTO mechanisms exhibit nonlinear characteristics. This requires detailed analysis in the time-domain but due to the computational effort this may not be suitable for an iterative procedure typical of optimisation methods. The extension of such exercises and methodologies is crucial to ensure that the objectives of WG1 are fulfilled. A non-exhaustive list of optimisation methods and commercial codes that implement these techniques is given below. Such list can be seen as a starting point to address the creation of an optimiser .DLL in the GH WaveFarmer Base Module.

4.2.1 Genetic Algorithms

A genetic algorithm (GA) is a directed random search technique which can find the global optimal solution in complex multi-dimensional search spaces. A GA is modelled on natural evolution in that the operators it employs are inspired by the natural evolution process. These operators, known as genetic operators, manipulate individuals in a population over several generations to improve their fitness gradually.

GAs do not use much knowledge about the problem to be optimised and do not deal directly with the parameters of the problem. They work with codes which represent the parameters. GAs operate with a population of possible solutions and not only one possible solution, assess the quality of already found solutions to improve them further.

4.2.2 Tabu Search

The Tabu search algorithm was developed for solving combinatorial optimisation problems. It is an iterative search algorithm and is characterised by the use of a flexible memory capable of finding the global minimum of a multimodal search space. The evaluation function selects the move that produces the most improvement or least deterioration in the objective function. A stopping criterion terminates the Tabu search procedure after a specified number of iterations have been performed either in total, or since the current best solution was found.

4.2.3 Simulated Annealing

The simulated annealing algorithm is based on the analogy between the annealing of solids and the problem of solving combinatorial optimisation problems. The algorithm consists of a sequence of iterations. Each iteration consists of randomly changing the current solution to create a new solution in the neighbourhood of the current solution. The neighbourhood is defined by the choice of the generation mechanism. Once a new solution is created the corresponding change in the cost function is computed to decide whether the newly produced solution can be accepted as the current solution. If the change in the cost function is negative the newly produced solution is directly taken as the current solution. Otherwise, it is accepted based according to Metropolis's criterion (more details can be found in Pham and Karaboga, 2000).

4.2.4 Artificial Neural Networks

Artificial Neural Networks (ANN) are modelled to simulate the mechanisms of the brain. Theoretically, they have a parallel distributed information processing structure. Two of the major features of neural networks are their ability to learn from examples and their tolerance to noise and

damage to their components. An ANN consists of a number of simple processing elements, also called nodes, units, short-term memory elements and neurons. Processing elements are connected to one another via links with weights which represent the strengths of the connections and determine the effect of the output of a neuron on another neuron. The structure of a network is determined by the way the inter-neuron connections are arranged and the nature of the connections. ANNs can be classified according to their structures and learning algorithms.

4.2.5 Particle Swarm Optimisation

The particle swarm optimisation (PSO) belongs to the class of direct methods used to find an optimal solution to an objective function in a search space. The PSO is a stochastic, population-based computer algorithm modelled on swarm intelligence. A communication structure is defined and neighbours assigned for each individual to interact with. Then a population of individuals defined as random guesses at the problem is initialized. These individuals are candidate solutions and an iterative process to improve these candidate solutions is set in motion. Movements through the search space are guided by these successes with the population usually converging on a better solution. The PSO in its basic form is best suited for continuous variables.

4.2.6 Commercial Codes

Several commercial codes have implemented some (or all) of the above optimisation techniques. Two examples are listed below; these can be seen as a guideline for the development on an optimiser .DLL in the GH WaveFarmer structure, in particular with regard to the flexibility in linking such techniques with external packages.

Friendship-Framework

The Friendship-Framework is a tool for the Computer Aided Engineering (CAE) of functional surfaces, developed by Friendship Systems, a GL company. This software allows the design and the optimisation of components in the marine industry such as turbomachinery, pumps and ship hulls, among others. It combines the geometric modelling and flow simulation allowing the optimisation of the design components with regard to specified objectives. The geometry is modelled parametrically and their physical characteristics numerically evaluated. The best geometries are then identified. Although currently applicable to the development of marine components, this parametric optimisation principle may be applicable to the design of arrays of WECs.

modeFRONTIER

modeFRONTIER is a multi-objective optimisation and design software developed by Esteco. It includes a large library of optimisation algorithms for both single and multi-objective optimisation such as Genetic Algorithms, Multi-Objective Particle Swarm, Multi-objective simulated annealing, among others. It couples different commercial tools such as Matlab and Excel as well as several CAD and engineering analysis programs. It allows multi-objective problems, i.e. where the objective functions are in conflict, resulting in a trade-off curve or Pareto Frontier where all objectives are treated separately and any of which could be considered an optimum solution.

5 IMPLEMENTATION STRATEGY

Following the overview of the proposed GH WaveFarmer structure (Section 1), the review of previous work in this field (arrays of WECs) and the description of the theoretical principles that provide the basis for the core modules (Sections 2 to 4), Section 5 outlines a draft implementation strategy. A list of the key design variables is provided in this section taking into account the conclusions originally presented in WG0 D1 (Section 5.1), along with a description of the representative scenarios to assess the applicability of the models (Section 5.2). The definitions for maximising the energy yield are presented next (Section 5.3), followed by a discussion regarding the limits of the performance models and the necessity of quantifying the boundary with a survivability model (Section 5.4). Finally, the key steps for the implementation of the frequency and time-domain models are presented in Section 5.5.

5.1 Key Design Variables

From a user's perspective, the input structure of GH WaveFarmer will need to define a series of fixed inputs while allowing iteration on a range of design variables. In addition, such iteration may follow a constrained or unconstrained optimisation exercise (in most practical cases of interest the optimisation exercise will be constrained). Penalties can also be assigned to specific characteristics, further conditioning the output of the optimiser. In summary, the following key categories can be defined:

- Fixed inputs (i.e. user inputs which are not subject to iteration for each simulation);
- Design constraints (i.e. design characteristics to be met for each simulation);
- Design variables (i.e. variables which will be iterated upon to derive the optimal array configuration);
- Objective function (i.e. the function that defines the goal of the optimisation process);
- Penalties (i.e. parameters that constrain the different objective functions).

With regard to the fixed inputs, a preliminary list of the parameters that can be grouped into this category is given below:

- WEC (geometry, type, PTO template)
- Number of WECs, i.e. the wave farm rating³
- Control methodology (passive, active or other)
- Mooring strategy (including maximum deviation from average position)
- Maximum site area (sea space usage)
- Bathymetry

³ In the advanced optimiser module it is foreseen that such parameters may migrate to the 'Design variables' category.

- Wave climate (i.e. range of sea states that describe the site conditions)

Note that by definition these inputs are fixed for each simulation. This merely implies that once a simulation is specified and started, the code will not iterate on such inputs (e.g. once the type of FDC is chosen, the simulation will not assess the possibility of having an array of different FDCs). The user can change the inputs and create a new simulation if a sensitivity study on a specific input is required.

The key design constraints to be specified prior to the optimisation process are:

- Minimum / maximum WEC distance
- Hardware limitations (note that the following list should be seen as a minimum)
 - controller limitations (range of applicable settings)
 - peak PTO and mechanical loads
 - maximum amplitude of motion
 - maximum velocity
 - peak instantaneous power
 - maximum cable export capacity
 - substations limitations / grid connection capacity

Having fixed the design characteristics and the key constraints, the optimiser is free to iterate on the key design variables (following the techniques outlined in Section 4.3). These include:

- Range of individual WEC PTO settings (i.e. control strategy for specific control methodology)
- Array layout (WEC geometrical locations)

Note that for each iteration the energy yield (or other objective function) will be computed for the full range of sea states used to describe the wave climate. The number of sea states used to describe the wave climate therefore has a significant impact on the computational effort required for each iteration of the optimiser (see discussion in Section 2).

Following the target capabilities described in Section 2.3, the GH WaveFarmer Base Module will be able to describe a site specific wave climate in a range of parameters which will be iterated upon to create a wave input database to the simulation. The definition of the required number of parameters and the quantification of their relative influence in the response of an array of WECs are the core tasks of the implementation stage with regard to the wave climate input. It will also be possible to iterate on the set of control parameters that define the control strategy (see Section 3), which in turn allows the definition of a (wave) farm control strategy. The definition of the strategy will lead to the quantification of the PTO loads associated with each WEC within the array, which can influence among other variables the O&M strategy (e.g. standardisation of the duty for each array element to ensure that the wave farm life cycle is as long as possible). The final key design variable listed above is the geometrical layout of the array, which will be iterated according to the optimisation

methodologies described in Section 4. Note that all iterations are subject to the key design constraints (see above).

Finally, the base module optimiser will include several options regarding the objective function and associated penalties. It is envisaged that for the base functionalities (Beta1 and Beta2) this will be limited to:

- Objective function
 - Maximisation of the energy yield (of the array)
- Penalties
 - Penalty for increasing distance between WECs (due to e.g. electrical cable costs)

Extensions to such base functionalities may include:

- Objective function
 - Minimisation of CoE
 - Maximisation of the life cycle (uniform PTO / mechanical duty, i.e. maximisation of the operational life by constraining the PTO operation)
 - Minimisation of the peak / average power ratio (physically such constraint may lead to an increase in the storage capacity within each element of the array, or a change in the control of the farm to maximise the average power while minimizing the peak)
- Penalties
 - Penalty with increasing number of cycles (fatigue of key components)

5.2 Outline of the Representative Scenarios

In the wave specification report (WG0 D1) a series of verification and validation case studies were presented, outlining the scenarios that will be used to verify and validate the developed software (respectively). This should not be confused with a set of representative scenarios that may be used to assess the functionalities of the GH WaveFarmer Base Module in its Beta1 and Beta2 versions; in fact, to ensure the independence between the case studies and the test scenarios, it is recommended that these differ considerably. A first outline of the representative scenarios that will be used to assess the software's functionalities is given in this Section. Note that these scenarios will be presented (with at least partial results) in D4 and D15 (A and B) as the tutorials to be included in the user manuals.

When defining representative scenarios the each category outlined in Section 5.1 should be covered. In particular:

- A range of Fundamental Device Concepts (FDCs) should be tested;
- Representative sites should be chosen with seasonal and annual descriptions (utilising appropriate long-term data sets) or their standard shape equivalents;

- In the first tests the array size should be limited to a few WECs (few MW wave farm) as this is the most likely scenario for deployment in the short / medium-term. To illustrate the full functionality of the software, a scenario that includes a large number of WECs is also defined (to be tested with the Beta2 version);
- The influence of the widest range of design variables should be assessed (e.g. array layout; PTO settings, i.e. control strategies; mooring configurations; additional constraints – e.g. electrical cable routing, min / max distance between FDCs, etc.).

This first category will show the flexibility of the developed software in its ability to assess the response of different types of FDCs. Such functionality will ensure a wide range of applicability of the software to the main end-users (e.g. utilities, investors, project developers and technology developers).

To ensure the realism of the test scenarios, and following the guidelines presented in Section 2, specific sites of interest to E-On and EDF may be used as the wave input to the simulation. Following the issue of WG1 WP1 D1B and during the implementation stage GH will engage in discussions with E-On and EDF to select the source of the data that can be used to describe the site specific long-term conditions. Given EMEC's involvement in the testing of the Beta1 version, a possibility would be to use EMEC data as part of their contribution to the PerAWaT project. Note that site specific data rather than standard shape spectra are used as the wave input to the representative scenarios the functionalities of the software will still be demonstrated, therefore the decision on which wave data to use is mostly dependent on the above mentioned dialogue with the end-users.

Furthermore, the representative scenarios should be applicable to the most immediate projects – which in terms of arrays of WECs are likely to be wave farms of relatively low rating (2 to 5MW) consisting of a small number of WECs. The coordination of work of the three partners (GH, UoOx, QUB) and the integration of the contribution from QUB on larger arrays will ensure the extension to large scale wave farms, suitable for a later stage of projects. The test of such implementation is covered in the last of the scenarios defined in Table 5.1 (scenario 6).

Finally the scenarios should cover a range of iterations in the key design variables specified in Section 5.1. As a minimum, the ability to assess (per sea state) different geometrical layouts and control strategies will be covered. The fundamental objective of addressing a range of iterations is to give the user a first indication of the potential of the software, its outputs and implications in the design of a wave farm. The recommended representative scenarios are summarised in Table 5.1. This table should be seen as a minimum to assess the functionalities of the software, allowing iterations in all key design variables (range of sea states that describe a wave climate, WEC PTO settings for each array element and array layout). In most scenarios both the mooring strategy and the bathymetry are set to the same configuration to allow cross-comparisons regarding the influence of the other fixed input and design variables. Depending on the site conditions (e.g. mean water depth) the bathymetry may or may not be relevant for the analysis. A comparison between a slack moored and a taught moored array of point absorbers is recommended (Scenarios 2 and 3 in Table 5.1) to quantify the influence of such fixed input. The influence of a penalty related to the inter-array WEC distance in Scenario 5 will also show the functionality of such category. For all the scenarios in Table 5.1 the objective function (maximisation of the energy yield) will be kept constant to allow the above mentioned cross-comparisons.

Further scenarios may address changes in specific fixed inputs (e.g. number of WECs in the array) and / or design constraints (e.g. modification of the type of hardware limitation); note that such additional studies, rather than assessing the applicability of the model to address different input conditions (an

aspect already covered in the scenarios outlined in Table 5.1), provide a sensitivity assessment suitable for specific exercises (i.e. they constitute an application exercise, not a representative scenario).

While the above methodology will allow an adequate overview of the functionalities of the developed software, it will not directly define the dividing line between the application of linear and nonlinear hydrodynamic modelling. This aspect is addressed in Section 5.3.

Table 5.1: List of Representative Scenarios

Scenario	Fixed Inputs		Design Constraints		Penalties
1	WEC type	Point Absorber	Min / Max inter-array distance	5 / 10 WEC diameters	None
	PTO template	Hydraulic			
	Number of WECs	4			
	Control Methodology	Passive			
	Mooring Strategy	Catenary Line	Hardware limitations	Max motion excursion (2 x wave amplitude)	
	Bathymetry	Flat bottom			
	Maximum Area	1km ²			
2	WEC type	Point Absorber	Min / Max inter-array distance	5 / 10 WEC diameters	None
	PTO template	Hydraulic			
	Number of WECs	4			
	Control Methodology	Active			
	Mooring Strategy	Catenary Line	Hardware limitations	A- Max motion excursion (2 x wave amplitude) B - Max PTO load (2 x nominal load)	
	Bathymetry	Flat bottom			
	Maximum Area	1km ²			

Table 5.1: List of Representative Scenarios (cont.)

Scenario	Fixed Inputs		Design Constraints		Penalties
3	WEC type	Point Absorber	Min / Max inter-array distance	5 / 10 WEC diameters	None
	PTO template	Direct-drive			
	Number of WECs	5			
	Control Methodology	Active			
	Mooring Strategy	Tension tether (Taut Line)	Hardware limitations	Max PTO load (2 x nominal load)	
	Bathymetry	Flat bottom			
	Maximum Area	1km ²			
4	WEC type	Attenuator	Min / Max inter-array distance	10 / 50 WEC diameters	None
	PTO template	Hydraulic			
	Number of WECs	4			
	Control Methodology	Active			
	Mooring Strategy	Catenary Line	Hardware limitations	Max PTO load (2 x nominal load)	
	Bathymetry	Flat bottom			
	Maximum Area	2km ²			

Table 5.1: List of Representative Scenarios (cont.)

Scenario	Fixed Inputs		Design Constraints		Penalties
5	WEC type	Attenuator	Min / Max inter-array distance	10 / 50 WEC diameters	Penalty (linear increase) associated with increasing inter-array WEC distance
	PTO template	Hydraulic			
	Number of WECs	4			
	Control Methodology	Active			
	Mooring Strategy	Catenary Line	Hardware limitations	Max PTO load (2 x nominal load)	
	Bathymetry	Flat bottom			
	Maximum Area	2km ²			
6	WEC type	Point Absorber	Min / Max inter-array distance	5 / 10 WEC diameters	None
	PTO template	Hydraulic			
	Number of WECs	50			
	Control Methodology	Passive			
	Mooring Strategy	Catenary Line	Hardware limitations	Max motion excursion (2 x wave amplitude)	
	Bathymetry	Flat bottom			
	Maximum Area	20km ²			

5.3 Definitions for Maximising the Energy Yield

The current GH WaveFarmer FD and TD code, described previously in Section 1.3, can run simulations for both regular waves and unidirectional irregular waves. The geometry input is limited to single WECs, which can have multiple connected bodies.

For the case of irregular waves the frequency spectrum can either be specified as a standard form (Pierson-Moskowitz, Bretschneider, or JONSWAP) or loaded from a file, which may contain a site specific frequency spectrum. At present the code does not run directional simulations. Moreover, there is no option to load unprocessed data such as displacement signals from a buoy or wave gauge array.

As highlighted in Section 5.1, the primary objective function of the WEC array modelling software is the maximisation of the energy yield. The methodology and definitions for the maximisation of the energy yield have been previously described in Cruz et al (2009) for the frequency-domain. GH has conducted a first study related to arrays of WECs using this methodology and assessed the influence of the control settings, sea state and array layout for a specific WEC geometry. More details regarding frequency-domain approaches, including a bibliographic review, are presented in Section 3.

In this approach the mean absorbed power is calculated by superimposing a wave amplitude spectrum to auxiliary power spectra (P_{aux}), which gives the absorbed power per square meter of incident wave amplitude (W/m^2). The auxiliary absorbed power P_{aux} is given by

$$P_{aux} = \frac{1}{2} B_m \omega^2 |\bar{\xi}|^2, \quad [5.1]$$

where $\bar{\xi} = \xi / A$ is the normalised complex amplitudes of oscillation ξ with the wave amplitude A , and B_m is the applied PTO damping. By definition the frequency spectrum $S(f)$ can be expressed by

$$S(f) = \frac{1}{2} \frac{A^2(f)}{df}, \quad [5.2]$$

thus the average absorbed power per WEC (or per array element when considering a wave farm), \bar{P}_n , under the action of irregular waves (using the superposition principle) can be given by

$$\bar{P}_n = \int 2P_{aux} S(f) df. \quad [5.3]$$

The average absorbed power by an array can be quantified by $\bar{P} = \sum_n^N \bar{P}_n$. The objective function is therefore the maximisation of \bar{P} .

Both the frequency and time-domain hydrodynamics for the GH WaveFarmer code (see Sections 3.2 and 3.3) are based on linear waves and the superposition of wave components with multiple frequencies and phases under Airy wave theory. However it is essential to distinguish nonlinear *forces* from nonlinear *waves*. The time-domain simulations in GH WaveFarmer initially assume a linear wave input whilst incorporating highly nonlinear force contributions from the external force (PTO, moorings) components (see Section 3).

Nonlinear *waves* refer to waves which do not obey the Airy principles (wave height small when compared to the wavelength and wavelength small compared to the water depth), and are particularly relevant when evaluating shallow water phenomena (e.g. cnoidal waves) and, in some cases, extreme events. Independent work conducted in several research facilities has shown that some extreme wave events, such as the 50 or 100-year wave, can be replicated by Airy wave superposition (e.g. Clauss et al., 2002; Clauss et al., 2003; Falcão, 2007) however the wave-structure interactions present in such conditions are more likely to be highly nonlinear. The applicability of both linear and nonlinear wave inputs (the nonlinear case requiring a fully nonlinear hydrodynamic forces representation) for both individual devices and arrays of WECs will be determined by comparing the results from the GH approach, described in Sections 2, 3 and 4, with those from the UoOx.

If justified, the development of a quasi-nonlinear approach will address the key aspects of potential wave-induced nonlinearities under more energetic performance sea states. The time-domain approach will firstly be based on the same principles as above, starting with the calculation of the instantaneous absorbed power per WEC. The individual WEC values will be used to derive the mean absorbed power of the array, which will be maximised for each input sea. Once the spectral wave model is coupled to the GH software following QUB's contribution (Beta2), and following the successful calibration of the sub-grid elements for a single WEC, the approach described above could be simplified (as these sub-grid elements would immediately return the average absorbed power per array element). As the average absorbed power will also be a function of the position in the array (and of other external settings such as the control strategy), the use of a sub-cluster of smaller arrays (which are assessed via the GH approach) in the context of a larger array will be necessary in a sub-grid element calibration exercise.

5.4 Performance vs. Survivability Conditions

As previously described in WG0 D1, the contribution of the partners (GH, UoOx and QUB) to the wave energy numerical modelling component of the PerAWaT project (WG1) is given in Figure 5.1.

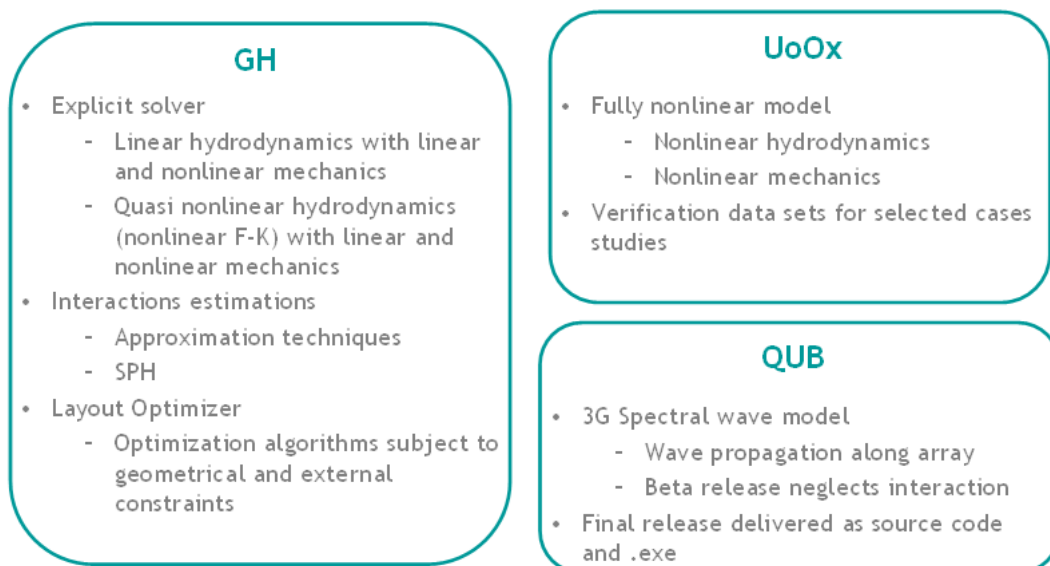


Figure 5.1: Overview of the numerical approach – WG1

As Figure 5.1 illustrates, GH will further develop a methodology based on linear and partly (quasi) nonlinear hydrodynamics (described in Section 3 of this report) while the UoOx will develop a fully nonlinear hydrodynamic model. In both approaches linear and nonlinear descriptions of the mechanically applied forces, due to the PTO and mooring system, will be implemented depending on the version of the solver (frequency or time-domain, respectively).

The main objectives of the comparisons between the models developed in WG1 by GH and the UoOx are:

- Understanding and quantifying the limitations of the linear hydrodynamics approach;
- Understanding when the nonlinear hydrodynamics are critical;
- Definition of the boundaries between a ‘Performance’ and a ‘Survivability’ model (as this is dependent on type of FDC, and UoOx are to model axisymmetric point absorbers only conclusions will be to some extent limited).

The quantification of the most energetic wave climate(s) to which the performance model can be applied will also have implications in e.g. the control strategy for the more energetic conditions. It is anticipated that for extreme seas (H_{50} , H_{100} , i.e. the 50 and 100-year return period events) the survivability model will be more accurate; however this may be irrelevant if external forces such as the PTO force are not correctly modelled for such events.

Therefore, it is recommended that in order to compare the performance and survivability response the two models approach:

- To the greatest extent possible, the same representative scenarios as outlined in Table 5.1 (UoOx nonlinear model will however be limited to point absorbers);
- Site specific conditions for more energetic seas (if using data from specific sites in the approach outlined in Section 5.2);
- As an alternative, select a standard shape for the frequency spectra and assess the response to progressively more energetic seas (e.g. influence of higher wave heights; influence of higher wave periods; influence of higher steepness ratios).

In summary, scenarios 1, 2 and potentially 3 (Table 5.1) will provide the benchmark between the model response to performance and survivability related conditions. Such input conditions will be primarily defined by sea states of increasing levels of incoming wave power. The scenarios are limited to the first three in Table 5.1 due to the computational effort: recall that the work being conducted by the UoOx (methodology described in WG1 WP1 D7) will be limited to arrays of four (potentially up to five) point absorbers. By using the GH and UoOx approach in these survivability scenarios, comparisons can be made and conclusions extrapolated to small arrays (with implications in the large array approach conducted by QUB).

5.5 Detailed Numerical Model Implementation Plan

5.5.1 Wave Data Input

As noted in Section 2, the most significant extension to the current wave modelling capabilities of the GH hydrodynamic modelling software will be the implementation of a flexible parametric method to describe the wave climate. The main difficulty in describing sea states using a limited number of parameters is that spectra often do not adhere to standard shapes, and there will be a range of different spectral shapes for a given parameter vector. Measured spectra often have multiple peaks due to the presence of a wind sea and one or more swell systems. Describing the full range of measured spectra using a limited number of parameters will inevitably simplify the real situation, so a key part of the analysis will be to investigate the significance of this simplification.

Sea states will be described parametrically by partitioning spectra into separate wave systems and fitting a JONSWAP frequency spectrum and wrapped normal directional distribution to each partition, similar to the approach taken by Kerbiriou et al. (2007). The JONSWAP spectrum can be described using three parameters: H_s , f_p and γ , or equivalently H_s , T_e and T_m (c.f. Eq. A.31 and A.32). These three parameters can be used to fit a spectrum, but this will neglect any frequency overlap of wave systems. The parametric fitting method will be compared to a least squares method, which accounts for frequency overlap of wave systems. The wrapped normal directional distribution can be described by two parameters: the mean direction and spread (see Appendices A4 and A6). This gives a vector of five parameters describing each wave system.

Once the measured spectra have been decomposed into separate systems, the data will be analysed to look for trends in the distribution of different spectral shapes. Most previous studies of wave climatology have used the bivariate H_s - T_e or H_s - T_z scatter diagram, so this will be the starting point of our analysis. Sea states will be binned by H_s and T_e and the following metrics will be calculated for each bin:

- Mean spectral shape
- RMS difference of spectra from mean spectral shape
- RMS difference of spectra from fitted spectra
- Percentage of total energy occurring in primary and secondary peaks
- Separation of peaks in frequency and direction
- Distribution of bandwidth, mean direction and spread

Previous studies have indicated that around 25% of spectra are bimodal or multimodal, but for higher sea states the relative occurrence of multimodal sea states decreases (e.g. Guedes Soares, 1991). An important part of this study will be to assess if multimodal sea states contribute significantly to the average annual WEC/array power production. The response is likely to be dependent on both the WEC and array layout, so the impact will be assessed for a both a point absorber and an attenuator in a number of different array configurations.

Ultimately, it will be desirable to reduce the number of sea state parameters used to describe WEC and array performance, so the sensitivity to various levels of parameterisation will be assessed. This will be gauged by calculating the annual energy yield using measured spectra for a full year compared to the annual energy yield calculated using:

1. A Bretschneider spectrum for each H_s - T_e bin
2. The mean spectral shape for each H_s - T_e bin
3. A number of fitted JONSWAP spectra for each bin, chosen to represent the full range of spectra (the number of spectra used for each bin will depend on the outcome of the study).

This should give an indication of the level of parameterisation necessary to obtain an accurate estimate of the annual energy yield.

5.5.2 Equation of Motion Solver – GH Multibody

The existing GH numerical modelling code is capable of solving frequency and time-domain equations of motion for a WEC model consisting of multiple rigid bodies. Each body has a nominal six degrees of freedom (surge, sway, heave, pitch, roll, yaw) but may be constrained to move in a subset of these either relative to the sea bed or relative to other bodies in the system. A first significant step in the implementation process will be to upgrade the equation of motion solver to the much more flexible, general purpose GH Multibody engine (GHMB). The GHMB code has been developed over a period of two and a half years to provide a framework for solving for the motion response, loading and deflections in systems of multiple rigid or flexible bodies (point masses, or modal, flexible members or structures) linked by user specified joints defining the structural geometry and restraint forces in the system. The code is well suited to modelling the wide variety of WEC designs currently being developed in the wave energy industry and provides a much more co-ordinated means of generating the equation of motion for a system than the current numerical code implementation. Previously in the numerical model, bodies have been defined as rigid objects constrained to move through direct manipulation of the system matrices in the equation of motion formulation; a user was required to think carefully about which degrees of freedom should be locked or constrained and in what co-ordinate system this locking should be applied. This can be a complex task for structures incorporating more than two or three moving components. It would be possible to upgrade this system to incorporate joint elements; however adopting the GHMB engine provides scope in the future to develop WaveFarmer as a tool capable of computing deflections and loading in flexible members (a much more involved task) and allows the software to benefit from the range of integrators and other modelling developments available to the established GH Bladed and GH Tidal Bladed tools.

The GHMB approach facilitates the rapid specification of the structural restraint forces in the system, and PTO, mooring and hydrodynamic forces can be specified at the bodies or hinges as ‘Applied Forces’ in the GHMB code. Each of the applied force calculation modules has access to a complete range of system states, which may be reported by GHMB in one of multiple co-ordinate systems. Applied force module state equations may still be passed to the integrator, which is separate from the core MB code, to be solved simultaneously with the equation of motion as described in Section 3.7.

5.5.3 The Hydrodynamic Model

The hydrodynamic excitation and radiation forces will be calculated in accordance with the linear theory presented in Sections 3.2 and 3.3; the time-domain radiation force expression incorporating the numerical convolution of past body velocity data with the impulse response or ‘memory’ functions for

the body geometry. The applied hydrostatic and excitation forces in the time domain remain linear, but this radiation force formulation allows nonlinear forces to be specified elsewhere in the equation of motion (such as in the PTO, moorings, control system or nonlinear joints in the structure) to induce a nonlinear WEC response akin to that expected from the complex systems employed by real WEC designs.

The initial beta releases of the GH WaveFarmer tool developed as part of the PerAWaT programme are based on the established GH hydrodynamics code. There is potential for improving the performance of this approach through the use of a system identification strategy to replace the radiation convolution integral term with a finite state-space model; the advantages of this approach, as well as a review of alternative system identification techniques are given in Section 3.3.4. The frequency-domain fitting system identification method is proposed for an initial implementation as this has been shown to produce acceptable performance in previous studies (Taghipour et al. 2008; McCabe et al., 2005) and may be readily implemented in the initial project time-frame. Alternative identification techniques may be added as the software develops and once the benefits of a state-space representation are proven.

To date, GH has used WAMIT as the hydrodynamic solver. The solver has the role of evaluating the frequency dependent hydrodynamic coefficients (added mass and radiation damping) and the wave exciting force amplitude for each of the WEC bodies. The WAMIT code also provides hydrostatic stiffness and the impulse response function data (although the latter can be readily calculated from the hydrodynamic coefficients). All of the output is tabulated in text files that can be easily read by external software. GH has compiled MATLAB code to read the WAMIT output files and initial numerical implementation work could lead to this being developed further to form a stand-alone ‘WAMIT Results Processor’ tool that converts the WAMIT data into a well-documented standard input format. Such modularisation of the WAMIT data processing allows any software user to write a plug-in to process results from an alternative hydrodynamic solver (commercial or custom-made) and keep the standard format.

In the context of more energetic sea states, the validity of a linear hydrodynamic formulation (albeit with a radiation force expression designed to cope with nonlinear external forces) remains uncertain and the limits of the established modelling approach will be assessed through a verification and validation process with the fully nonlinear data provided by the UoOx WG1 WP1 deliverables and the WG2 experimental data, respectively.

The beta releases of the software base module developed as part of the implementation deliverables WG1 WP1 D2 and D3, will incorporate power take-off, control system and moorings definition and calculation modules following the key implementation steps described in the proceeding sections.

5.5.4 Power Take-Off (PTO) Module

The PTO module will allow the user to select from two alternative mathematical PTO representations. The first of these, the *Simple Mathematical Expression, No Internal States* option, described in section 3.6.1, allows a user to compile a function of the form:

$$f_{PTO} = g(\underline{z}),$$

where the PTO force, f_{PTO} at time t is calculated as a user defined function of the body states in the equation of motion, \underline{z} . In the frequency-domain, the function g must be linear and the user interface

will be constrained accordingly (i.e. the user will only be able to specify a linearised PTO force profile). In the time-domain, the function may be either linear or nonlinear (e.g. the PTO force can depend on the square of the body velocity in one or more degrees-of-freedom). GH has existing graphical user interface code for the input of user defined mathematical expressions in the ‘Channel Combination’ post-processing tool in GH Bladed; this may potentially be adapted to meet the software specification.

The second PTO definition option to be developed in the initial implementation stage is the concept of a PTO ‘*template*’, as described in section 3.6.1. The PTO template modelling option allows a user to obtain a more accurate prediction of device performance than the simple model described above through the specification of templates that incorporate internal states to be solved for by the time domain integrator. A single template will be created initially, designed to formulate a PTO force calculation based on just one internal state, ζ as shown in Figure 3.5. The template design is described by the equations and variables compiled in Table 5.2, where the mathematical models presented are based on the concept of an incompressible working ‘flow’ which has a rate and potential associated with it. This is equivalent to a current and voltage in an electrical system, or a volumetric flow rate and pressure in a hydraulic system. The internal state, ζ is defined as the ‘*charge*’ within a flow smoothing element, Φ , which can be most readily visualised as a hydraulic accumulator or electrical capacitor type arrangement.

The individual calculation blocks have been defined to characterise the core functionality of the PTO. A typical PTO is responsible for transforming the absorbed energy from the irregular, oscillatory form delivered by a wave-driven actuator into a smooth, rectified form for use by the generator; the first template presented in Table 5.2 reflects this. The generator electrical model is very simple in this template (although the user may define a more complex model within limits) and this block is likely to be developed as the tool evolves, potentially incorporating some of the more detailed electrical modelling options provided in the most recent versions of GH Bladed. A PTO template can approximate the characteristics of some PTO designs, but is not intended to model individual component performance: the aim is simply to produce a more realistic instantaneous power take-off force output value, f_{PTO} as well a more reliable estimate of absorbed energy. Systems based on very different operating principles will be most readily modelled using a range of PTO template designs; for example, a direct-drive WEC or other design making use of very different PTO technologies may require a completely new template to that presented in Figure 3.5 and Table 5.2 in order to accurately recreate its operating characteristics. It is proposed that a library of templates be built up as necessary over time. This type of approach is synonymous with the range of powertrain models available in the GH Bladed wind turbine modelling software, which has become an industry standard tool for performance assessment and load calculation in the wind industry.

The template calculations outlined in Table 5.2 can be solved in conjunction with the equation of motion by calling the charge state derivative calculation (as defined in the smoothing element) during the equation of motion numerical integration process. All of the other system variables are either control signals or explicit functions of the present system state. Where multiple mathematical models have been provided, the user will be given the option to select one option for use. These typically include a user defined option, where the user may enter explicit mathematical expressions based on the inputs and outputs of template blocks. Each of the template calculations will be implemented in practice as a software function that can be called to return the output variable as calculated from a number of fixed inputs (as detailed in the fixed calculation formats in Table 5.2) and potentially a number of locally defined parameters.

The above PTO implementation options represent the first phases of the PTO module development only. At a more advanced stage, the template option will act as the baseline specification for the .dll format to be generated by technology developers to override the PTO and control modules, i.e. when not using the tool to optimise such aspects, relying purely on the information supplied directly by the technology developer (note that the first '*Simple Mathematical Expression*' option can also provide some simple flexibility of a similar form to the .dll whilst the complete .dll interface is being developed).

Table 5.2: Governing calculations for the initial PTO template. The template is designed to describe a hydraulic or electrical rectification and smoothing type arrangement.

Actuation			
User Defined Parameters			
<i>Name</i>	<i>Symbol</i>	<i>Description</i>	
Flow Coefficient	C_F	Simple velocity coefficient used to calculate PTO ‘flow’ rate	
Control Parameters			
<i>Name</i>	<i>Symbol</i>	<i>Description</i>	
Actuator Locking	I_{LOCK} B_{LOCK}	Variables used to ‘lock’ actuator motion by applying a damping B_{LOCK} whenever the Boolean parameter I_{LOCK} is set to ‘true’.	
Control Flow Coefficient	C_{FC}	Controller defined flow coefficient term. Used to mimic discreet actuator switching or other form of variable flow actuation.	
Inputs and Outputs (I/O) (Working Variables)			
<i>Name</i>	<i>Symbol</i>	<i>I/O</i>	<i>Description</i>
EOM States	\underline{z}	I	Equation of motion states – typically body displacement, z_1 and velocity, z_2 .
Actuation Potential	Γ_A	I	Potential Difference across actuator
PTO Force	f_{PTO}	O	Instantaneous power take-off force output.
Actuator Flow	Q_A	O	Energy carrying flow rate out from actuation component.
Calculations – User may select from multiple calculation models if available			
<i>Calculation Name</i>	<i>Model Number</i>	<i>Model Description</i>	
Actuator Flow	1	$Q_A = (C_F + C_{FC})z_2$	
	2	User Defined. Format must fit: $Q_A = f(C_F, C_{FC}, \underline{z})$	
PTO Force	1	$f_{PTO} = (C_F + C_{FC})\Gamma_A + B_{LOCK}z_2$	
	2	User Defined. Format must fit: $f_{PTO} = f(C_F, C_{FC}, \Gamma_A, \underline{z}, B_{LOCK})$	

Rectification Circuit			
User Defined Parameters			
<i>Name</i>	<i>Symbol</i>	<i>Description</i>	
Rectification Volumetric Proportional Flow Loss Coefficient.	η_{RV}	Proportional loss coefficient. Allows user to specify a flow loss in proportion to the charge in the smoothing circuit and the actuator flow. Loss is representative of a leakage in a hydraulic system.	
Rectification Constant Flow Loss	Q_{L-RC}	Constant flow leakage loss regardless of pressure or flow rate.	
Rectification Resistance	R_R	Flow resistance due to valves or resistors in the rectification circuit.	
Control Parameters			
<i>Name</i>	<i>Symbol</i>	<i>Description</i>	
Control Resistance	R_{RC}	A controllable flow resistance.	
Control Potential	Γ_C	Additional controller induced actuator potential	
Inputs and Outputs (I/O) (Working Variables)			
<i>Name</i>	<i>Symbol</i>	<i>I/O</i>	<i>Description</i>
Actuator Flow	Q_A	I	Energy carrying flow rate out from actuation component.
Smoothing Potential	Γ_S	I	Potential difference across generator power-train. Maintained by smoothing circuit.
Actuation Potential	Γ_A	O	Potential difference across actuator
Smoothing Flow	Q_S	O	Energy carrying flow rate out into smoothing circuit.
Calculations – User may select from multiple calculation models if available			
<i>Calculation Name</i>	<i>Model Number</i>	<i>Model Description</i>	
Actuation Potential	1	$\Gamma_A = \Gamma_S + Q_A R_R + Q_A R_{RC} + \Gamma_C$	
	2	User Defined. Format must fit: $\Gamma_A = f(\Gamma_S, R_R, R_{RC}, Q_A, \Gamma_C)$	
Smoothing Flow	1	$Q_S = Q_A - C_{L-RP} Q_A \Gamma_S - Q_{L-RC}$	
	2	User Defined. Format must fit: $Q_S = f(C_{L-RP}, Q_{L-RC}, Q_A, \Gamma_S)$	

Smoothing Circuit			
User Defined Parameters (Note than in this case, use is dependant on calculation selection)			
<i>Name</i>	<i>Symbol</i>	<i>Description</i>	
Accumulator Pre-Charge Potential	Γ_0	Pre-charge pressure for the gas accumulator model.	
Accumulator Size	Φ_0	Total accumulator volume for the gas accumulator model.	
Capacitance	C_y	Capacitance for the electrical model.	
Other User Defined Parameters	$C_{SU_1}, C_{SU_2}, \dots$	User defined constants for use in a user defined smoothing model.	
Control Parameters			
<i>Name</i>	<i>Symbol</i>	<i>Description</i>	
User defined control variable	V_{SU_1}	Control variable for use with a user defined smoothing potential mathematical model.	
Inputs and Outputs (I/O) (Working Variables)			
<i>Name</i>	<i>Symbol</i>	<i>I/O</i>	<i>Description</i>
Smoothing Flow	Q_S	I	Energy carrying flow rate into smoothing circuit.
Consumption	Q_C	I	Energy carrying flow passing though the generator power train.
Smoothing Potential	Γ_S	O	Potential difference across generator power-train. Maintained by smoothing circuit.
Calculations – User may select from multiple calculation models if available			
<i>Calculation Name</i>	<i>Model Number</i>	<i>Model Description</i>	
Net Smoothing Flow	1	$Q_{S_NET} = Q_S - Q_C$	
Smoothing Potential	1	Gas Accumulators System (Polytropic) $\dot{\Phi} = Q_{S_NET}$ $\Gamma_S = \Gamma_0 \left(\frac{\Phi_0}{\Phi_0 - \Phi} \right)^n$	
	2	Electrical Capacitor System $\dot{\Phi} = Q_{S_NET}$	

		$\Gamma_S = \frac{\Phi}{C_y}$
	3	User Defined. Format must fit $\dot{\Phi} = Q_{S_NET}$ $\Gamma_S = f(\Phi, V_{SU_1}, \dots)$
States		
<i>State Name</i>	<i>Description</i>	<i>State Derivative Calculation Name</i>
Charge, Φ	Quantity of fluid or charge stored in the smoothing circuit.	Smoothing Potential

Load Drive Element			
User Defined Parameters			
<i>Name</i>	<i>Symbol</i>	<i>Description</i>	
Load Resistance	R_L	Loading on the generator drive components.	
Smoothing Outflow Resistance	R_{OUT}	Resistance to outflow from the smoothing model.	
Powertrain Mechanical Efficiency	η_{DM}	'Mechanical' efficiency of generator drive componentry.	
Powertrain Volumetric Efficiency	η_{DV}	Volumetric efficiency of generator drive componentry.	
Control Parameters			
<i>Name</i>	<i>Symbol</i>	<i>Description</i>	
Powertrain Control Resistance.	R_{DC}	Control resistance used to modulate flow to the powertrain.	
Maximum Consumption	Q_{DC_MAX}	Controller applied limit on the powertrain flow consumption.	
Inputs and Outputs (I/O) (Working Variables)			
<i>Name</i>	<i>Symbol</i>	<i>I/O</i>	<i>Description</i>
Smoothing Potential	Γ_S	I	Potential difference across generator power-train. Maintained by smoothing circuit.
Consumption	Q_C	O	Energy carrying flow passing though the generator power train.
Generator Power	P_G	O	Generator Drive Power
Calculations – User may select from multiple calculation models if available			
<i>Calculation Name</i>	<i>Model Number</i>	<i>Model Description</i>	
Consumption	1	$Q_C = MIN\left(\frac{1}{\eta_{DV}} \frac{\Gamma_S}{R_{OUT} + R_L + R_{DC}}, \frac{Q_{DC_MAX}}{\eta_{DV}}\right)$	
Generator Drive Power	1	$P_G = \eta_{DM} \eta_{DV} Q_C \Gamma_S$	

Efficiency (Electrical Generator)			
User Defined Parameters			
<i>Name</i>	<i>Symbol</i>	<i>Description</i>	
Generator Efficiency	η_{GEN}	Electrical generator efficiency.	
User Defined Parameters	$C_{SU_1}, C_{SU_2}, \dots$	User defined constants for electrical generator model. May be used to describe power electronics effects thereby providing a more comprehensive model of the generator and power converter until a more sophisticated electrical model is available.	
Inputs and Outputs (I/O) (Working Variables)			
<i>Name</i>	<i>Symbol</i>	<i>I/O</i>	<i>Description</i>
Generator Power	P_G	I	Generator input power
Electrical Power Output	P_E	O	Electrical power output
Calculations – User may select from multiple calculation models if available			
<i>Calculation Name</i>	<i>Model Number</i>	<i>Model Description</i>	
Electrical Power Output	1	$P_E = \eta_{GEN} P_G$	
	2	User defined model $P_E = f(P_G, C_{SU_1}, C_{SU_2}, \dots)$	

5.5.5 Control System

The PTO implementation options will each be supported by a control strategy implementation as described in Section 3.6.2. In the case of the simple mathematical expression PTO model, a control force, f_C will simply be imposed on the uncontrolled PTO force calculation output, f_{PTO_U} so that a controlled instantaneous PTO force value, f_{PTO_C} , is returned to the equation of motion. The control force, f_C may be a function of the equation of motion states, the uncontrolled PTO force value and the incident or past wave data, W :

$$f_{PTO_C} = f_{PTO_U} + f_C(z, f_{PTO_U}, W). \quad [5.1]$$

If the PTO force function is linear, then the form of f_C may be calculated by the software to approximate one of the idealised control strategies described in Section 3.6.2: constant reactance tuning, complex conjugate control, or latching. The user will be able to select which option is implemented through the user interface and, for a time-domain, irregular waves simulation, will have the option of either a passive or active strategy for the constant reactance tuning. In the passive case the control strategy is optimised for a single, user supplied sea state, whilst the active case will conduct a frequency analysis of the short-term future or past wave data to determine a closer to optimal control strategy for the wave conditions being experienced (whilst keeping the control strategy to a single term, the applied PTO damping).

In the constant reactance tuning and complex conjugate control formulations, the applied control force, $f_C(z, f_{PTO_U}, W)$ will be calculated to fill the damping and, in the case of complex conjugate control, reactance deficit between that provided by the PTO and the optimal case values described in Section 3.6.2. The latching implementation will be through the application of a large, user-defined damping to the PTO force as the velocity in the PTO mode crosses zero. The damping force will be applied until a certain time before the peak wave excitation force is experienced. The exact release timing will depend on the wave amplitude and will initially be determined using a lookup table that will in turn be optimised over time through the synchronisation error in peak PTO mode velocity and peak excitation force amplitude.

Note that in all cases, the automatic GH WaveFarmer control will only approximate the ideal case as possible additional nonlinearity in the moorings system may have an impact on performance.

A user specifying a nonlinear PTO expression will always be responsible for manually defining the control strategy through the creation of a MATLAB function that completes the $f_C = f(z, f_{PTO_U}, W)$ calculation in Equation (5.1)

A template PTO can support more complex control logic based on the template defined control variables. The control logic will be specified by the user in a control system .dll, which will allow external parties to develop (in-house) WEC specific templates once a complete .dll interface is developed over the course of the project (it is not envisaged that this option will be available in time for the beta1 release).

5.5.6 Moorings Implementation

A moorings system is required to oppose the mean wave drift force acting on a WEC device. The user will initially be able to select between two alternative moorings implementation options in the time-domain. The first, which will be the only frequency-domain option, is a simple linear dynamic model which takes the form:

$$f_{\text{moorings}} = M_{\text{moor}}\ddot{x} + B_{\text{moor}}\dot{x} + K_{\text{moor}}x$$

where x is the body displacement matrix, M_{moor} is a moorings inertial coefficient, B_{moor} an effective linear damping value and K_{moor} an effective stiffness. Each of the moorings system coefficients, which may be referred to in a combined way simply as a ‘moorings impedance’, will need to be determined externally by the user in an approach similar to that suggested by Fitzgerald and Bergdahl (2008), which aims to linearise the system properties about an operating point. A linear moorings model of this form will be solved directly as part of the equation of motion solution process and the impedance coefficients, M_{moor} , B_{moor} and K_{moor} will need to be entered as values representing the effects of the complete moorings system on the motion of each body about its centre of mass.

The second option, applicable to the time-domain only, is a quasi-static approach whereby the reaction force produced by each of the mooring lines in response to the displacement of the WEC from its equilibrium position is calculated from a lookup table, or nonlinear mathematical expression, describing the static displacement-force relationship. Multiple lookup tables or a number of alternative expressions may potentially be provided for operation about a number of different equilibrium positions. This approach neglects system dynamics, but means that nonlinear moorings characteristics can be incorporated to some extent. The quasi-static model would allow the effects of individual lines on the WEC to be accounted for independently, a user being able to specify the seabed anchoring position and attachment point on a body (relative to the body’s centre of mass) for each line element. The quasi-static assumption means that during simulation, each mooring line may be assumed to provide a force vector in a plane that is perpendicular to the nominal (undisturbed) free-surface and that passes through the attachment and anchoring point locations. The angle in this plane at which the force is applied is dependent on the length of the line and the instantaneous straight line off-set of the attachment point from the anchoring point at a given simulation time. At each time-step, the equation of motion solver may call a ‘quasi-static moorings’ function, passing the body displacements in the global coordinate system as arguments. These will then be used to calculate the global position of the mooring line attachment point, which in turn will yield the angle (calculated using the line length, neglecting line stretching) and magnitude of the applied moorings line force (provided by the quasi-static displacement-force lookup).

As the software develops, it is expected that there will be an increased requirement for more advanced mooring models. GL Noble Denton, another member of the GL Group have developed a frequency domain dynamic moorings package called ROMEO which may potentially be incorporated to provide a more accurate moorings representation for frequency domain calculations. The requirement for a software link with or the development of a full time-domain moorings simulation model will also be investigated.

5.5.7 Optimiser Implementation

The optimiser module will be designed to allow users to create and optimise wave farm layouts and estimate their energy yields whilst obeying a range of user-defined physical and technical constraints.

Three initial methodologies have been envisaged. These are introduced and detailed in this Section and classified as ‘scenarios’. Note that the numbering of such scenarios is associated with the beta releases: scenarios 1 will be incorporated in the Beta 1 version while scenarios 2 will only be available in the Beta2 version (which will also, by default, incorporate the approaches implement for Beta1).

Scenario 1A method can be considered as the baseline tool for the optimisation process and serves as a verification tool for other alternative optimisation methodologies such as 1B and 2A. The formulation of the optimisation module requires several data inputs which are summarised below. Note that these will depend on the methodology under use.

- Array geometry (initial seed or fixed layout)
- Specification of the site wave climate
- Definition of the control methodology
- Additional constraints

The optimiser model will include several sub-routines which will require the above data to be provided by the user. A more complete description of the proposed sub-routines and the information required to the use is described next.

Baseline Methodology: Scenario 1A

Scenario 1A is effectively an exhaustive search tool where all possibilities are sequentially tested in order to determine the best solution which respects the input constraints. The solution will include the locations of the devices in the array and their PTO damping settings. The key functionalities are highlighted in Figure 5.2

Among the above mentioned sub-routines, the layout generator tool will define the physical area and geographical locations available for device placement. The model will assume that every WEC in a layout should be in a grid point as defined by the layout generator. For a sufficiently fine grid, the grid points can be sufficiently close so that the search area can be considered as approximately continuous (i.e. the possible locations account for any position in the available sea area).

1. Fixed array layout

The layout generator will also allow the evaluation a fixed layout in which the coordinates are defined by the user. This should be seen as a particular case of the optimisation problem where the array layout is not considered a variable but rather an input from the user. In this case, the model will not iterate on the locations of the devices, limiting the optimisation exercise to other variables such as the farm control strategy. Such option also allows direct comparisons between the outputs of the software and known, analytical solutions (verification exercises).

2. Geometrical input data

For the general case where the WEC position coordinates within the array are to be optimised, the following geometrical information should be provided by the user:

- Number of WECs in the array
- The wave farm boundaries (maximum sea space usage)
- The minimum and maximum inter-WEC separation distances
- Grid resolution
- Water depth

An initial grid resolution of 25m will be assumed by default and a grid over the sea space usage created. The WEC positions will be limited to these grid points. It should be noted however that this grid resolution may change depending on the size of the sea space available, the number of devices or even the dominant incident wave length and therefore it should be investigated the effect of these on the calculations. The grid size will be a compromise between computational effort, running time, storage requirements and accuracy and therefore this value will be primarily linked with the available sea area so that the total number of grid points is not excessive. It is acknowledged that this feature will impact the accuracy of the model and therefore other grid resolutions will be tested in order to verify its suitability.

The grid resolution will ultimately be better described as a proportion of the incoming wave length. It should be noted however that offshore floating WECs are expected to present surge and sway motions which are limited by the respective mooring configurations. This will affect the WEC instantaneous location over time, and thus the average position shall be considered.

With the geometrical input data defined above, the model will create a database of all possible combinations of array layout configurations. The total number of possible combinations will be given by:

$$G = nC_w = \binom{n}{w} = \frac{n!}{w!(n-w)!},$$

where n is the total number of grid points and w the number of WECs. It is assumed that the order is not important which is equivalent to consider that the WECs have all similar geometries (i.e. the wave farm is made of n equivalent WECs).

The locations that violate the minimum inter-device separation distance or exceed the maximum inter-device separation distance must be subtracted to G . The final number of possible combinations of device locations is therefore G_c . The layout generator routine will consider the G_c viable layout configurations and output such information to a data file (which corresponds to the geometrical input database).

The following step is to create G_c mesh layout for input in the flow solver (WAMIT). Parametric tools will be used to allow this procedure to be more time effective.

3. Wave climate inputs

It is expected that the optimum array configuration (array locations and device PTO settings) for a given sea state will be sub-optimum for another sea state. For that reason, and when evaluating the performance of an array at specific site, the model should be able to iterate over different sea states allowing a weighted average to be computed for a user-defined, site specific wave climate. Similarly, regular waves must be allowed as input to facilitate investigations on e.g. particular effects for specific frequencies and directions and comparisons with initial tank testing data.

As a minimum, the following data should be specified by the user:

Regular Waves

- Range of wave periods
- Range of incidence wave headings

Irregular Waves

- Range of sea states (representative of the wave climate at the site) – see Section 5.5.1

In the baseline methodology (Scenario 1A), a hydrodynamic flow solver such as WAMIT will run once for each of the G_c layout scenarios. The following outputs will be available as a result of such simulations:

- Hydrodynamic coefficients (added-mass and hydrodynamic damping)
- Exciting forces
- Free-surface elevation at field points
- Fluid velocity vector at field points
- The above outputs are a function of the wave frequency and layout coordinates for a each element of the geometrical input database.

4. Control methodology

The software will use WAMIT outputs along with data defined by the user to evaluate the performance of the array. The following data should be loaded by the user when setting-up the model:

- WEC definition (e.g. locked modes – hinged joints, sliding joints, etc.)
- Power Take-Off (PTO) setting (e.g. damping range) per array element
- Control strategy (e.g. passive, active, complex conjugate, etc.)

For each layout configuration, incident wave frequency and heading, the software will iterate and find the optimum PTO settings that maximises the power output within the constraints defined by the user.

The outputs of each run will include the displacement response amplitude operators (RAOs), average absorbed power of each device, relative capture width (RCW) and PTO optimal settings.

Once these outputs are available, the wave climate representative of the site will be considered (superimposed) and the PTO and array layout configurations that lead to the highest absorbed energy yield will be saved to an output file.

5. Constraints

From an engineering design perspective it is highly recommend to limit the optimisation exercise to a feasible range with regard to each design variable. Therefore the model should verify that the solution respects user-defined constraints before considering the solution as valid. Some constraints have been defined earlier such as inter-devices distances or sea space usage. However, other constraints may be relevant, namely those related to the WEC itself. These include:

- controller limitations (range of applicable settings)
- peak PTO and mechanical loads
- maximum amplitude of motion
- maximum velocity
- peak instantaneous power
- maximum cable export capacity
- substations limitations / grid connection capacity

Only the iterations that meet these constraints will be considered as valid potential solutions.

Advanced Methodology: Scenario 1B

An advanced version of Scenario 1A is planned for Scenario 1B. It is expected that if the number of G_c layout scenarios is significant, the required computational time can become prohibitively large. A more intelligent iterative procedure will therefore be required.

In Scenario 1B the model will run only for a subset of layout scenarios when compared to Scenario 1A. The subset of the G_c layout scenarios to be iterated will be selected according to critical variables such as the radiation pattern of the WEC. Additional selection criteria will be further investigated and coupled with the optimisation algorithms described in Section 4.2. As the number of layout configurations reduces, it is expected that the model will converge faster to the optimum solution. This optimum solution should be equivalent to the solution found in Scenario 1A if the same input data was used (e.g. if only one, fixed layout was being assessed, scenarios 1A and 1B should yield the same results if the subset of layouts includes the optimal layout).

Stand-Alone Methodology: Scenario 2A

Scenario 2A is expected to further develop the previously described methodology. Under this method, WAMIT is used once for each WEC (single unit) and its outputs saved in a database which can be loaded at a further stage when necessary. The information is compiled in a database and subject to the agreement of the developer may be used by third-parties when evaluating a wave farm with such technology (similarly to what occurs in wind energy with a power curve). This is expected to represent a significant save on the computational time of the optimisation procedure.

In contrast with the previous scenarios where the hydrodynamic interactions between devices are evaluated in WAMIT, these will be calculated within the optimiser module in scenario 2A. The interactions can be evaluated applying the superposition principle (Airy linear theory) but may also be estimated through approximations techniques such as plane-wave or point-absorber methods. It is anticipated that such methodology will feed directly into the work of QUB (calibration of sub-grid elements for small cluster of wave farms), allowing the extension of the software for large arrays.

Note that the layout generator module will be embedded in the based module of the software in Scenario 2A. An intelligent optimisation algorithm is expected to be included in the model. Potential optimisation algorithm candidates include Genetic Algorithms (GA), Simulated Annealing (SA), Tabu Search (TS), Neural Networks (NN), Sequential Quadratic Programming (SQP) or Parabolic Intersection (PI). The applicability of these optimisation algorithms must be fully investigated before conclusions are reached, which will lead to the coding of several alternatives.

Stand-Alone Methodology: Scenario 2B

In its final form the optimiser module will incorporate the work of QUB. This involves the use of phase-resolving or phase-averaged models in which a WEC is modelled as a sub-grid element (source / sink) at certain locations of the wave field. The previous scenarios will feed calibrated terms for smaller arrays (sub-clusters) which will allow the calibration of the above mentioned sub-grid elements. As in scenario 2A, the information (calibrated terms) is compiled in a database and subject to the agreement of the developer may be used by third-parties when evaluating a wave farm with such technology. Examples of such models are MildWave, SWAN or MIKE21. Scenario 2B will share with scenario 2A the search engine, i.e. the optimisation algorithms. The limits of applicability of such models will be investigated specifically in WG1 WP2 and WG2 WP2.

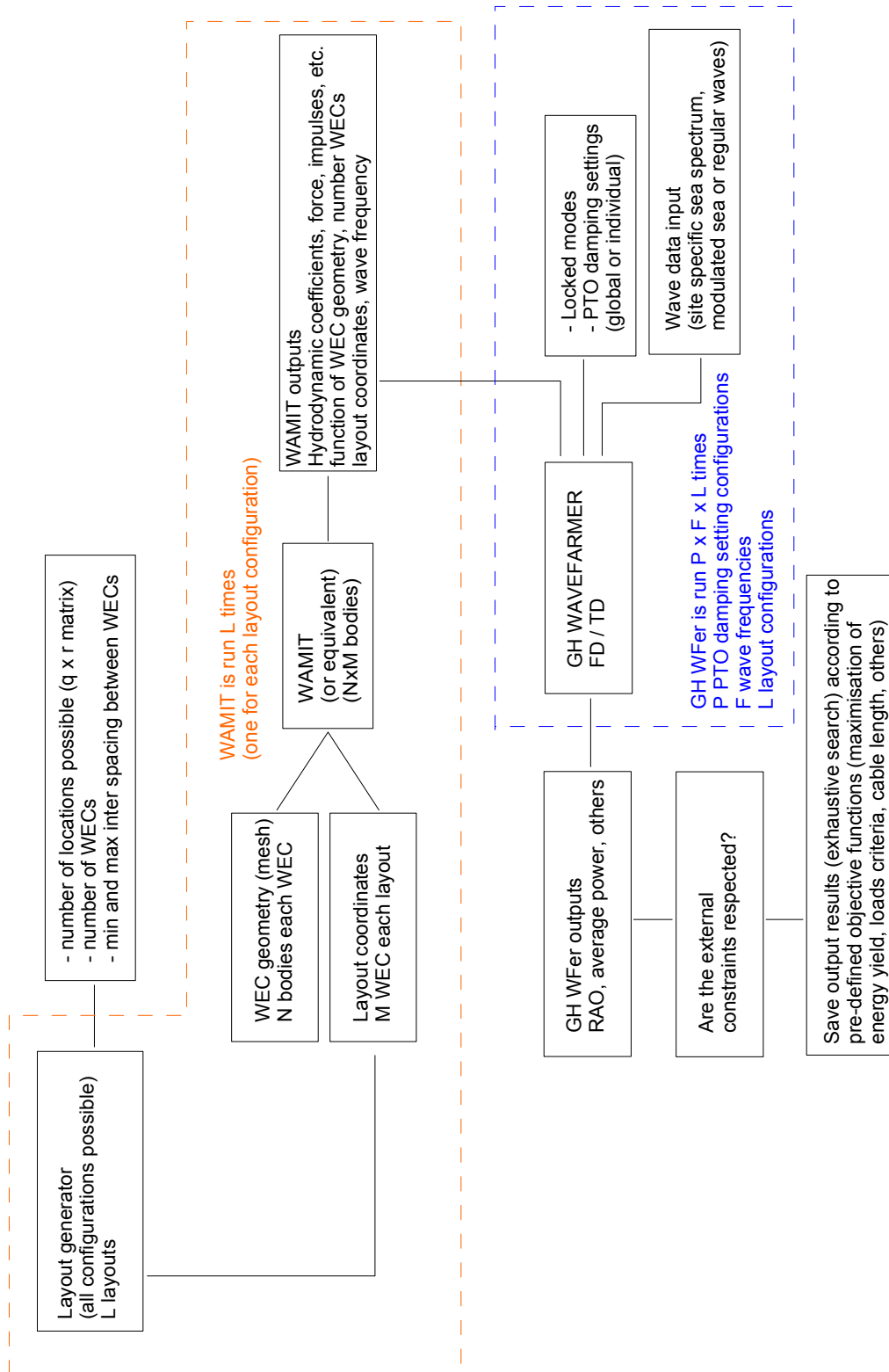


Figure 5.2: Flowchart – Optimiser I/O structure (Scenario 1A)

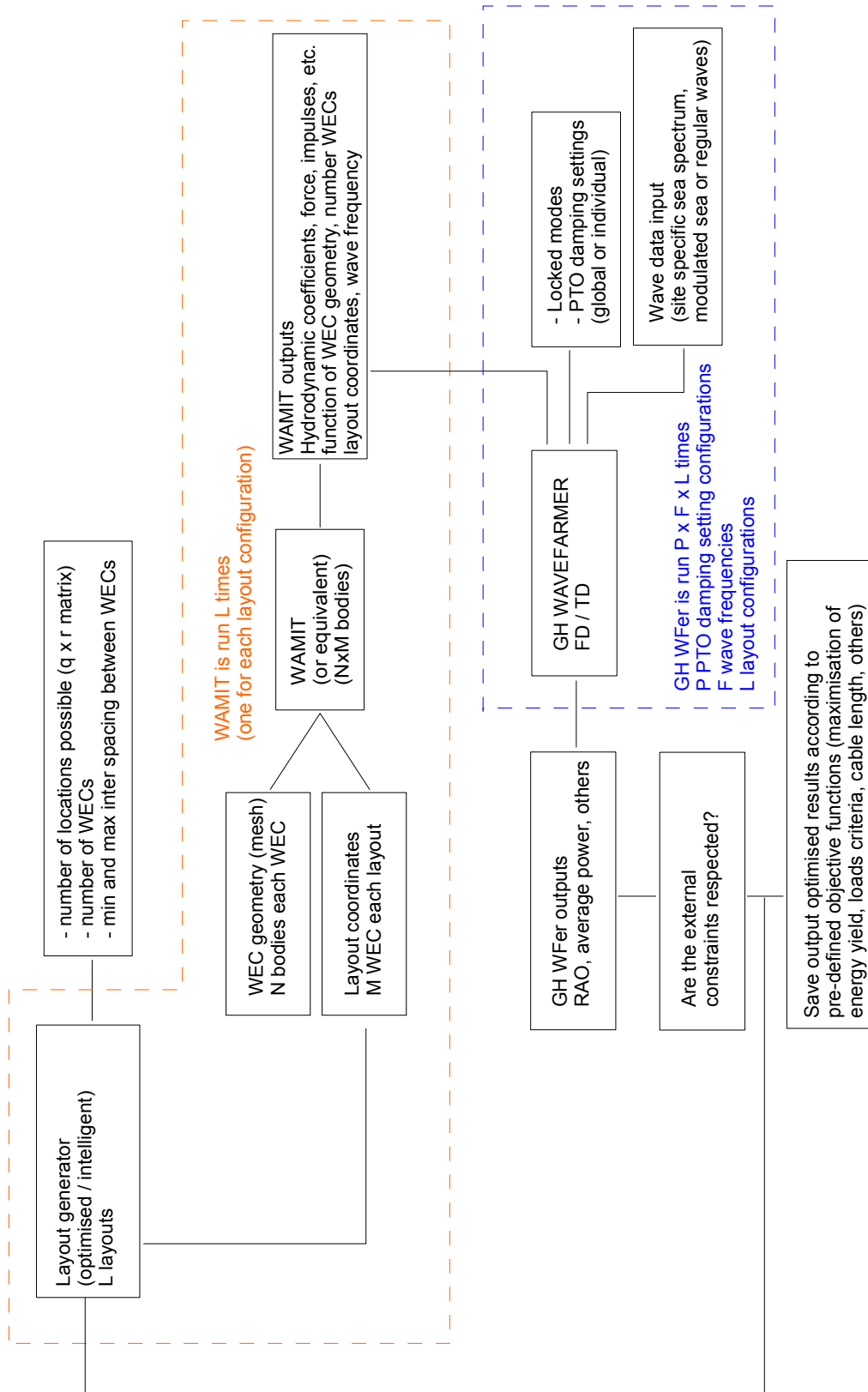


Figure 5.3: Flowchart – Optimiser I/O structure (Scenario 1B)

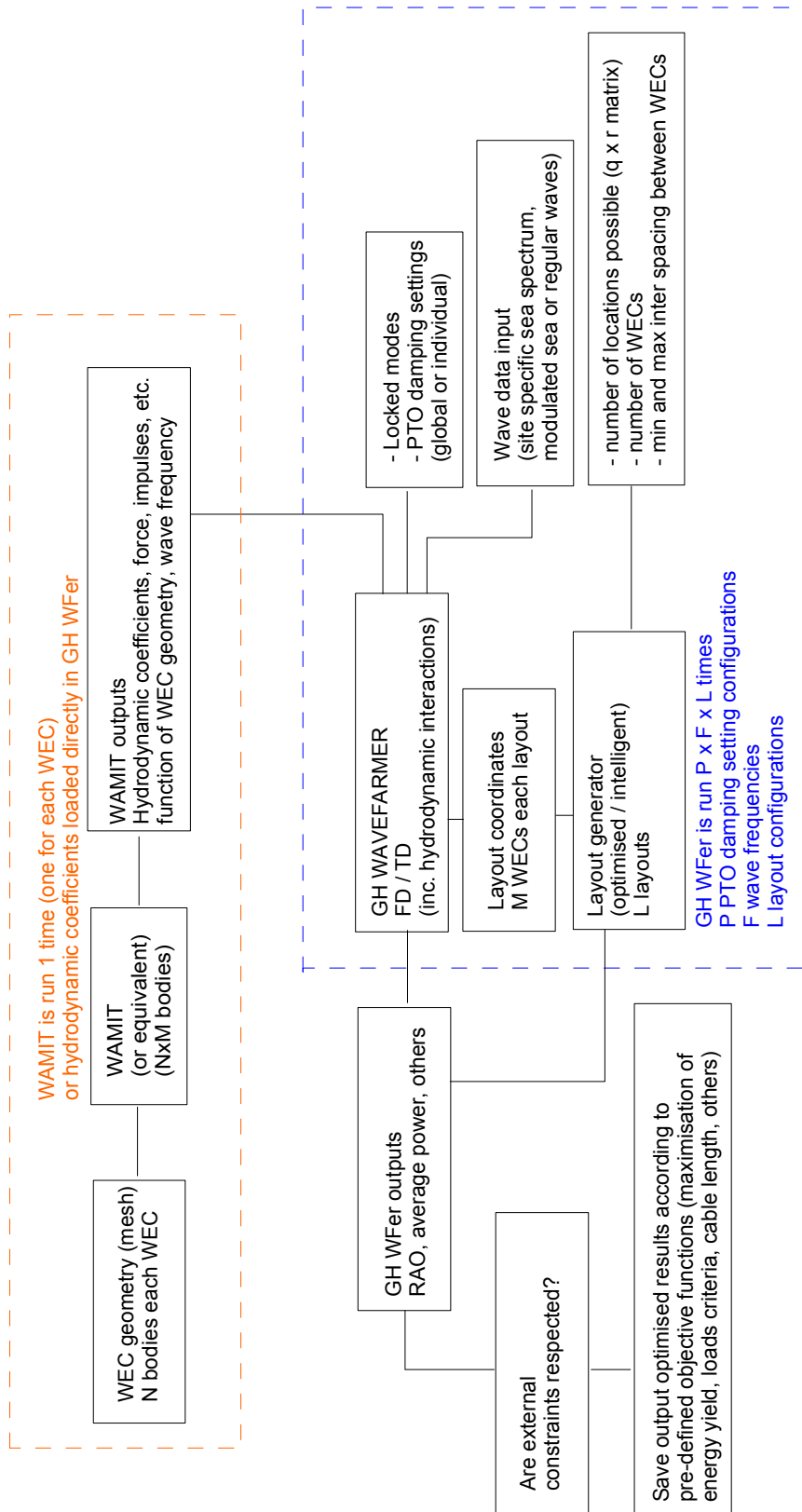


Figure 5.4: Flowchart – Optimiser I/O structure (Scenarios 2A and 2B)

5.5.8 A Summary of the Key Implementation Steps – FD and TD Core Algorithms

The implementation process described in this report aims to build up the frequency and time-domain core algorithms code for the beta releases by systematically completing a series of implementation steps. Note that GH has an existing numerical modelling code (Cruz et al., 2009) which will act as the basis for the software development. The key steps can be summarised as follows:

1. Definition of the wave climate inputs and associated sensitivity studies (use of different spectral parameter vectors as inputs);
2. An upgrade of the equation of motion solver to incorporate the GH Multibody modelling engine.
3. Development of a stand-alone WAMIT results postprocessor designed to save WAMIT output data in a documented format. The user will have the option of running the processor from within the software. The hydrodynamics module will read in the processed WAMIT data so that it can be used for formulation of each of the hydrodynamic force terms.
4. Creation of a radiation impulse response function system identification algorithm based on the frequency-domain fitting technique. The performance (and accuracy) of the resulting state-space simulation will be compared with the existing time-domain numerical convolution method using an irregular wave input and a simple viscous damper PTO model. Favourable results will lead to a system identification option being incorporated as a pre-processing stage.
5. Creation of a user interface capable of receiving constrained mathematical expressions. The interface will be able to limit the user to entering a linear expression if necessary. The mathematical expression interface will allow frequency and time-domain simulations to be defined using the simple mathematical expression PTO model, with its associated control representation, and will act as the basis for the input of user-defined functions in the PTO templates.
6. Construction of a linearised dynamics moorings model. This initial moorings model will ask the user to enter inertial, damping and stiffness coefficients representing the complete moorings system.
7. Construction of the first PTO Template, which will be capable of representing some hydraulic and electrical PTO designs with a single internal state. The state derivative equation will be solved by the equation of motion solver and the template will be designed to operate under specific control logic called every time-step.
8. Construction of the structural restraint forces and quasi-static moorings models, including a user interface designed to obtain data on the geometrical configuration and force properties of the system.
9. Construction of the optimiser module is a staged approach (1A to 2B) alongside all of the above.
10. Construction of a final post-processing module, allowing the specification of batch runs leading to the creation of site specific power matrices.

REFERENCES

References (Section 2)

DTI, 2007. Preliminary Wave Energy Performance Protocol. DTI Report: 07/807.

Kerbiriou MA, Prevosto M, Maisondieu C, Clement A, Babarit A, 2007. Influence of Sea-States Description on Wave Energy Production Assessment. Proc. 7th European Wave and Tidal Energy Conference, Porto, Portugal, 2007.

Mackay EBL, Bahaj AS, Challenor PG (2010a). Uncertainty in wave energy resource assessment. Part 2: Variability and predictability. *Renewable Energy*, 35(8), 1809-1819

Saulnier JB, Ricci P, Pontes MT, Falcão AF, 2007. Spectral Bandwidth and WEC Performance Assessment. Proc. 7th European Wave and Tidal Energy Conference, Porto, Portugal, 2007.

References (Section 3)

Alves, M (2002). "Incident Wave Identification", MARETEC / AWS Internal Report 2/2002, Lisbon, Portugal

American Petroleum Institute (1997); API RP 2SK, Recommended Practice for Design and Analysis of Stationkeeping Systems for Floating Structures, USA.

Babarit A, Duclos G, Clément A.H, 2004. Comparison of latching control strategies for a heaving wave energy device in random sea. *Applied Ocean Research* 26, 227-238.

Babarit A, Clément A.H, 2006. "Optimal latching control of a wave energy device in regular and irregular waves"; Published in *Applied Ocean Research* 28, 77-91.

Brito-Melo, A, Sarmiento, A, Clément, A and Delhommeau, G (1998). "Hydrodynamic Analysis of Geometrical Design Parameters of Oscillating Water Columns", Proc. 3rd European Wave Energy Conference, Patras, Greece, Vol. 1, pp.23-30.

Brito-Melo, A, Hofmann, T, Sarmiento, A, Clément, A and Delhommeau, G (2000a). "Numerical Modelling of OWC-shoreline Devices Including the Effect of the Surrounding Coastline and Non-Flat Bottom", Proc. 10th International Offshore and Polar Eng Conference, Seattle, USA, Vol.1, pp.743-748.

Brito-Melo, A and Sarmiento, A (2000b). "Numerical Study of the Performance of a OWC Wave Power Plant in a Semi-Infinite Breakwater", Proc. 4th European Wave Energy Conference, Aalborg, Denmark, pp. 283-289.

Brito Melo, A (2002). "AWS Physics Characterisation", IST Internal Report, Instituto Superior Técnico, Lisbon, Portugal.

Brooke, J (2003). *Wave Energy Conversion*, Elsevier Science.

Budal, K and Falnes, J (1975). “A resonant point absorber of ocean-wave power”, *Nature*, Vol. 256, pp. 478-479.

Budal, K (1977). “Theory of absorption of wave power by a system of interacting bodies”, *Journal of Ship Research*, Vol. 21, pp. 248-253.

Budal, K and Falnes, J in Count B (Editor), 1980. Power from Sea Waves. Academic Press (London). ISBN: 0-12-193550-7.

Bryden, I (1983). “Long floating cylinders in three-dimensional seas,” PhD Thesis, The University of Edinburgh.

Callaghan, J and Bould, R (2006). *Future Marine Energy*, The Carbon Trust.

Centre for Marine and Petroleum Technology (CMPT), 1998. Floating Structures: A guide for design and analysis. Volume 2. Oilfield Publications Limited. ISBN 1 870553 357.

Clare, R, Evans, DV and Shaw, TL (1982). “Harnessing sea wave energy by a submerged cylinder device”, *Journal of The Institution of Civil Engineers*, Vol. 73, pp. 356-385.

Clément, A, Babarit, A, Gilloteaux, J, Josset, C and Duclos, G (2005). “The SEAREV Wave Energy Converter, Proc. 6th European Wave & Tidal Energy Conference, Glasgow, United Kingdom.

Count B M, Jefferys E R, Wave power, the primary interface. Proceedings of the 13th Symposium on Naval Hydrodynamics, Paper 8. p1-10. The Shipbuilding Research Association of Japan, Tokyo.

Cruz, J and Salter, S (2006). “Numerical Modelling of a Modified Version of the Edinburgh Duck Wave Energy Converter”. *Proc. IMechE Part M: Journal of Engineering for the Maritime Environment*, Vol. 220, pp. 129-147.

Cruz, J and Sarmiento, A (2007). “Sea state characterisation of the test site of an offshore wave energy plant”, *Ocean Engineering*, Vol. 34 (5-6), pp. 763-775.

Cruz, J, (2008). *Ocean Wave Energy* (Editor), Springer-Verlag.

Cummins W.E, 1962. The impulse response function and ship motions. *Schiffstechnik* 9, p101–109.

Jefferys in Count B (Editor), 1980. Power from Sea Waves. Academic Press (London). ISBN: 0-12-193550-7.

Dean, R, and Darymple, R (1991). *Water Wave Mechanics for Engineers and Scientists*, World Scientific.

Delauré, Y and Lewis, A (2003). “3D hydrodynamic modelling of fixed oscillating water column by a boundary element methods”, *Ocean Engineering*, Vol. 30 (3), pp. 309-330.

Det Norske Veritas (DNV) Software. ‘Mimosa’ Flyer. Available online, February 2010.

Det Norske Veritas (DNV) Software. ‘Riflex – Riser System Analysis Program’ Flyer. Available online, February 2010.

Det Norske Veritas (DNV), 2004. DNV-OS-E301, Position Mooring, Norway.

Duclos G, Clément A H, Chatry G, 2001. Absorption of Outgoing Waves in a Numerical Wave Tank using a Self-Adaptive Boundary Condition. *Int. Journal of Offshore and Polar Engineering*, 11(3), 168–175.

Edinburgh University Wave Power Project, 1987. Solo Duck Linear Analysis. A report to the wave energy steering committee covering work supported by the United Kingdom department of Energy.

Eatock Taylor, R and Jeffreys, E (1985). “Variability of Hydrodynamic Load Predictions for a Tension Leg Platform”, *Ocean Engineering*, Vol. 13 (5), pp. 449-490.

Evans, DV (1976). “A theory for wave-power absorption by oscillating bodies”, *Journal of Fluid Mechanics*, Vol. 77 (1), pp. 1-25.

Evans, DV (1979). “Some theoretical aspects of three-dimensional wave-energy absorbers”, Proc. 1st Symp. Wave Energy Utilization, Gothenburg, Sweden.

Evans, DV, Jeffrey, DC, Salter, SH and Taylor JR (1979). “Submerged cylinder wave energy device: theory and experiment”, *Applied Ocean Research*, Vol. 1 (1), pp. 3-12.

Evans, DV (1981a). “Power from Water Waves”, *Annual Review of Fluid Mechanics*, Vol. 13, pp. 157-187.

Evans, DV (1981b). “Maximum wave-power absorption under motion constraints”, *Applied Ocean Research*, Vol. 3, pp. 200-203.

Evans, DV and Falcão, AF (1986). *Hydrodynamics of Ocean Wave-Energy Utilization* (Editors), Proceedings IUTAM Symposium, Lisbon, Portugal, 8-11 July 1985, Springer-Verlag.

Evans, D., Linton, CM (1993). “Hydrodynamics of wave-energy devices”, Annex Report B1: Device Fundamentals/Hydrodynamics, Contract JOU2-0003-DK, Commission of the European Communities.

Falcão, A (2003). “First-generation wave power plants: current status and R&D requirements”, Proc. 22nd International Conference on Offshore Mechanics and Arctic Engineering, Cancun, Mexico, Paper No. OMAE2003-37366.

Falcão A F de O, 2007. Modelling and control of oscillating-body wave energy converters with hydraulic power take-off and gas accumulator. *Ocean Engineering*, vol. 34, 2021–2032.

Falcão A F de O, 2008. Phase control through load control of oscillating-body wave energy converters with hydraulic PTO system. ‘*Ocean Engineering*’ 35, p358–366.

Falnes, J (1980). “Radiation impedance matrix and optimum power absorption for interacting oscillators in surface waves”, *Applied Ocean Research*, Vol. 2, pp. 75-80.

Falnes J, 2002. *Ocean Waves and Oscillating Systems. Linear Interactions Including Wave Energy Extraction*. Cambridge University Press. ISBN 0-521-01749-1.

Faltisen, O (1990). *Sea loads on ships and offshore structures*, Cambridge University Press.

Fitzgerald J, Bergdahl L, 2007. Considering Mooring Cables for Offshore Wave Energy Converters. Proceedings of the 7th European Wave and Tidal Energy Conference, Porto, Portugal

Fitzgerald J, Bergdahl L, 2008. Including moorings in the assessment of a generic offshore wave energy converter: A frequency-domain approach. *Marine Structures* Volume 21, Issue 1. 23-46

Iserles, A, 1996. *A First Course in the Numerical Analysis of Differential Equations*. Cambridge University Press. ISBN 0521556554.

Goodman T R, Breslin J P, 1976. Statics and dynamics of anchoring cables in water. *Journal of Hydronautics* vol. 10, no. 4, 113-120.

Greenhow, M and Ahn, SI (1988). "Added Mass and Damping of Horizontal Circular Cylinder Sections", *Ocean Engineering*, Vol. 15 (5), pp. 495-504.

Haskind, M (1957). "The exciting forces and wetting of ships in waves", *Izv. Akad. Nauk. SSSR, Otd. Tekh. Nauk*, Vol. 7, pp. 65-79.

Havelock, T (1942). "The damping of the heaving and pitching motion of a ship", *Philosophical Magazine*, Vol. 33 (7), pp. 666-673.

Havelock, T (1955). "Waves due to a floating sphere making periodic heaving oscillations", *Proc. Royal Society*, Vol. 231, pp. 1.

Henderson, R, 2006. Design, simulation, and testing of a novel hydraulic power take-off system for the Pelamis wave energy converter. Published in 'Renewable Energy' Vol. 31, 271–283.

Henderson, R (2008). "Case Study: Pelamis", In: Chapter 5, *Ocean Wave Energy* (Ed.: J Cruz), Springer-Verlag.

Hess, J and Smith, A (1964). "Calculation of nonlifting potential flow about arbitrary three-dimensional bodies", *Journal of Ship Research*, Vol. 8, pp. 22-44.

Hess, J (1990). "Panel methods in computational fluid dynamics", *Annual Review of Fluid Mechanics*, Vol. 22, pp. 255-274.

Ho B, Kalman R, 1966. Effective Reconstruction of Linear State-Variable Models from Input/Output Functions. *Regelungstechnik* 14 (12), 417-441

Jeffrey, DC, Keller, GJ, Mollison, D, Richmond DJ, Salter, SH, Taylor, JM, Young, IA (1978). "Study of mechanisms for extracting power from sea waves", Fourth Year Report of the Edinburgh Wave Power Project, The University of Edinburgh.

John, F (1950). "On the Motion of Floating Bodies", *Communications on Pure and Applied Mathematics*, Vol. 3, pp. 45-101.

Justino, P and Clément A (2003). "Hydrodynamic performance for small arrays of sub-merged spheres", Proc. 5th European Wave Energy Conference, Cork, Ireland, pp. 266-273.

Johanning L, Smith G H, Wolfram J. Towards Design Standards for WEC Moorings. Proceedings of the 6th European Wave and Tidal Conference, Glasgow UK, 223-230

Josset C, Babarit A, Clément A H, 2007. A wave-to-wire model of the SEAREV wave energy converter. Proceedings of the IMechE vol. 221 Part M: J. Engineering for the Maritime Environment.

Katory, M (1976). "On the motion analysis of large asymmetric bodies among sea waves: an application to a wave power generator", *Naval Architecture*, pp. 158-159.

Kinsman, B (1965). *Wind Waves*, Prentice-Hall, pp. 460-471.

Koterayama W, 1978. Motions of a moored floating body and dynamic tension of mooring lines in regular waves. Report of the Research Institute for Applied Mechanics, Kyushu University, Fukuoka, vol. 6 no. 82.

Kristiansen E, Egeland O, 2003. Frequency Dependent Added Mass in Models for Controller Design for Wave Motion Damping. 6th IFAC Conference on Maneuvering and Control of Marine Craft, 17th – 19th September 2003, University of Girona, Spain.

Kung S Y, 1978. A New Identification and Model Reduction Algorithm via Singular Value Decompositions. Proc. Twelfth Asilomar Conf. on Circuits, Systems and Computers, November 6-8, 1978, 705-714.

Lamb, H (1932). *Hydrodynamics*, 6th Ed., Cambridge University Press.

Le Méhauté, B (1976). *An Introduction to Hydrodynamics & Water Waves*, Springer-Verlag.

Lee, C-H, Maniar, H, Newman, JN and Zhu, X (1996a). "Computations of Wave Loads Using a B-Spline Panel Method", Proc. 21st Symposium on Naval Hydrodynamics, Trondheim, Norway, pp. 75-92.

Lee, C-H, Newman, JN and Nielsen, F (1996b). "Wave Interactions with Oscillating Water Column", Proc. 6th International Offshore and Polar Engineering Conference, Los Angeles, USA, Vol.1, pp. 82-90.

Lee, C-H, Farina, L and Newman, J (1998). "A Geometry-Independent Higher-Order Panel Method and its Application to Wave-Body Interactions", Proc. 3rd Engineering Mathematics and Applications Conference, Adelaide, Australia, pp. 303-306.

Lin, C-P (1999). "Experimental studies of the hydrodynamic characteristics of a sloped wave energy device", PhD Thesis, The University of Edinburgh.

Linton, CM (1991). "Radiation and diffraction of water waves by a submerged sphere in finite depth, *Ocean Engineering*, Vol. 18 (1/2), pp. 61-74.

Livingstone M J, 2009. Modelling and Control of a Wave Energy Converter Power Take-Off. Final Year Project Supported by Garrad Hassan and Partners Ltd. Machine Systems Group. University of Bath.

Livingstone M J, Plummer A R, 2010. The design, simulation and control of a wave energy converter power take-off. (submitted for publication in Proceedings of the 7th International Fluid Power Conference, Aachen, Germany).

Longuet-Higgins M S, 1977. The mean forces exerted by waves on floating or submerged bodies with applications to sand bars and wave power machines. Proceedings of the Royal Society of London A. 352, 463-480.

Maniar, H (1995). "A three-dimensional higher order panel method based on B-splines", PhD Thesis, Massachusetts Institute of Technology.

Martins, E, Ramos, FS, Carrilho, L, Justino, P, Gato, L, Trigo, L and Neumann, F (2005). "CEODOURO: Overall Design of an OWC in the new Oporto Breakwater", Proc. 6th European Wave Energy Conference, Glasgow, UK, pp. 273-280.

Mavrakos, S and McIver, P (1997). "Comparison of methods for computing hydrodynamic characteristics of arrays of wave power devices", *Applied Ocean Research*, Vol. 19, pp. 283-291.

McCabe A P, Aggidisa G A, Stallard T J, 2006. A time-varying parameter model of a body oscillating in pitch. *Applied Ocean Research* 28, 359-370.

McCormick, M (1981). *Ocean Wave Energy Conversion*, John Wiley & Sons.

McIver, P (1993). "The hydrodynamics of arrays of wave-energy devices", Annex Report B1: Device Fundamentals/Hydrodynamics, Contract JOU2-0003-DK, Commission of the European Communities.

McIver, P and McIver, M (1995). "Wave-power absorption by a line of submerged horizontal cylinders", *Applied Ocean Research*, Vol. 17, pp. 117-126.

Mei, CC (1976). "Power Extraction from Water Waves", *Journal of Ship Research*, Vol. 20, pp. 63-66.

Mei, CC (1989). *The Applied Dynamics of Ocean Surface Waves*, Advanced Series on Ocean Engineering, Vol. 1, World Scientific (revised edition in 2005).

Montgomery, DC (2001). *Design and Analysis of Experiments*, John Wiley & Sons, 5th Edition.

Mynett, AE, Serman, DD and Mei, CC (1979). "Characteristics of Salter's cam for extracting energy from ocean waves", *Applied Ocean Research*, Vol. 1 (1), pp. 13-20.

Nebel, P (1992). "Optimal Control of a Duck", Report of the Edinburgh Wave Power Project, Edinburgh, UK.

Newman, JN (1976). "The interaction of stationary vessels with regular waves", Proc. of the 11th Symposium on Naval Hydrodynamics, London, UK, pp. 491-501.

Newman, JN (1977). *Marine Hydrodynamics*, MIT Press.

Newman, JN (1985). "Algorithms for the free-surface Green's function", *Journal of Engineering Mathematics*, Vol. 19, pp. 57-67.

Newman, JN (1992). "Panel methods in marine hydrodynamics", Proc. 11th Australasian Fluid Mechanics Conference, Hobart, Australia, Keynote Paper K-2.

Newman, JN and Lee, CH (1992). "Sensitivity of Wave Loads to the Discretization of Bodies", Proc. of the 6th Behaviour of Offshore Structures (BOSS) International Conference, London, UK, Vol. 1, pp. 50-63.

Newman, JN and Lee, CH (2002). "Boundary-Element Methods in Offshore Structure Analysis", *Journal of Offshore Mechanics and Artic Engineering*, Vol. 124, pp. 81-89.

Ogilvie, TF (1963). "First and second-order forces on a submerged cylinder submerged under a free-surface", *Journal of Fluid Mechanics*, Vol. 16, pp. 451-472.

O'Leary, M (1985). "Radiation and scattering of surface waves by a group of submerged, horizontal, circular cylinders", *Applied Ocean Research*, Vol. 7 (1), pp. 51-57.

Orcina Ltd. OrcaFlex Manual Version 9.2a.

Payne, G (2002). "Preliminary numerical simulations of the Sloped IPS Buoy", Proc. of the MAREC Conference, Univ. Newcastle upon Tyne, UK.

Payne, G (2006). "Numerical modelling of a sloped wave energy device", PhD Thesis, The University of Edinburgh.

Pinkster, JA (1997). "Computations for Archimedes Wave Swing", Delft University Technology, Delft, The Netherlands, Report No. 1122-O.

Pizer, D (1992). "Numerical Predictions of the Performance of a Solo Duck", Report of the Edinburgh Wave Power Project, Edinburgh, UK.

Pizer, D (1993). "The Numerical Prediction of the Performance of a Solo Duck", Proc. European Wave Energy Symposium, Edinburgh, UK, pp. 129-137.

Pizer, D (1994). "Numerical Models", Report of the Edinburgh Wave Power Project, Edinburgh, UK.

Pizer, D, Retzler, C, Henderson, R, Cowieson, F, Shaw, F, Dickens, B and Hart, R (2005). "PELAMIS WEC - Recent Advances in the Numerical and Experimental Modelling Programme", Proc. 6th European Wave Energy Conference, Glasgow, UK, pp. 373-378.

Prado, M., and Gardner, F (2005). "Theoretical analysis of the AWS dynamics during the submergence operation", Proc. 6th European Wave Energy Conference, Glasgow, UK, pp. 395-400.

Prado, M, Neumann, F, Damen, M and Gardner, F (2005). "AWS Results of Pilot Plant Testing 2004", Proc. 6th European Wave Energy Conference, Glasgow, UK, pp. 401-408.

Prado, M (2008). "Archimedes Wave Swing", In: *Ocean Wave Energy* (Ed.: J Cruz), Springer-Verlag.

Press, W, Teukolsky, S, Vetterling, W and Flannery, B (1992). *Numerical Recipes in FORTRAN*. 2nd Ed., Cambridge University Press.

Rademakers, L, Van Schie, R, Schitema, R, Vriesema, B and Gardner, F (1998). "Physical Model Testing for Characterising the AWS", Proc. 3rd European Wave Energy Conference, Patras, Greece, Vol. 1, pp. 192-199.

Retzler C, Pizer D, Henderson R, Ahlqvist J, Cowieson F and Shaw M (2003). "PELAMIS: Advances in the Numerical and Experimental Modelling Programme", Proc. 5th European Wave Energy Conference, Cork, Ireland, pp. 59-66.

Roache, PJ (1997). "Quantification of Uncertainty in Computational Fluid Dynamics", *Annual Review of Fluid Mechanics*, Vol. 29, pp 123-160.

Roache, PJ (1998). *Verification and Validation of Computational Science and Engineering*, Hermosa Publishers.

Roache, PJ (2003). "Error Bars for CFD", 41th Aerospace Sciences Meeting, Reno, USA.

Romate, JE (1988). "Local Error analysis in 3-D Panel Methods", *Journal of Engineering Mathematics*, Vol. 22, pp. 123-142.

Romate, JE (1989). "The Numerical Simulation of Nonlinear Gravity Waves in Three Dimensions using a Higher Order Panel Method", PhD Thesis, Universiteit Twente.

Ross, D (1995). *Power from the Waves*, Oxford University Press.

Salter, SH (1974). "Wave Power", *Nature*, Vol. 249, pp. 720-724.

Sarmiento, A (1992). "Wave flume experiments on two-dimensional oscillating water column wave energy devices", *Experiments in Fluids*, Vol.12, pp. 286-292.

Sarmiento, A, Luís, A, Lopes, D (1998). "Frequency-Domain Analysis of the AWS", Proc. 3rd European Wave Energy Conference, Patras, Greece, Vol. 1, pp. 15-22.

Sarpkaya, T and Isaacson, I (1981). *Mechanics of Wave Forces on Offshore Structures*, Von Nostrand Reinhold Company.

Shaw, R (1982). *Wave Energy - A Design Challenge*, Ellis Harwood Ltd, John Wiley & Sons.

Skyner, D (1987). "Solo Duck Linear Analysis", Report of the Edinburgh Wave Power Project, Edinburgh, UK.

Standing, MG (1980). "Use of Potential Flow theory in Evaluating Wave Forces on Offshore Structures", *Power from Sea Waves*, Proc. Conf. Institute of Mathematics and its Applications (Ed. B. count), pp. 175-212, Academic Press, London.

Sumer, BM and Fredsøe, J (1997). *Hydrodynamics around Cylindrical Structures*, Advanced Series on Ocean Engineering, Vol. 12, World Scientific.

Sykes, R, Lewis, A and Thomas, G (2007). “A Physical and Numerical Study of a Fixed Cylindrical OWC of Finite Wall Thickness”, Proc. 7th European Wave and Tidal Energy Conference, Porto, Portugal, September 2007.

Taghipour R, Perez T, Moan T, 2008. Hybrid frequency-time-domain models for dynamic response analysis of marine structures. *Ocean Engineering* 35, 685-705.

Thomas, GP and Evans DV (1981). “Arrays of three-dimensional wave-energy absorbers”, *Journal of Fluid Mechanics*, Vol. 108, pp. 67-88.

Thomas in Cruz J (Editor), 2008. *Ocean Wave Energy, Current Status and Future Perspectives*. Springer-Verlag. ISBN978-3-540-74894-6

Triantafyllou M S, Bliedl A, Shin H, 1986. Static and fatigue analysis of multi-leg mooring system. MIT Sea Grant Program Report, August 1986.

Tucker, MJ and Pitt, EG (2001). *Waves in Ocean Engineering*. Elsevier Science Ltd.

Ursell F, 1964. The decay of the free motion of a floating body. *Journal of Fluid Mechanics* 19, 305-319

van Daalen, E (1993). “Numerical and Theoretical Studies of Water Waves and Floating Bodies”, PhD Thesis, University of Twente, The Netherlands.

van der Pluijm, D and Voors, E (2002). “Power from ocean waves – A study on power conversion with the Archimedes Wave Swing”, MSc Thesis, Delft University of Technology.

Vugts, JH (1968). “The Hydrodynamic Coefficients for Swaying, Heaving and Rolling Cylinders in a Free-surface”, Netherlands Ship Research Centre TNO, Report No. 112 S.

Walker N S. GMOOR32 Manual v9.2. Global Maritime Consultancy Limited.

WAMIT Inc, 2006. WAMIT User Manual Versions 6.3, 6.3PC, 6.3S, 6.3S-PC

Wehausen, J and Laiton, E (1960). “Surface Waves”, *Encyclopaedia of Physics*, Vol. 9, pp. 446-778.

Wehausen, J.V., 1971. The motion of floating bodies. *Annual Review of Fluid Mechanics* 3, 237–268

Yeung, RW (1982). “Numerical methods in free-surface flows”, *Annual Review of Fluid Mechanics*, Vol. 14, pp. 395-442.

Yemm, R, Pizer, D and Retzler, C (1998). “The WPT-375 – a near-shore wave energy converter submitted to Scottish Renewables Obligation 3”, Proc. 3rd European Wave Energy Conference, Patras, Greece, Vol. 2, pp.243-249.

Yu Z, Falnes J, 1995. State-space modelling of a vertical cylinder in heave. *Applied Ocean Research* 17, 265-275.

Zentech Inc. ZenMoor by Zentech Flyer. Available online, February 2010.

References (Section 4)

Alexandre, A. et al., Transformation of wave spectra across a line of wave devices. Proc. 8th Wave and Tidal Energy Conf., Uppsala, Sweden, 2009

Babarit, S. et al., Assessment of the influence of the distance between two wave energy converters on the energy production, Proc. 8th Wave and Tidal Energy Conf., Uppsala, Sweden, 2009

Babarit, A., Impact of long separating distances on the energy production of two interacting wave energy converters, Ocean Engineering, 2010

Backer, G. et al., Performance of closely spaced point absorbers with constrained floater motion, Proc. 8th Wave and Tidal Energy Conf., Uppsala, Sweden, 2009

Beels, C., Troch P., De Backer G., De Rouck J., Moan T., Falcao A., A model to investigate wave power devices. Proc. Int. Conf. Ocean Energy, 94-101, Bremerhaven, Germany, October 23-25, 2006.

Beels, C. et al., Optimal pattern of interacting wave power devices., Civil Engineering Department, Ghent University.

Budal, K., Theory for absorption of wave power by a system of interacting bodies. J. Ship Res., 21(4), 248-253, 1997

Child, B.F.M. and Venugopal, V., Interaction of waves with an array of floating wave energy devices. Proc. 7th Wave and Tidal Energy Conf., Porto, Portugal, 11-13 September, 2007

Child, B.F.M. and Venugopal, V., Modification of power characteristics in an array of floating wave energy devices. Proc. 8th Wave and Tidal Energy Conf., Uppsala, Sweden, 2009

Cruz, J. et al, Wave Farm Design: Preliminary studies on the influences of wave climate, array layout and farm control, Proc. 8th Wave and Tidal Energy Conf., Uppsala, Sweden, 2009

Falcão, A., Wave-power absorption by a periodic linear array of oscillating water columns, Ocean Engineering, 2001

Falcão, A., Hydrodynamic interaction between wave energy converters in arrays, Instituto Superior Tecnico, Lisboa, 2008

Falnes, J., Radiation impedance matrix and optimum power absorption for interacting oscillators in surface waves. Applied Ocean Research, 2, 75-80, 1980

Fitzgerald, C., Optimal configurations of arrays of wave-power devices, Master of Science thesis, National University of Ireland, Cork, 2006

Fitzgerald, C. and Thomas, G., A preliminary study on the optimal formation of an array of wave power devices. Proc. 7th Wave and Tidal Energy Conf., Porto, Portugal, 11-13 September, 2007

Folley, M. and Whittaker, T., The effect of sub-optimal control and the spectral wave climate on the performance of wave energy converter arrays, Applied Ocean Research, 2009

Garrett, C.J.R., Wave forces on a circular dock, Journal of Fluid Mechanics, 46(1):129-139, 1971

Greengard, L. and Rokhlin, V., A fast algorithm for particle simulations, *Journal of Computational Physics*, 73(2):325-348, 1987

Justino, P. and Clément, A., Hydrodynamic performance for small arrays of submerged spheres, *Proc. 5th Wave and Tidal Energy Conf.*, University College Cork, Ireland, 2003

Kagemoto, Hiroshi and Yue, D.K.P., Interactions among multiple three-dimensional bodies in water waves: an exact algebraic method. *Journal of Fluid Mechanics*, 166:189-209, 1986

Li, Y., Mei, C.C., Bragg scattering by a line array of small cylinders in a waveguide. Part 1. Linear aspects, *Journal of Fluid Mechanics*, vol.583, p.161-187, 2007

Mackay, E., EquiMar project deliverable WP5, University of Southampton, 2008

Maniar, H.D., Newman, J.N., Wave diffraction by a long array of cylinders, *Journal of Fluid Mechanics*, 339:309-30, 1997

Mavrakos, S.A. and McIver, P., Comparison of methods for computing hydrodynamic characteristics of arrays of wave power devices, *Applied Ocean Research*, vol. 19, 283-291, 1997.

McIver, P., Wave forces on arrays of floating bodies, *Journal of Engineering Mathematics*, 18, 273-285, 1984

McIver, P. and Evans, D. V., Approximation of wave forces on cylinder arrays, *Applied Ocean Research*, 6, 101-107, 1984

McIver, P., Wave interaction with arrays of structures, *Applied Ocean Research*, 2001

Millar, D.L., Smith H.C.M., Reeve, D.E., Modelling analysis of the sensitivity of shoreline change to a wave farm. *Ocean Engineering*, 34, 884-901, 2007

modeFRONTIER 3.1 User Manual, ESTECO, 2004

Newman, J.N., Wave effects on multiple bodies, *Hydrodynamic in Ship and Ocean Engineering*, 2001

Ohkusu, M., Hydrodynamic forces on multiple cylinders in waves. In *Proceedings of the International Symposium on Dynamics of Marine Vehicles and Structures in Waves*. Institute of Mechanical Engineers, London, 1974.

Pham, D.T. and Karaboga, D., *Intelligent Optimisation Techniques*, Springer, 2000

Siddorn, P. and Taylor, R.E., Diffraction and independent radiation by an array of floating cylinders, *Ocean Engineering*, 2008

Simon, M., Multiple scattering in arrays of axisymmetric wave-energy devices. Part 1. A matrix method using a plane-wave approximation, *Journal Fluid Mechanics*, vol. 120, pp.1-25, 1982

Smith H.C.M., Millar, D.L., Reeve D.E., Generalisation of wave farm impact assessment on onshore wave climate. *Proc. 7th Wave and Tidal Energy Conf.*, Porto, Portugal, 11-13 September, 2007

Thomas, G.P. and Evans, D.V., Arrays of three-dimensional wave-energy absorbers. *J. Fluid Mechanics*, 108, 67-88, 1981

Thompson, I. et al., A new approximation method for scattering by large arrays, 22nd International Workshop on Water Waves and Floating, Croatia, 2007

Venugopal V. and Smith G.H., Wave climate investigation for an array of wave power devices. Proc. 7th Wave and Tidal Energy Conf., Porto, Portugal, 11-13 September, 2007

Weber, J. and Thomas, G., An efficient flexible engineering tool for multi-parametric hydrodynamic analysis in the design and optimisation of WECs, 6th Wave and Tidal Energy Conf., Glasgow, United Kingdom, 2005

Weller, S. et al., Experimental measurements of irregular wave interaction factors in closely spaced arrays, Proc. 8th Wave and Tidal Energy Conf., Uppsala, Sweden, 2009

Weller, S. et al., Optimisation of a heterogeneous array of heaving bodies, Proc. 8th Wave and Tidal Energy Conf., Uppsala, Sweden, 2009

NOMENCLATURE

Standard Index (S I) Units are used unless stated otherwise

An overdot, \dot{x} indicates differentiation of the quantity x with respect to time.

A X^* indicates the complex conjugate of the complex quantity X

The complex operator, $j = \sqrt{-1}$

A standard glossary of terms can be found in the 2007 Ocean Energy Glossary (IEA-OES), which was followed throughout this document. This document is available at

http://www.wavec.org/client/files/Ocean_Energy_Glossary_Dec_2007.pdf.

Section 2	
A	Wave Amplitude
c_g	Group Speed
c_p	Phase Speed
$D(f, \theta)$	Directional Spreading Function (or Directional Distribution)
$E(f)$	Omnidirectional spectrum or Frequency Spectrum
f	Frequency
f_m	Mean Frequency
g	Acceleration due to gravity
H_s	Significant Wave Height
$k = 2\pi / \lambda$	Wave Number
m_n	nth moment of the omnidirectional spectrum
$MDIR$	Mean Direction
P_{aux}	Auxiliary Absorbed Power
\bar{P}	Average absorbed power by an array

\bar{P}_n	Average absorbed power per array element
$S(f, \theta)$	Directional Variance Spectrum
$SDIR$	Mean Spread
T	Period
T_e	Energy Period
T_m	Mean Period
T_z	Zero-Crossing Period
ξ	Oscillation Amplitude (for an unspecified degree of freedom)
θ	Direction of wave propagation
λ	Wavelength
ν	Bandwidth
η	Sea surface elevation
$\omega = 2\pi f$	Angular frequency
σ	Variance or Directional Spread (Definition depends on context)
ϕ	Phase
<u>Section 3</u>	
A	Wave Amplitude
A_i, A_r, A_t	Incident, Reflected and Transmitted Wave Amplitudes
A', B', C', D'	System State Matrices
B	Damping
B_m	Mechanical Damping
B_r	Radiation Damping (or Radiation Resistance)

$c(t)$	Causal Impulse Response Function (Context Specific)
$D(\omega)$	Transfer Function (Context Specific)
E	Reactance
E_r	Radiation Reactance
f_{drift}	Mean Drift force
f_e	Excitation force
f_{ext}	External forces
f_f	Fluid forces
f_{hs}	Hydrostatic force
f_r	Radiation force
F_e	Complex excitation force amplitude
F_{inc}	Incident Excitation force component
F_{diff}	Diffacted Excitation force component
g	Acceleration due to gravity
$G(\omega)$	Transfer Function (Context Specific)
$H(\omega)$	Transfer Function (Context Specific)
$h(t)$	Impulse Response Function
$k(t)$	Radiation Impulse Response ('Memory') Function (Velocity)
$K(\omega)$	Fourier Transform of the Radiation Impulse Response Function
K_{hs}	Hydrostatic Stiffness

K_m	Mechanical Stiffness
m_m	Physical Body Mass
$l(t)$	Radiation Impulse Response ('Memory') Function (Acceleration)
$m_r(\omega)$	Added Mass
\bar{P}_m	Time averaged power absorbed by the PTO
\underline{q}	State Vector (Contains all states with state equations solved by the equation of motion solver).
t	Time
u	Velocity
\underline{u}	Vector of inputs to state-space formulation (context specific)
U	Complex Velocity Amplitude
x	Displacement
X	Complex Displacement Amplitude
\underline{y}	Simulation outputs
\underline{z}	State Vector (Equation of Motion States)
Z	Impedance
Z_m	Mechanical Impedance
Z_r	Radiation Impedance
α_i	Parameters (Prony Approximation – Context Specific)
β_i	Parameters (Prony Approximation – Context Specific)
δ	Time-Step Size
θ	System Identification Parameters

$\omega = 2\pi f$	Angular frequency
ϕ	Phase
$\underline{\zeta}$	State Vector (External States)
<u>Section 4</u>	
β	Incident wave angle
N	Number of individual devices
q	' q -factor'

KEY TO ACRONYMS

ADCP	Acoustic Doppler Current Profiler
AIC	Akaike's Information Criterion
BCS	Body-fixed Coordinate System
BDM	Bayesian Directional Method
BEM	Boundary Element Method
DDD	Double Direction Decomposition
DFTM	Direct Fourier Transform Method
DOF	Degree-Of-Freedom
EMEC	European Marine Energy Centre
EMLM	Extended Maximum Likelihood Method
EMEP	Extended Maximum Entropy Principle
EWTEC	European Wave and Tidal Energy Conference
FD	Frequency-Domain
FDC	Fundamental Device Concept
FSP	Full-Scale Prototype
GH	Garrad Hassan and Partners Ltd
GCS	Global Coordinate System
IMLM	Iterated Maximum Likelihood Method
NURBS	Non-Uniform Rational B-Splines
OWC	Oscillating Water Column
PM	Pierson-Moskowitz
PR	Power Ratio (ratio between measured and expected power)
PTO	Power Take-Off
QUB	Queen's University Belfast
RAO	Response Amplitude Operator

RCW	Relative Capture Width
RMS	Root-Mean-Square
SDD	Single Direction Decomposition
TD	Time-Domain
TFSM	Truncated Fourier Series Decomposition Method
UoOx	University of Oxford
WEC	Wave Energy Converter
WR	Waverider

APPENDIX A – DESCRIPTION OF OCEAN WAVES (LINEAR THEORY)

The definitions presented in this Appendix are given in the context of linear theory, in which it is assumed that the amplitude of a wave is small in comparison to its wavelength. The concepts presented here are standard theory and, unless otherwise referenced, can be found in texts such as Tucker and Pitt (2001) or EMEC (2009).

The tests of wave energy converters described in the main section of this report use both regular and irregular waves. Regular waves refer to a single wave train with long, parallel crests, whose shape repeats exactly once per wavelength. In linear theory this shape is a sinusoid. Regular waves are sometimes referred to as monochromatic because there is only one wave frequency present. The basic equations for regular linear waves are presented in Section A.1. Irregular waves refer to a sea composed of waves with more than one frequency, potentially travelling in different directions. Due to the presence of multiple frequencies, irregular waves are sometimes referred to as polychromatic or panchromatic. The term polychromatic implies that many frequencies are present, whereas panchromatic implies that all frequencies are present (which is perhaps slightly misleading). Irregular waves are described using the concept of the wave spectrum, introduced in Section A.2. The wave spectrum can be summarised using the spectral parameters defined in Sections A.3 and A.4 and standard shapes described in Sections A.5 and A.6. Finally, the simulation of waves from a given spectrum is discussed in Section A.7.

A.1 Regular Linear Waves

The linear solutions to the hydrodynamic equations which describe wave motion give the sea surface elevation, η , at location (x, y) and time t , as:

$$\eta(x, y, t) = A \cos [k(x \cos \theta + y \sin \theta) - \omega t + \varphi] \quad [\text{A.1}]$$

where:

A is the wave amplitude

$k = 2\pi / \lambda$ is the wave number and λ is the wavelength

$\omega = 2\pi f$ is the angular frequency and f is the frequency

θ is the direction of wave propagation

φ is the phase

The equation which governs the relationship between wavelength and period is called the dispersion relation. It is given by

$$\omega^2 = gk \tanh kh \quad [\text{A.1}]$$

where g is the acceleration due to gravity and h is the water depth. The speed that the wave crests move (in a direction perpendicular to the wave crest) is called the phase speed and denoted c_p . It is given by

$$c_p = \frac{\lambda}{T} = \frac{\omega}{k} = \left(\frac{g}{k} \tanh kh \right)^{1/2} \quad [\text{A.2}]$$

The speed at which the energy propagates is known as the group speed, denoted c_g . It is given by

$$c_g = \frac{d\omega}{dk} = \frac{1}{2} c_p \left(1 + \frac{2kh}{\sinh 2kh} \right) \quad [\text{A.3}]$$

A.2 The Wave Spectrum

For real seas the surface elevation, η , at location (x, y) and time t , is assumed to be a linear superposition of a large number of regular components:

$$\eta(x, y, t) = \sum_{n=1}^{\infty} A_n \cos[k_n(x \cos \theta_n + y \sin \theta_n) - \omega_n t + \phi_n], \quad [\text{A.4}]$$

with phases distributed randomly over $[0, 2\pi]$ with uniform probability density.

The directional variance spectrum $S(f, \theta)$ describes how the energy in the wave field is distributed with frequency and direction. For small δf and $\delta \theta$ we have

$$\sum_f^{\delta f} \sum_{\theta}^{\delta \theta} \frac{1}{2} A_n^2 = S(f, \theta) \delta f \delta \theta \quad [\text{A.5}]$$

That is, the spectral density is the sum of the variances of the individual sinusoidal components over a given frequency and directional range.

The directional spectrum can be decomposed into two functions, one representing the total energy at each frequency, and the other describing how the energy at each frequency is distributed with direction:

$$S(f, \theta) = E(f) D(f, \theta) \quad [\text{A.6}]$$

$E(f)$ is called the omnidirectional spectrum (or sometimes the frequency spectrum) and is related to the directional spectrum by

$$E(f) = \int_0^{2\pi} S(f, \theta) d\theta \quad [\text{A.7}]$$

$D(f, \theta)$ is the directional spreading function (or directional distribution) and satisfies two properties:

$$1. \quad \int_0^{2\pi} D(f, \theta) d\theta = 1 \quad [\text{A.8}]$$

$$2. \quad D(f, \theta) \geq 0 \text{ over } [0 \ 2\pi] \text{ [A.9]}$$

A.3 Non-Directional Spectral Parameters

The wave height and period parameters are defined in terms of moments of the omnidirectional spectrum. The n^{th} moment of the spectrum is defined as

$$m_n = \int_0^{\infty} f^n E(f) df \quad \text{[A.10]}$$

In practice the upper limit of the integral in Equation (2.11) is normally taken as half the sampling frequency of the measuring device (the Nyquist frequency). Wave height and period parameters are defined as follows:

$$\text{Significant wave height} \quad H_s = 4\sqrt{m_0} \quad \text{[A.11]}$$

$$\text{Energy period} \quad T_e = m_{-1} / m_0 \quad \text{[A.12]}$$

$$\text{Mean period} \quad T_m = m_0 / m_1 \quad \text{[A.13]}$$

$$\text{Zero-crossing period} \quad T_z = \sqrt{m_0 / m_2} \quad \text{[A.14]}$$

The bandwidth, ν , of the spectrum is defined as:

$$\nu = \sigma / f_m \quad \text{[A.15]}$$

where $f_m = 1 / T_m$ is the mean frequency of the spectrum and

$$\sigma^2 = \frac{1}{m_0} \int_0^{\infty} (f - f_m)^2 E(f) df \quad \text{[A.16]}$$

is the variance of the spectral energy about the mean frequency. The bandwidth parameter can be expressed in terms of spectral moments as:

$$\nu = \sqrt{\frac{m_0 m_2}{m_1^2} - 1} \quad \text{[A.17]}$$

The bandwidth parameter is sensitive to the high frequency end of the spectrum and therefore the upper limit of the integral [A.11]. Therefore some authors recommended that the cut-off frequency is chosen as a function of the mean frequency.

A.4 Directional Parameters

The mean direction, $\theta_m(f)$, and directional spread, $\sigma(f)$, at each frequency are given by (Tucker and Pitt, 2001):

$$\theta_m(f) = \text{ATAN2} \left[\int_{-\pi}^{\pi} D(f, \theta) \sin(\theta) d\theta, \int_{-\pi}^{\pi} D(f, \theta) \cos(\theta) d\theta \right] \quad [\text{A.18}]$$

$$\sigma(f) = \left[\int_{-\pi}^{\pi} D(f, \theta) (\theta - \theta_m)^2 d\theta \right]^{1/2} \quad [\text{A.19}]$$

where $\text{ATAN2}(y, x)$ is the four-quadrant inverse tangent function, which uses logic on the signs of x and y to resolve the 180° ambiguity in direction. The directional spread is the standard deviation of the directional distribution. Note that the notation $\sigma(f)$ is used for directional spread to agree with conventions, and it should not be confused with the definition in Eq. [A.16] and [A.17]. This conflict of notation is unfortunate, but has been used here to agree with the majority of literature on the subject.

A mean direction and spread over the whole spectrum, weighted by the energy at each frequency, can be defined as

$$\text{MDIR} = \text{ATAN2} \left[\int_0^{\infty} E(f) \sin(\theta_m(f)) df, \int_0^{\infty} E(f) \cos(\theta_m(f)) df \right] \quad [\text{A.20}]$$

$$\text{SDIR} = \frac{\int_0^{\infty} E(f) \sigma(f) df}{\int_0^{\infty} E(f) df} \quad [\text{A.21}]$$

A.5 Standard Shapes for the Frequency Spectrum

The two most commonly used forms are the Pierson-Moskowitz (PM) and JONSWAP spectra. Roughly speaking, the PM spectrum is used to describe a fully developed sea and the JONSWAP spectrum is used in cases where there are fetch or duration limitations on sea state development (i.e. the amount of energy transferred from the wind to the sea is limited by the distance or time over which the wind is blowing). The PM spectrum is most easily presented in its generalised form, also known as the Bretschneider spectrum, in terms of wave height and period parameters. It is given by

$$E_{PM}(f) = Af^{-5} \exp(-Bf^{-4}) \quad [\text{A.22}]$$

where

$$A = \frac{1}{4} H_s^2 B \quad [\text{A.23}]$$

$$B = 1.25 T_p^{-4} = 0.675 T_e^{-4} = 0.443 T_m^{-4} = 0.318 T_z^{-4} \quad [\text{A.24}]$$

The JONSWAP spectrum can be written as the product of a PM spectrum with a function $G(f)$

$$E_J(f) = G(f) E_{PM}(f) \quad [\text{A.25}]$$

where

$$G(f) = \gamma \exp\left\{-\frac{(f-f_p)^2}{2\sigma^2 f_p^2}\right\} \quad [\text{A.26}]$$

The parameter γ is called the peak enhancement factor. It is the ratio of the maximum spectral density of the JONSWAP spectrum to that of the corresponding PM spectrum. The parameter σ controls with width over which the spectral peak is increased. The values usually taken for γ and σ are those found by Hasselmann et al. (1973):

$$\gamma = 3.3 \quad [\text{A.27}]$$

$$\sigma = \begin{cases} 0.07 & \text{for } f < f_p \\ 0.09 & \text{for } f \geq f_p \end{cases} \quad [\text{A.28}]$$

The formulation of the JONSWAP spectrum given in Eq. [A.26]-[A.29] is not especially useful for fitting the spectrum for given values of H_s and period parameters. The formula $B = 1.25 T_p^{-4}$ is still valid for the JONSWAP spectrum, but the ratios between A and B and the other period parameters are dependent on the values of γ and σ . The spectrum can be integrated numerically to find the ratios between T_p and other period parameters and the ratio between the H_s of the JONSWAP spectrum and that of the corresponding PM spectrum. For the values of σ given in Eq. [A.29] and for the range $1 \leq \gamma \leq 20$, the ratio of H_s is well fitted by a fourth order polynomial and the ratios between period parameters are well described by a logarithm law:

$$\frac{H_s(JS)}{H_s(PM)} = -6.109 \times 10^{-6} \gamma^4 + 3.383 \times 10^{-4} \gamma^3 - 7.575 \times 10^{-3} \gamma^2 + 0.1244 \gamma + 0.8926 \quad [\text{A.29}]$$

$$T_e / T_p = 0.8625 + 0.03411 \ln(\gamma) \quad [\text{A.30}]$$

$$T_m / T_p = 0.7713 + 0.05374 \ln(\gamma) \quad [\text{A.31}]$$

$$T_z / T_p = 0.7018 + 0.06528 \ln(\gamma) \quad [\text{A.32}]$$

These approximations are illustrated in Figure A.1. The appropriate value of B can then be found by substituting one of the above relationships into the formula $B = 1.25 T_p^{-4}$, and A is given by substituting Eq. [A.30] into Eq. [A.24].

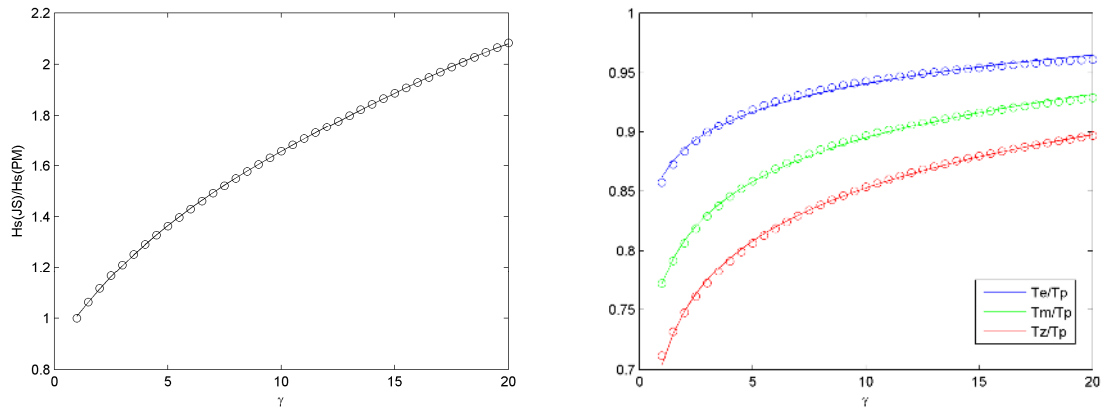


Figure A1. The ratios of H_s and period parameters for various values of peak enhancement factor γ . Circles are values obtained by integrating the spectrum, solid lines are the approximations given in Eq. A30-A33.

A.6 Standard Shapes for the Directional Distribution

There are two parametric forms which are commonly used to describe the directional distribution. The first is known as the ‘cosine2s’ distribution and is given by

$$D(\theta, f) = F(s) \cos^{2s} \frac{1}{2} (\theta - \theta_m(f)) \quad [A.33]$$

where $F(s)$ is a factor necessary to satisfy Eq. [A.9]:

$$F(s) = \frac{1}{2\sqrt{\pi}} \frac{\Gamma(s+1)}{\Gamma(s+1/2)} \quad [A.34]$$

For a narrow beam spectrum the angular spread, as defined in Eq. [A.20], is approximated by

$$\sigma^2 \approx \frac{2}{1+s} \quad [A.35]$$

The second commonly used formulation is the wrapped-normal distribution:

$$D(\theta, f) = \frac{1}{\sigma(f)\sqrt{2\pi}} \sum_{k=-\infty}^{\infty} \exp \left[-\frac{1}{2} \left(\frac{\theta - \theta_m(f) - 2\pi k}{\sigma(f)} \right)^2 \right] \quad [A.36]$$

This formulation directly includes the spread parameter σ , so is slightly more straight forward to use. The summation over k in Eq. [A.37] is to ensure that energy outside the interval $[0, 2\pi]$ is added back in. In practice the summation can be taken over range $k = -2, \dots, 2$. For $\sigma < 30$ the ‘cosine2s’ and wrapped-normal distribution have very similar shapes.

For fetch-limited sea states the directional distribution is bimodal at frequencies greater than about twice the peak frequency (see e.g. Young et al., 1995; Ewans, 1998; Hwang et al., 2000). Ewans (1998) has proposed the use of a double Gaussian distribution to model this bimodality. It can be written as

$$D(f, \theta) = \frac{1}{\sigma(f)\sqrt{8\pi}} \sum_{k=-\infty}^{\infty} \left\{ \exp \left[-\frac{1}{2} \left(\frac{\theta - \theta_1(f) - 2\pi k}{\sigma(f)} \right)^2 \right] + \exp \left[-\frac{1}{2} \left(\frac{\theta - \theta_2(f) - 2\pi k}{\sigma(f)} \right)^2 \right] \right\} \quad [\text{A.37}]$$

where

$$\theta_1(f) = \theta_m + \Delta\theta(f) / 2$$

$$\theta_2(f) = \theta_m - \Delta\theta(f) / 2$$

and $\Delta\theta$ is the separation between the peaks of the two modes. Note that the parameter σ in Eq. [A.38] no longer corresponds to the directional spread defined in Eq. [A.20]. The values of $\Delta\theta$ and σ are given as functions of frequency:

$$\Delta\theta = 14.93 \text{ for } f < f_p \quad [\text{A.38}]$$

$$\Delta\theta = \exp \left[5.453 - 2.750 \left(\frac{f}{f_p} \right)^{-1} \right] \text{ for } f \geq f_p \quad [\text{A.39}]$$

$$\sigma = 11.38 + 5.357 \left(\frac{f}{f_p} \right)^{-7.929} \text{ for } f < f_p \quad [\text{A.40}]$$

$$\sigma = 32.13 - 15.39 \left(\frac{f}{f_p} \right)^{-2} \text{ for } f \geq f_p \quad [\text{A.41}]$$

The resulting distribution is unimodal for $f < 2f_p$ and becomes bimodal at higher frequencies. This formulation results in a directional distribution which is qualitatively the same as earlier studies (e.g. Mitsuyasu et al., 1975; Hasselmann et al., 1980; Donelan et al., 1985) in the way that the spread varies with frequency. However earlier studies made the *a priori* assumption that the distribution was unimodal. Mitsuyasu et al. (1975) and Hasselmann et al. (1980) also suggested that the distribution was dependent on the wave age (a function of the wind speed and phase speed of the waves), whereas no such dependence was noted in later studies.

A.7 Simulation of sea surface elevation from the wave spectrum

The sea surface elevation can be simulated from the wave spectrum using a summation similar to Eq. [A.5]. The number of frequencies used is chosen as a function of the duration of the simulation, T . Suppose that we are interest in simulating waves within the frequency range $[f_0, f_i]$ with frequency resolution df . Choosing $df = 1/T$ and f_0 as an integer multiple of df ensures that repeat period of simulated waves is T and that the energy content of the simulated waves is exactly equal to that of the spectrum, since the period of the n^{th} wave component is T/n and therefore repeats exactly n times within the duration of the simulation. The amplitude of the n^{th} wave component is given by (c.f. Eq. [A.6])

$$A_n = \sqrt{2E(f_n)df} \quad [\text{A.43}]$$

The phase of each component is chosen as a random number from a uniform distribution over the interval $[0, 2\pi]$. For directionally spread seas, a small number, M , of directions at each frequency is used, with the directions chosen as random numbers, $\theta_{n,m}$, from the distribution $D(f_n, \theta)$. The resultant sea surface is given by

$$\eta(x, y, t) = \frac{1}{\sqrt{M}} \sum_{n=1}^N \sum_{m=1}^M A_n \cos \left[k_n (x \cos \theta_{n,m} + y \sin \theta_{n,m}) - \omega_n t + \varphi_n \right]. \quad [\text{A.45}]$$

References

- Donelan MA, Hamilton J, Hui WH, 1985. Directional spectra of wind-generated waves. Philos. Trans. Roy. Soc. London., A315, 509-562.
- EMEC, 2009. Assessment of Wave Energy Resource. Report prepared for EMEC by EG Pitt
- Ewans KC, 1998. Observations of the Directional Spectrum of Fetch-Limited Waves. J. Phys. Oceanogr., 28, 495-512.
- Hasselmann DE, Dunckel M, Ewing JA, 1980. Directional wave spectra observed during JONSWAP 1973. J. Phys. Oceanogr., 10, 1264-1280.
- Hwang PA, Wang W, Walsh EJ, Krabill WB, Swift RN, 2000. Airborne Measurements of the Wavenumber Spectra of Ocean Surface Waves. Part II: Directional Distribution. J. Phys. Oceanogr., 30, 2768-2787.
- Kahma K, Hauser D, Krogstad HE, Lehner S, Monbaliu JAJ, Wyatt LR, 2005. Measuring and Analysing the Directional Spectra of Ocean Waves. EU COST Action 714, EUR 21367, ISBN 92-898-0003-8.
- Mitsuyasu H, and Coauthors, 1975. Observations of the directional spectrum of ocean waves using a cloverleaf buoy. J. Phys. Oceanogr., 5, 750-760.
- Tucker MJ and Pitt EG, 2001. Waves in ocean engineering. Elsevier Science.

Young IR, Verhagen LA, Banner ML, 1995. A note on the bimodal directional spreading of fetch-limited waves. *J. Geophys. Res.*, 100 (C1), 773-778.

APPENDIX B – ESTIMATION OF THE WAVE SPECTRA FROM MEASUREMENTS

B.1. Frequency spectrum

The frequency spectrum is estimated from a time series of surface elevation using a Fast-Fourier Transform (FFT) algorithm. If Z , is the Fourier transform of the surface elevation signal, η , then the spectral density is then given by

$$E(f_i) = \frac{2Z(f_i)Z^*(f_i)}{f_s N} \quad [\text{B.1}]$$

where $f_i = if_s / N$ and f_s is the sampling frequency, N is the number of samples in the record, and H_i^* denotes the complex conjugate of H_i .

B.2. Directional spectrum

Estimates of the directional spectrum require the use of three or more signals. For buoy measurements, the three signals are heave, pitch and roll or heave and two horizontal displacements. For wave probe arrays in a tank three or more surface elevation signals can be used.

A good introduction to the various analysis methods available is given by Benoit et al (1997). For buoy measurements Benoit et al (1997) recommend the use of the Iterated Maximum Likelihood Method (IMLM) or Maximum Entropy Method (MEM). Directional parameters can also be estimated without fitting a distribution, using the method of Kuik et al (1988). This section starts by describing the relationship between cross-spectra, the directional distribution and its Fourier coefficients. We then describe the IMLM, MEM and parametric methods implemented in the Wave Analysis module.

B.2.1 The cross-spectral matrix

Consider an arbitrary device recording N signals, P_1, \dots, P_N . Denote the cross-spectrum between signals P_m and P_n as G_{mn} . It can be shown that G_{mn} and G_{nm} are complex conjugates so cross-spectra need only be computed for $m \leq n$. The real part of the cross-spectra, C_{mn} , are called coincident spectral density functions or co-spectra, and the imaginary parts, Q_{mn} , are called quadrature spectral density functions or quad-spectra.

Within the framework of linear theory, cross-spectra are related to the directional spectrum by

$$G_{mn}(f) = E(f) \int_0^{2\pi} H_m(f, \theta) H_n^*(f, \theta) \exp[-i\mathbf{k} \cdot \mathbf{x}_{mn}] D(f, \theta) d\theta \quad [\text{B.2}]$$

where H_m is the transfer function between the surface elevation and signal P_m , * denotes the complex conjugate, \mathbf{k} is the wave number vector and $(\mathbf{x}_m - \mathbf{x}_n)$ is the vector between the locations of signals m and n .

The transfer function $H_m(f, \theta)$ can be expressed as

$$H_m(f, \theta) = h_m(f) \cos^{\alpha_m} \theta \sin^{\beta_m} \theta \quad [\text{B.3}]$$

The values of h_m , α_m , and β_m for commonly used measurement types are presented in Table B.1.

Wave Signal	h_m	α_m	β_m
Surface elevation	1	0	0
Surface slope (x-axis)	ik	1	0
Surface slope (y-axis)	ik	0	1
Displacement (x-axis)	$i \frac{\cosh(k(d+z))}{\sinh(kd)}$	1	0
Displacement (y-axis)	$i \frac{\cosh(k(d+z))}{\sinh(kd)}$	0	1
Displacement (z-axis)	$\frac{\sinh(k(d+z))}{\sinh(kd)}$	0	0
Velocity (x-axis)	$\omega \frac{\cosh(k(d+z))}{\sinh(kd)}$	1	0
Velocity (y-axis)	$\omega \frac{\cosh(k(d+z))}{\sinh(kd)}$	0	1
Velocity (z-axis)	$-i\omega \frac{\sinh(k(d+z))}{\sinh(kd)}$	0	0
Acceleration (x-axis)	$-i\omega^2 \frac{\cosh(k(d+z))}{\sinh(kd)}$	1	0
Acceleration (y-axis)	$-i\omega^2 \frac{\cosh(k(d+z))}{\sinh(kd)}$	0	1
Acceleration (z-axis)	$-\omega^2 \frac{\sinh(k(d+z))}{\sinh(kd)}$	0	0

Table B.1. Linear transfer functions for various wave signals. d is the water depth and z is the height of the measurement from the still water level (positive upwards).

B.2.2 Fourier series decomposition

The directional spectrum can be described by a Fourier series representation:

$$D(f, \theta) = \frac{1}{\pi} \left\{ \frac{1}{2} + \sum_{n=1}^{\infty} [a_n(f) \cos(n\theta) + b_n(f) \sin(n\theta)] \right\} \quad [\text{B.4}]$$

where the coefficients are given by

$$a_n(f) = \int_0^{2\pi} D(f, \theta) \cos(n\theta) d\theta \quad [\text{B.5}]$$

$$b_n(f) = \int_0^{2\pi} D(f, \theta) \sin(n\theta) d\theta \quad [\text{B.6}]$$

For buoy measurements only the first four Fourier coefficients can be computed from the cross-spectra. From Table B.1, after some algebra, we see that

$$a_1 = \frac{Q_{12}}{\sqrt{C_{11}(C_{22} + C_{33})}} \quad [\text{B.7}]$$

$$b_1 = \frac{Q_{13}}{\sqrt{C_{11}(C_{22} + C_{33})}} \quad [\text{B.8}]$$

$$a_2 = \frac{C_{22} - C_{33}}{C_{22} + C_{33}} \quad [\text{B.9}]$$

$$b_2 = \frac{2C_{23}}{C_{22} + C_{33}} \quad [\text{B.10}]$$

It is possible to estimate the directional distribution in terms of a truncated Fourier series using the first four coefficients, however this can result in negative values, violating the definition given in Eq. (B-7). As a solution to this problem Longuet-Higgins et al (1963) proposed the use of a weighting function to ensure that the estimate of $D(f, \theta)$ is always positive. However, this results in a diffusion of energy with direction and artificially broadens the distribution. This method is therefore not recommended. However, the relations between the Fourier coefficients and cross-spectra have been presented here as they are used in the maximum entropy method and can also be used to estimate directional parameters.

B.2.3 Model-free directional parameters

Kuik et al (1988) note that the use of MLM and MEM methods may suggest a misleadingly high directional resolution for buoy measurements. As an alternative, they propose a method to estimate directional parameters directly from the cross-spectra, without fitting a directional distribution. These parameters are model-free (i.e. they do not assume a particular form of the directional distribution) and can be expressed analytically in terms of the cross-spectra, and are thus much faster to compute than MLM and MEM estimates.

The directional parameters defined by Kuik et al (1988) are

$$\theta_m = \text{ATAN2}(b_1 / a_1) \quad [\text{B.11}]$$

$$\sigma_c = [2(1 - m_1)]^{1/2} \quad [\text{B.12}]$$

where a_1 and b_1 are the first two Fourier coefficients of the directional distribution and

$$m_1 = (a_1^2 + b_1^2)^{1/2} \quad [\text{B.13}]$$

Kuik et al note that θ_m can be interpreted as the vector mean of the directional distribution (in fact this definition is consistent with Eq. A.19). The parameter σ_c can be interpreted as the circular-moment analogue to the line-moment definition of RMS spread (Eq. A.20). They show that for narrow directional distributions (σ less than about 40°) this definition closely matches the line-moment equivalent.

B.2.4 Maximum likelihood methods

The maximum likelihood method (MLM) estimate of the directional spectrum is given by

$$\hat{D}_0(f, \theta) = \frac{\kappa}{\sum_{m,n} H_m(f, \theta) G_{mn}^{-1}(f, \theta) H_n^*(f, \theta)} \quad [\text{B.14}]$$

where G_{mn}^{-1} are the elements of the inverse of G and κ is determined by the condition in Eq. A.9.

The cross-spectra computed from the MLM estimate are not consistent with the cross-spectra from the wave signals. Pawka (1983), Oltman-Shay and Guza (1984) and Krogstad et al (1988) have suggested iterative methods to improve the MLM estimate so that the cross-spectra are consistent. The method of Krogstad et al (1988) has been will be implemented for the Wave Analysis module. Iterative improvements to the MLM estimate are given by:

$$\hat{D}_i(f, \theta) = \hat{D}_{i-1}(f, \theta) + \gamma \left(\hat{D}_0(f, \theta) - \Delta_{i-1}(f, \theta) \right) \quad [\text{B.15}]$$

where $\Delta_{i-1}(f, \theta)$ is the MLM estimate calculated from the cross-spectra of $\hat{D}_{i-1}(f, \theta)$. Krogstad et al (1988) show that the number of iterations required for convergence depends on the value of γ , with the range $0.5 < \gamma < 1.5$ giving the best performance. A value of $\gamma = 0.5$, is a reasonable compromise between the rate of convergence and the possibility of adjusting the estimate too far in the wrong direction. Iterations are terminated when $i > 50$ or

$$\int_0^{2\pi} \left| \hat{D}_i(f, \theta) - \Delta_{i-1}(f, \theta) \right| d\theta \leq 0.01 \quad [\text{B.16}]$$

B.2.5 Maximum entropy methods

There are two types of MEM estimates which use different definitions of entropy. Lygre and Krogstad (1986) define an estimate of the directional distribution which maximises the Burg definition of entropy:

$$H_B(D) = - \int_0^{2\pi} \ln(D(\theta)) d\theta, \quad [\text{B.17}]$$

whereas Kobune and Hashimoto (1986) define an estimator which maximises the Shannon definition of entropy:

$$H_S(D) = - \int_0^{2\pi} D(\theta) \ln(D(\theta)) d\theta. \quad [\text{B.18}]$$

The MEM distribution of Lygre and Krogstad can be expressed as an analytical function of the measured cross-spectra and is therefore very quick to compute. However, it has been shown by numerous authors to produce double peaks in cases of unimodal directional distributions (see e.g. Brissette and Tsanis, 1994; Kim et al, 1994). The MEM of Kobune and Hashimoto is more computationally intensive, but has been shown to produce more robust estimates of the directional distribution. This latter method has been implemented in GH WAVES.

To start with, consider the case of buoy measurements. Kobune and Hashimoto showed that the estimate which maximises [B.18] has the form

$$\hat{D}(f, \theta) = \exp\left(-\sum_{j=0}^4 \lambda_j(f) \alpha_j(\theta)\right), \quad [\text{B.19}]$$

where $\alpha_0(\theta) = 1$, $\alpha_1(\theta) = \cos(\theta)$, $\alpha_2(\theta) = \sin(\theta)$, $\alpha_3(\theta) = \cos(2\theta)$ and $\alpha_4(\theta) = \sin(2\theta)$. The λ_j 's are Lagrange multipliers, found by solving the system of nonlinear equations given by equating the Fourier coefficients calculated from the measured data and the estimated directional distribution, subject to the constraint in Eq. [A.9]. This system of equations can be written as

$$\int_0^{2\pi} \exp\left(-\sum_{j=0}^4 \lambda_j(f) \alpha_j(\theta)\right) \alpha_j(\theta) d\theta = \phi_j(f), \quad j = 0, \dots, 4 \quad [\text{B.20}]$$

where $\phi_0(f) = 1$, $\phi_1(f) = a_1(f)$, $\phi_2(f) = b_1(f)$, $\phi_3(f) = a_2(f)$ and $\phi_4(f) = b_2(f)$. This formulation was proposed by Nwogu et al (1987), and includes λ_0 as an iteration parameter to improve convergence for narrow spreading functions. This differs slightly from the formulation proposed by Kobune and Hashimoto (1986) who expressed λ_0 as a function of the other four λ_j 's. The system of equations given in [B.20] is solved by standard numerical methods. Occasionally there are convergence problems when trying to solve these equations. Kim et al (1994) proposed an approximation scheme which can be used when this occurs. They showed that by expanding the exponential term in [B.20] to second order, the λ_j 's can be expressed as

$$\lambda_0 = \ln \left[\int_0^{2\pi} \exp\left(\sum_{j=1}^4 \lambda_j \alpha_j(\theta)\right) d\theta \right] \quad [\text{B.21}]$$

$$\lambda_1 = 2\phi_1\phi_3 + 2\phi_2\phi_4 - 2\phi_1 \sum_{j=0}^4 \phi_j^2 \quad [\text{B.22}]$$

$$\lambda_2 = 2\phi_1\phi_4 - 2\phi_2\phi_3 - 2\phi_2 \sum_{j=0}^4 \phi_j^2 \quad [\text{B.23}]$$

$$\lambda_3 = \phi_1^2 - \phi_2^2 - 2\phi_3 \sum_{j=0}^4 \phi_j^2 \quad [\text{B.24}]$$

$$\lambda_4 = 2\phi_1\phi_2 - 2\phi_4 \sum_{j=0}^4 \phi_j^2 \quad [\text{B.25}]$$

Kim et al showed that this approximation scheme produces estimates close to those from [B.20], and gives reasonable results for unimodal and bimodal distributions, although with a slight tendency to reduce the directional width.

Maximum entropy methods for arrays of wave probes have been proposed by Nwogu (1989) and Hashimoto et al (1994). The method of Hashimoto et al, known as the extended maximum entropy principle (EMEP), is a slight improvement on Nwogu's method and has been implemented in GH WAVES. The estimate of the directional distribution is given by

$$\hat{D}(f, \theta) = \frac{1}{\kappa} \exp \left(\sum_{j=1}^J [A_j \cos(j\theta) + B_j \sin(j\theta)] \right), \quad [\text{B.26}]$$

where

$$\kappa = \int_0^{2\pi} \exp \left(\sum_{j=1}^J [A_j \cos(j\theta) + B_j \sin(j\theta)] \right) d\theta. \quad [\text{B.27}]$$

and the coefficients A_j and B_j are unknowns. The coefficients are found by minimising the differences between the measured co- and quad-spectra and those calculated by substituting [B.26] in [B.2]. If L is the number of independent, non-zero co- and quad-spectra, and ε_l is the difference between the l^{th} measured and modelled co- or quad-spectra then the EMEP estimate is obtained by minimising $\sum_{l=1}^L \varepsilon_l^2$.

The optimal number of terms, J , used in [B.26] is determined as the value which minimises Akaike's Information Criterion:

$$AIC = L \left(\ln(2\pi\hat{\sigma}^2) + 1 \right) + 4J \quad [\text{B.28}]$$

where $\hat{\sigma}^2$ is an estimate of the variance of the ε_l (which are assumed to be independent and normally distributed with zero mean). The computation is performed for each value of J , starting with $J = 1$, until the value of AIC starts to increase.

References

- Benoit M, Frigaard P, Schaffer HA, 1997. Analysing multidirectional wave spectra: A tentative classification of available methods. Proc. IAHR Seminar: Multidirectional Waves and their Interaction with Structures, 27th IAHR Congress, San Francisco, August 1997.
- Brissette FP and Tsanis IK, 1994. Estimation of wave directional spectra from pitchroll buoy data. J. Waterway, Port, Coastal and Ocean Eng., 120(1), 93-115.
- Hashimoto N, Nagai T, Asai T, 1994. Extension of Maximum Entropy Principle Method for directional wave spectrum estimation. Proc. 24th Int. Conf. on Coastal Eng. (ASCE), Kobe, Japan, pp232-246
- Kim T, Lin L, Wang H, 1994. Application of the maximum entropy method to the real sea data. Proc. 24th Int. Conf. on Coastal Eng., (ASCE), Kobe, Japan, pp 340-355.
- Kobune K and Hashimoto N, 1986. Estimation of directional spectra from the maximum entropy principle. Proc. 5th Int. Offshore Mechanics and Arctic Eng. Symp., Tokyo, Japan, Vol 1, pp 80-85.
- Krogstad HE, Gordon RL, Miller MC, 1988. High resolution directional wave spectra from horizontally mounted acoustic Doppler current meters. J. Atmos. and Oceanic Technol., 5, 340-352.
- Kuik AJ, Van Vledder GP, Holthuijsen LH, 1988. A Method for the Routine Analysis of Pitch-Roll-Heave Buoy Wave Data. J. Phys. Oceanography, 18, 1020-1034.
- Longuet-Higgins MS, Cartwright DE, Smith ND, 1963. Observations of the directional spectrum of sea waves using the motions of a floating buoy. Ocean Wave Spectra, Prentice Hall, 111–136.
- Lygre A and Krogstad HE, 1986. Maximum entropy estimation of the directional distribution in ocean wave spectra. J. Phys. Oceanography, 16, 2052-2060.
- Nwogu OU, 1989. Maximum entropy estimation of directional wave spectra from an array of wave probes. Applied Ocean Research, 11(4), 176-193
- Nwogu OU, Mansard EPD, Miles MD, Isaacson M, 1987. Estimation of directional wave spectra by the maximum entropy method . Proc. 17th IAHR Seminar - Lausanne, Switzerland.
- Oltman-Shay J and Guza RT, 1984. A data-adaptive ocean wave directional-spectrum estimator for pitch-roll type measurements. J. Phys. Oceanography, 14, 1800-1810.
- Pawka SS, 1983. Island shadows in wave directional spectra. J. Geophys. Res., 88, 2579-2591.